ABSTRACT

Title of thesis: DEVELOPMENT OF HORDEIN-PECTIN NANOPARTICLE COMPLEX FOR THE ENCAPSULATION OF BIOACTIVE COMPOUNDS FOR ENHANCED FUNCTIONALITIES

Kevin Tarwa, Master of Science, 2023

Thesis directed by: Professor Qin Wang, Department of Nutrition and Food Science

Nanoparticle delivery systems composed of food polymers are a sustainable and eco-friendly approach to protect functional ingredients and promote healthier food options. In this research, a hordein-pectin nanoparticle complex (HP-NPC) was fabricated using an anti-solvent precipitation and electrostatic deposition (pH 4) method for the encapsulation of hydrophobic bioactive compounds to enhance their functionalities.

First, hordein was extracted from whole barley grains to obtain a dried powder to synthesize hordein nanoparticles (HNP). Then pectin with a degree of esterification (DE) around 71% was applied as a coating material. The average particle size of the freshly prepared nanoparticle complex was relatively small (~246 ± 11 nm), and Fourier transform infrared spectroscopy (FTIR) indicated that cationic hordein interacted with anionic pectin mainly though newly formed hydrogen bonds and electrostatic interaction as indicated by their opposite surface charges. Scanning electron microscopy (SEM) revealed that the morphology of the nanoparticle complex was spherical with a smooth surface. The pectin coating was shown to have a protective effect against pH (3.0-9.0), heat (80 °C for 0-120 mins), and salt (0-100 μM) which are all factors known to degrade proteins.

Second, lutein, a hydrophobic bioactive xanthophyll was encapsulated into HP-NPC to develop a lutein-hordein/pectin nanoparticle complex (L-HP-NPC). Since lutein has low water solubility and low bioavailability in the gastrointestinal tract (GIT), the effect of the encapsulation system on the functional properties of lutein was investigated. The loading capacity (LC%) and encapsulation efficiency (EE%) was around 15.5 and 82%, respectively. *In vitro* digestion resulted in a higher bioaccessibility of lutein for encapsulated HP-NPC (~22.3%), which is defined as the percentage of lutein accessible for absorption in the simulated intestinal fluid (SIF) compared to lutein encapsulated into HNP (~9%). The ability of pectin to produce gels in acidic media was shown to have a significant effect against gastric enzymes that can degrade both hordein and lutein. Also, lyophilization (an important step in food processing) had no significant effect on the stability of L-HP-NPC. This encapsulation system could potentially be used as a functional ingredient in the food industry to develop healthy and nutritious foods for consumers.

Third, carvacrol, a phenolic monoterpene known for its antimicrobial properties was encapsulated into HP-NPC to develop a carvacrol-hordein/pectin nanoparticle complex (CA-HP-NPC). Special focus was on the solubility of encapsulate carvacrol due to its known low solubility in aqueous solutions. The antimicrobial effectiveness of the encapsulated nanoparticle complex was tested against non-pathogenic gram-positive *L. innocua* and gram-negative *E. coli K12.* CA-HP-NPC was still able to maintain a relatively small particle size (~207 ± 8 nm) after being dispersed into water post-lyophilization. Carvacrol was shown to be effective against the two bacteria, however, CA-HP-NPC did not show antimicrobial effectiveness. Although carvacrol was successfully encapsulated into the nanoparticle complex, further studies on their release properties need to be investigated to further understand their functional properties for food applications.

DEVELOPMENT OF HORDEIN-PECTIN NANOPARTICLE COMPLEX FOR THE ENCAPSULATION OF BIOACTIVE COMPOUNDS FOR ENHANCED FUNCTIONALITIES

by

Kevin Tarwa

Thesis Submitted to the Faculty of the Graduate School of the
University of Maryland, College Park, in Partial Fulfillment
of the requirements for the degree of
Master of Science
2023

Advisory Committee:
Dr. Qin Wang, Professor, Department of Nutrition and Food Science, UMCP (chair)
Dr. Rohan V. Tikekar, Associate Professor, Department of Nutrition and Food Science, UMCP
Dr. Paul C. Turner, Associate Professor, Maryland Institute for Applied Environmental Health, UMCP

Acknowledgements

I would like to give a special thanks to all the individuals in my life who have contributed to or helped me in receiving my master's degree. First and foremost, I would like to give a sincere thank you to Dr. Qin Wang for all the feedback and guidance that she had provided me in this project. I would also like to thank my committee members, Dr. Rohan V. Tikekar, and Dr. Paul C. Turner for taking the time out of their busy schedules to assist as my committee members. I would also like to give special thanks to my friends here at the University of Maryland, Peihua Ma, Xiaoxue Jia, Shuyi Feng, Ethan Lee, Abby Gao, Rose Fan, and many more. Thank you for making my time spent here at UMD an enjoyable and memorable experience. I would also like to give a warm and special thanks to Aishwarya Rao for being such a kind and spirited friend during this entire process. Thanks for always reminding me that things will be fine even during times when my work was not going in the right direction. It was a pleasure being a teaching assistant with you and I look forward to working with you during my PhD. I would also like to thank Dr. Boce Zhang from the University of Florida. Without his guidance during my undergraduate experience at the University of Massachusetts of Lowell, I don't think I would be in the position I am today. I will never forget feeling lost until I took your introduction to food science and food safety course. You helped me realize that food science was a field that I was passionate about, and I cannot thank you enough for guiding me in that direction. Also, a huge thanks to Dr. Ryan Blaustein, Dr. Seong Ho Lee, Dr. Liangli Yu, Dr. Abani Pradhan, and Dr. Aldo Ponce for their help and for allowing me to use their labs to conduct some of my experiments. I would like to give a special thanks to some of the closest people that I have met during my transition here to Maryland. Thank you, Ryan, Michelle, Bek, Meet, Nathan, and Alanna, I am forever thankful for meeting you guys. I have shared some of the most memorable experiences

here in Maryland with you all and I look forward to so many more in our life-long friendships. I am also so grateful for my time working at Cielo Rojo and for the amazing individuals that I have met. Manuela, Tatianna, Carlos, Lilian, Kheyana, Qadeera, Marvin, and Heidi, you have all made work such an enjoyable experience and I hope our friendships continue even after we move on to bigger and better things. To my friends back home, Mike, Yvonne, Hippert, Ben, and Luke, we have built a relationship that is life-long, and I will always be grateful for you guys always checking up to see if I am doing well. You all hold a special place in my heart, and I love you guys forever. Lastly, I would like to give a warm and sincere thanks to my family, my parents, and my brother. Thank you all for supporting me no matter how much of a pain I can be. I appreciate everything you all have done and continue to do for me. You are all my inspiration to succeed in life and I hope that one day, I will be able to repay you all somehow. I am forever thankful for the sacrifices that you have made and thank you for inspiring me to become a better man every day.

Life is never an easy experience, and every day is a constant battle. You may win some, and sometimes you will lose some. Although those wins are rewarded with celebrations, we never really truly appreciate those losses. Those losses have helped me grow stronger as an individual because it's not about how hard you fall; it's about how you decide to get back up.

"You should never view your challenges as a disadvantage. Instead, it's important for you to understand that your experience facing and overcoming adversity is one of your biggest advantages" -Michelle Obama

Table of Contents

List of tables

List of figures

Chapter 1. Introduction

1.1. Food nanotechnology

The unit "nanometer" refers to any material that is a thousandth of a thousandth of a thousandth of a meter (10^{-9}) in at least one dimension. To put that into perspective, one nanometer (nm) is roughly 80,000-100,000 times smaller in width than human hair, and approximately as long as the growth of human fingernails per second (Sekhon, 2010). Food nanomaterials generally have a particle size around 1-100 nm with varying physical and chemical characteristics which allows us to determine the overall stability and properties of interfacial biopolymer mixtures containing protein, lipids, carbohydrates, artificial additives, and surfactants (Sonkaria et al., 2012). Nanosized biopolymers are more active biologically as compared to larger-sized particles of the same components due to the surface area per mass (Chau et al., 2007). Applications of nanotechnology were first addressed by the United States Department of Agriculture (USDA) in September 2003 with attempts to control food characteristic traits, enhance processing functionalities such as flavor, texture, processing efficiency, heat tolerance, shelf-life, traceability, safety, bioavailability of nutrients and cost-effective food analysis with a major focus to control and manipulate the properties and characteristics of substances close to the molecular level (Momin et al., 2013).

According to the latest report from Technavio, the food nanotechnology market is expected to increase at a compound annual gross rate (CAGR) of around 25%, with potential growth of USD 187.84 billion from 2020 to 2025 (Technavio, 2022). Food nanotechnology offers a promising way to develop food products with a higher capability to alter their characteristics and nutritional value compared to conventional processing methods, lower cost, and enhanced sustainability. Applications in food nanotechnology are aimed at enhancing nutrients

bioavailability (Kaya-Celiker & Mallikarjunan, 2012), and extending the shelf-life of products through active packaging (Kaya-Celiker & Mallikarjunan, 2012; Mihindukulasuriya & Lim, 2014). However, one of the limitations to utilizing nanotechnology in the food industry is the fact that there are no worldwide guidelines on its use, which may deteriorate consumer acceptance (Sozer & Kokini, 2009). Thus, it is expected that the applications of nanotechnology in the food industry will focus on active food packaging. Although with limited consumer acceptance on food nanotechnology, its applications still offer benefits due to the use of biodegradable and non-toxic food biopolymers, which allow its extended applications in the pharmaceutical and cosmetic industries (Anusha & Priya, 2022; Singh et al., 2022).

1.1.1. Synthesis techniques

Synthesis techniques for nanotechnology applications in food are applied by two approaches, either “top down” or “bottom up” (Ravichandran, 2010). The top-down approach utilizes physical machinery (i.e., food processing), to convert materials into their nanometer size range by applying processes such as grinding, milling, etching, and lithography (Sanguansri & Augustin, 2006). The bottom-up approach starts with atoms or molecules to form nanomaterials where smaller components at the atomic or molecular-scale self-assemble through a natural physical principle or an externally applied driving force, to develop more organized systems (Arole & Munde, 2014). As depicted in **Fig 1.1**, the top-down approach allows the reduction of bulk materials into the nanoscale while the bottom-up approach is the formation of large nanostructures from smaller atoms and molecules (Abid et al., 2022). Although the top-down approach is simple to use, its limitations are due to its ineffectiveness in obtaining proper particle size and shape. Thus, the bottom-up approach is a more feasible approach to developing nano-

scaled materials due to the self-assembly of atoms and molecules, lower energy required and lower cost.

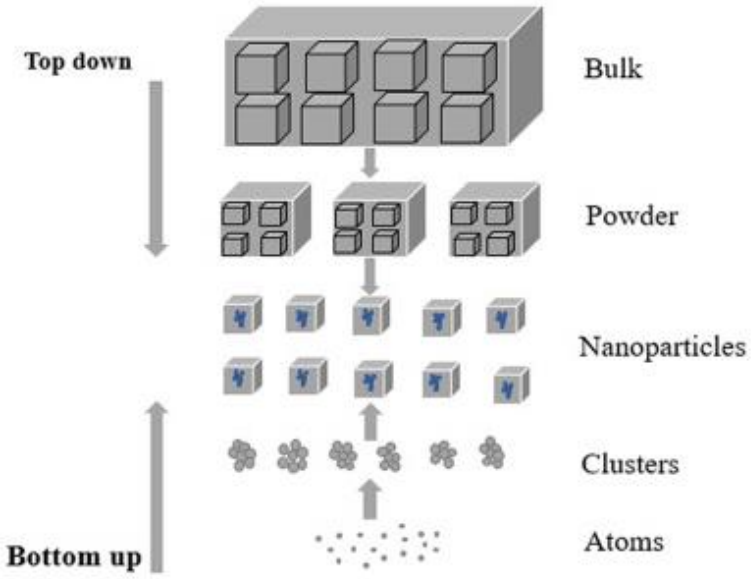

Fig 1.1. Top-down and bottom-up approach for developing nano-scaled materials (Abid et al., 2022)

1.1.2. Self-assembly of food polymers

The process in which molecules spontaneously organize or aggregate into stable structures is known as self-assembly. The process of self-assembly is driven by inter- and intramolecular forces such as van der Waals forces, hydrogen bonding, hydrophobic interactions, electrostatic forces, and π-π aromatic stacking (Stoffelen & Huskens, 2016). Thus, self-assembly offers an environmentally friendly, biocompatible, convenient, and low toxic approach to developing food nanomaterials and has been applied to the fields of medicine, nutraceuticals, food safety, and cancer therapy (Kalita et al., 2012; D. Li et al., 2020; Pathak et al., 2015; Zhang et al., 2007). Several types of nanostructures can be fabricated through the self-assembly of food biopolymers

such as nanoparticles, nanoemulsons, nanoliposomes, and nanofibers. The next section will highlight some characteristics of these mentioned nanostructures and some of their applications.

1.2. Types of food nanomaterials

1.2.1. Nanoparticles

Nanoparticles ranging from 1-100 nm are used in the food science field and have the potential to produce healthier, safer, and high-quality foods. Food biopolymers such as proteins, carbohydrates, and lipids are finding increasing application as ingredients in the food industry due to their unique physiochemical properties and functional attributes. The dimensions of food nanoparticles play a major role in its functional performance such as its physiochemical properties (optics, rheology, and stability), encapsulation characteristics (e.g., loading, retention, and release), and behavior within the gastrointestinal tract (GIT; e.g., transport, degradation, interactions, and penetration) (Joye & McClements, 2014). Food nanoparticles have a wide range of applications such as active food packaging to prevent food spoilage (Omerović et al., 2021; Souza & Fernando, 2016), encapsulation of bioactive compounds for targeted delivery and controlled release (Rostamabadi et al., 2021; Weiss et al., 2008), enhancing nutrition by providing information about the location of a nutrient or bioactive component in specific tissues or cells (Srinivas et al., 2010), agriculture in developing nanofertilizer and nano-fertilizers to increase crop productivity (Goswami & Mathur, 2019) and so on.

1.2.2. Nanoemulsions

Nanoemulsions are another field of food nanotechnology that can be applied as carriers or delivery systems for bioactive compounds such as nutraceuticals (Jamali et al., 2020), drugs (Wilson et al., 2022), flavors (Saffarionpour, 2019), antioxidants, and antimicrobial agents

(Seibert et al., 2019). The structure of nanoemulsions consists of a lipid phase dispersed in an aqueous continuous phase, with each oil droplet being surrounded by a thin interfacial layer consisting of emulsifier molecules (Silva et al., 2012). Nanoemulsion droplets range from 5-100 nm which enhances their kinetic stability due to no gravitational separation and droplet aggregation due to the reduced attractive forces between the small size droplets (Aswathanarayan & Vittal, 2019). Another driving force leading to the kinetic stability of nanoemulsions is the Brownian motion, which overcomes the gravitational forces in nanoemulsions, thus making it kinetically stable and resistant to particle aggregation (Dasgupta et al., 2019). Fortification of beverages and aqueous-based foods such as sauces, yogurts, salad dressings, and desserts can be achieved through nanoemulsions.

1.2.3. Nanoliposomes

Another category of food nanomaterials are nanoliposomes (> 100 nm) whose structures form vesicles composed of membranes of one or more lipid bilayers (e.g., phospholipids and sterols) (Bondu & Yen, 2022). Nanoliposomes present two distinct phases: a lipid phase in an aqueous phase, where the aqueous phase is the continuous phase, and the lipid phase is the dispersed phase. Conventional nanoemulsions are often limited as potential drug delivery systems since only lipophilic molecules can be encapsulated (Kuznetcova et al., 2020). Nanoliposomes can alleviate this limitation due to their structural morphology, which can promote the encapsulation of both hydrophilic and lipophilic molecules. Other advantages of utilizing nanoliposomes in the food industry are their ability to improve the texture, flavors, and preservation of food products. Since phospholipids can be used as materials to develop these colloidal dispersions, nanoliposomes can be applied as nanocarrier systems for the protection and delivery of both hydrophilic and hydrophobic bioactive agents due to the amphiphilicity of

phospholipids (i.e., polar, and nonpolar regions) (Reza Mozafari et al., 2008). Thus, nanoliposomes are an attractive nano-structure due to their ability to enhance the functional properties of drugs, nutraceuticals, and other bioactive compounds to promote human health.

1.2.4. Nanofibers

Electrospinning is a simple and cost-effective technique to produce nanofibers (Kumar et al., 2019). The process of electrospinning nanofibers involves converting a polymer solution into a fiber mat using two electrodes that have high-voltage static electric fields between them. The polymer solution is then pulled through a nozzle syringe which then leads to the formation of a thin polymer jet (Aman Mohammadi et al., 2022). The jet is then traveled through the air, creating a matt of nanofibers on a collector plated as the solvent is evaporated. As shown in **Fig 1-2**, the fabrication of food packaging can be achieved by electrospinning smart and active nanofibers. These smart and active nanofibers can enhance the quality of food products by detecting changes in freshness or volatile gases, or even act as antimicrobial and antioxidizing agents and oxygen scavengers to extend the shelf-life of products.

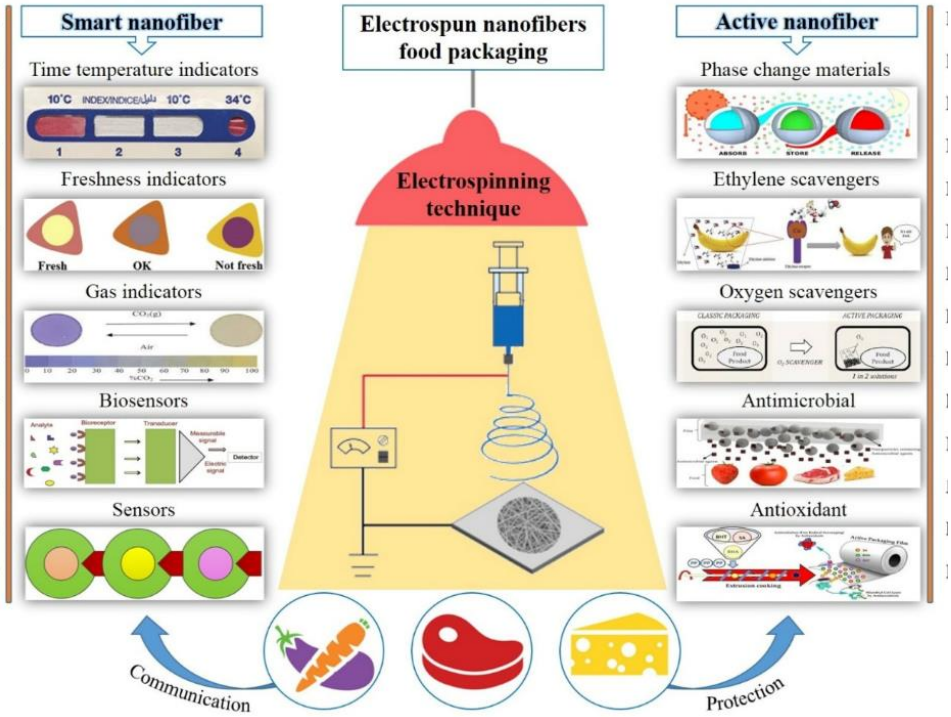

Fig. 1-2. Graphical depiction of the types and benefits of active and smart electrospun nanofibers in food packaging systems (Aman Mohammadi et al., 2022).

1.3.Protein nanoparticles

Proteins are an essential part of functional ingredients because of their advantages such as wide abundance, easy extraction, biocompatibility, biodegradability, excellent nutritional value, acceptance in the food industry, good surface activity, and excellent emulsion stabilizers (Zhang et al., 2021). Proteins are excellent candidates to develop nanoparticles because of some of their unique functional attributes, however it is important to understand some of the factors affecting their nanoparticle preparation.

(1) Protein composition has an influence on the preparation of nanoparticles since proteins are composed of various molecular weight fractions which can influence the nanoparticle characteristics (Pathak & Thassu, 2009). Thus, it is important to purify proteins before the

nanoparticle synthesis with methods such as salting out, dialysis, gel-filtration chromatography, ion-exchange chromatography, or affinity chromatography. (2) Protein solubility is another concern that can influence the preparation method and characteristics of nanoparticles. The isoelectric point (pI) of proteins influences their water solubility and is pH dependent. Hydrophobic interactions of proteins are reduced away from their pI, resulting in less aggregation. However, when the pH approaches the protein's pI, their solubility decreases due to greater hydrophobic interactions, leading to increased aggregation. (3) The surface properties of proteins have a significant influence on their nanoparticle formation due to the surface functional groups of the proteins (amine, carboxyl, and thiol groups) that may be exposed to conformational changes of the protein macromolecules when exposed to various conditions (pH, salt, heat, or enzymatic changes in the GIT) (Tarhini et al., 2017). These functional groups give the protein nanoparticles unique functionalities where hydrophobic bioactive compounds and various drugs can be encapsulated via electrostatic interactions and can interact directly with biological membranes.

The diverse functional properties of proteins have allowed their applications as nanocarriers to encapsulate both hydrophilic and hydrophobic bioactive compounds. Protein-based nanoparticles have been developed from a variety of sources, which include animal sources (casein, whey protein, and gelatin) (Giroux & Britten, 2011; Peñalva et al., 2018; Shutava et al., 2009) or plant sources (such as zein, hordein, gliadin, and soy) as nanocarriers (Duclairoir et al., 2002; He et al., 2020; Peñalva et al., 2015; Teng et al., 2012). Nanoparticles developed from cereal grain proteins (derived from wheat, barley, corn, and sorghum) often have limited applications in many food products due to their low solubility, and structural enzymatic changes

due to environmental stress (pH, salt, and heat). Thus, chemical, physical, or enzymatic modification of protein nanoparticles are necessary to enhance their stability and functionalities.

1.4. Protein-polysaccharide nanoparticles

Proteins and polysaccharides have been used to develop nanoparticles through various types of biopolymer-biopolymer associative interactions (Jones et al., 2010). Polysaccharides are another group of important biological material abundant in large quantities in various plants and animals, usually hydrophilic, and consist of glycosidic bonds linked by various monosaccharides (Xue & Luo, 2023). Proteins and polysaccharides can interact covalently and non-covalently. The covalent interactions consist of a Maillard-type reaction leading to protein-polysaccharide conjugates with increased stability against heat. Non-covalent interactions are driven by electrostatic, hydrophobic, hydrogen bonding, and Van der Waals interactions, which can influence their properties and functionalities in various food systems (Gentile, 2020). A variety of polysaccharides have been used in the development of protein-polysaccharide nanoparticles such as: chitosan (De Queiroz et al., 2018), pectin (Wang et al., 2020), alginate (Zou et al., 2016), cellulose (Song et al., 2009), Arabic gum (Wu et al., 2018), and many others.

Polysaccharides are promising materials to be incorporated into protein nanoparticles due to their wide abundance, non-toxicity, biodegradability, and biocompatibility. Protein-polysaccharide nanoparticles can be synthesized using both top-down and bottom-up approaches, however only the bottom-up approaches will be mentioned since the top-down method was not utilized in this project. The bottom-up approach allows the construction of protein-polysaccharide nanoparticles due to changes in environmental conditions, such as pH, ionic, strength, temperature or concentration and typically allow the production of very fine particles (Joye & McClements, 2014). When designing protein-polysaccharide nanoparticles for food

applications, it is important to consider the molecular and physiochemical properties such as molecular weight, charge, branching, flexibility, polarity, and solubility when selecting which polysaccharide to use.

Non-toxic and GRAS of food polymer nanoparticles

Food polymers have gained lots of attention in the fabrication of nanoparticles as compared to synthetic materials due to their generally recognized as safe (GRAS) status. Although food nanoparticles have a wide range of applications in the food industry, their applications are still in their infancy due to consumer preferences (Calzolai et al., 2012). Food nanoparticles offer a promising method for the delivery of bioactive compounds as functional ingredients in food products. However, for fortified foods containing nanomaterials, it is important to consider their uptake in the gastrointestinal system due to changes in environmental conditions (temperature, pH, ionic strength, enzyme, activity, and mechanical forces) that could dramatically alter their structure and physiochemical properties (Yada et al., 2014). Compared to inorganic materials such as silver (Ag), silicon dioxide (SiO_2), and zinc oxide (ZnO), organic nanoparticles such as lipid, proteins, and carbohydrates were observed to be more quickly metabolized in the human body (de Oliveira Mallia et al., 2022). In addition, their biodegradability, biocompatibility, and environmental stability are all key features that make their applications in the food industry promising.

1.5. *Hordein overview*

Hordein is the major storage protein in the endosperm of the barley and constitutes up to 30-50% of the total protein content and belongs to the prolamin family of cereal grains due to its high content of glutamine (Glu) and proline (Pro) in their amino acid sequence. Hordein is

separated into four different subunits and each fraction is differentiated based on their amino acid composition, molecular weight, and extractability characteristics (Jaeger et al., 2021). B-hordein is sulfur-rich (S-rich) and considered the most prominent subunit located at the hor-2 locus and comprises 70-80% of the total barley prolamin (Anderson, 2013). The other subunits include S-poor C-hordein, constituting 10-20% and A- and D-hordein making up less than 5%. The molecular weight of B-hordein is around 30,000-50,000 DA but can be further distinguished into subunits B1, B2, and B3 based on their electrophoretic capabilities.

1.5.1. Hordein structure

The most extensively studied storage protein structures for barley are B- and C-hordein that account for ~95% of the alcohol-soluble fraction. Though both subunits differ in which B-hordeins are S-rich in contrast to the S-poor C-hordeins, nucleotide sequencing of the cDNA clones, and direct sequencing of C-hordein peptides confirms evidence from hybridization studies revealing homologies between the mRNAs of both subunits (Forde et al., 1985). Hor-1 and Hor-2 are two complex loci found on chromosome 5 in barley and encodes the C- and B-hordein polypeptides, respectively (Brandt et al., 1985). Although both loci are linked, they are not identical due to differences in molecular weight, charge at low pH, isoelectric point, and amino acid composition.

1.5.2. Hordein amino acid composition

The amino acid composition of the four barley fractions is depicted in **Table 1-1** (Linko et al., 1989). Hordein and glutelin are rich in Pro and Glu amino acids and non-polar amino acids such as leucine (Leu), isoleucine (Ile), valine (Val), and phenylalanine (Phe). However, albumin

and globulin, which are considered the water-soluble and salt-soluble fractions, respectively, contain rich amounts of asparagine (Asp) and lower amounts of Glu and Pro.

Amino Acid	**Albumin**	**Globulin**	**Hordein**	**Glutelin**
Ala	9.3	7.9	2.6	10.0
Asp	10.6	10.5	1.8	11.5
Cys	6.5	5.6	2.4	*
Glu	19.2	14.5	35.0	21.0
Gly	10.8	12.7	3.1	12.5
Ile	3.8	3.0	5.3	6.0
Leu	6.8	8.4	7.8	10.9
Lys	3.4	7.8	0.6	0.8
Met	2.5	1.6	1.2	1.9
Phe	3.6	4.4	6.8	5.3
Pro	6.1	7.3	20.1	2.1
Ser	6.7	7.9	5.8	9.7
Tyr	4.4	3.0	3.3	1.1
Val + Thr	6.4	5.5	4.3	7.2

Table 1-1. Amino acid composition of barley grain fractions (mol%) (Linko et al., 1989)

Like other cereal grains, barley is not considered a source of complete protein due to the low contents of lysine (Lys), methionine (Met), and Val amino acids (Åssveen, 2009). However, the amino acid composition of barley grains has been shown to differ among various cultivars (Åssveen, 2009), use of nitrogen fertilizers (Bulman et al., 1994; de Ruiter & Karl, 2001), and seasonal differences during harvest (Weibull, 1987).

1.5.3. Hordein functionalities

Foaming

One functionality of hordein is its ability to develop foams which is a principal component in the making of beer products. Two ideal mechanisms have been proposed for the foaming nature of hordein in beer (Kapp & Bamforth, 2002). The first involves two specific albumin proteins including protein Z and lipid transfer protein 1 (LTP1) which display high stability to heating and proteolysis (Perrocheau et al., 2005). Another proposed mechanism is that various polypeptides have contributed to the foam stabilization in beer, which share a common characteristic of amphipathicity with higher hydrophobicity leading to more foam-active properties. Kapp et al. (2002) investigated the foaming characteristics of albumin and hordein controlling denaturation and proteolysis treatments resembling the events of malting and brewing (Kapp & Bamforth, 2002). As depicted in **Fig 1-3**, fluorescence intensity using 1-anilino-8-naphtalenesulphonic acid (ANS) indicated a positive correlation between hydrophobicity and foam stability. Denaturation was carried out by altering the pH of the protein solutions (pH 1.0-4.5) and heat treatment (95 °C for 10 mins). Interestingly, denaturation led to

an increase in hydrophobicity which positively correlated to increased foaming stability. Albumin displayed a high capacity to develop foams under denaturation as compared to hordein. However, when subjected to proteolysis, hordein's foam-stabilizing capabilities were increased compared to albumin. This was attributed to albumin's resistance to digestion by cysteine proteinases which hydrolyze the hordein fraction.

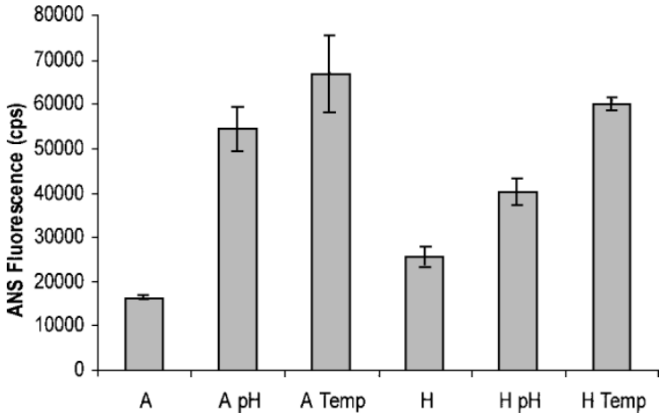

Figure 1-3. Hydrophobicity of partially denatured barley proteins at 75 µg ml^{-1}: albumin (A); albumin natured by acid (A pH); albumin denatured by heat (A Temp); hordein (H); hordein denatured by acid (H pH); hordein denatured by heat (H Temp) (Kapp & Bamforth, 2002).

Film-forming capacity

Edible films are used as selective barriers to extend the shelf life of food products and prevent contact from the surrounding environment and reducing exposure to spoilage (microorganisms, oxygen, water vapor, and off-flavors) (Otoni et al., 2017). Previous food packaging materials were developed from petroleum-based polymers and plastics however their non-biodegradability and renewability increases pollution and reduces sustainability for the environment (Mohamed et al., 2020). Recent trends have shifted to developing edible films from protein, polysaccharide, and lipid-based polymers because of their biodegradability and non-

toxic properties (Coupland et al., 2000; Kocira et al., 2021; Rhim, 2004). The film forming capacity of hordein is attributed to the abundance of non-polar amino acid, proline. Yong Cho et al. (2009) wanted to determine the functional and film-forming capacity of the different barley protein fractions (albumin, globulin, glutelin, and hordein) (Cho & Rhee, 2009). Hordein and glutelin displayed the lowest water absorption capacity (WAC) with 145.7 mL water/100 g solid and 156.7 mL water/100 g solid, respectively, compared to albumin, which had a WAC of 183.0 mL/water/100 g solid. However, the difference in WAC between the barley fractions was attributed to their contrasting solubilities. Hordein also obtained the highest oil absorption capacity (136 mL oil/g solid) which was due to the strong hydrophobicity of the non-polar side chain interacting with the hydrocarbon chain of the oil. The water vapor permeability (WVP) of the films were lowest among the films synthesized with hordein and showed a WVP value of 1.91 ng·m/m2·Pa·sec. The film forming capacity of hordein displayed high water barrier properties but produced a mechanically weak edible film because of the processing conditions influencing its structure.

Electrospinning ability

One of the ideal interests in electrospinning of micron/submicron- and nano-scaled fibers is their large surface area to volume ratio and pore-interconnectivity. The electrospinning process is influenced by various factors such as viscosity, conductivity, and surface tension of the solution as well as processing parameters (applied voltage, distance from needle tip to the collector, etc.) (Celebioglu et al., 2018). Electrospinning utilizing food polymers offers a promising approach to developing nanofiber materials that are biodegradable, cost-efficient, and sustainable to the environment. Prolamins have gained attraction as materials for developing electrospun fibers due to their hydrophobicity which makes them ideal candidates as

hydrophobic grease-proof coatings in the areas of food, medicine, textile, and paper (Li et al., 2010; Shukla & Cheryan, 2001). The hydrophobic nature of hordein favors its use as compared to hydrophilic electrospun fabrics, that often lose their overall shape or rapidly disperse in water and resist non-specific protein adsorption and prevent cell attachment (Wang et al., 2015).

Encapsulation

With more consumer awareness towards the promotion of healthier lifestyles, functional foods fortified with bioactive components are gaining increased attention worldwide (Islam et al., 2023). However, the fortification of foods with bioactive components are often limited due to their unpleasant taste, odor, flavor, poor stability, and bioavailability which have drastic effects on the nutritional value and quality of food products. Thus, encapsulation techniques have been designed to overcome these limitations. As shown in **Fig 1-4**, the benefit of encapsulation involves the controlled release of bioactive compounds at target sites, increased stability, environmental protection, and enhancing bioavailability. Hordein's unique amino acid sequence contains a large proportion of non-polar amino acids allows it to possess unique function properties, including greater adhesion, extensibility, and gelation, which are all essential characteristics needed as carriers for controlling the release of hydrophobic and hydrophilic compounds (He et al., 2020).

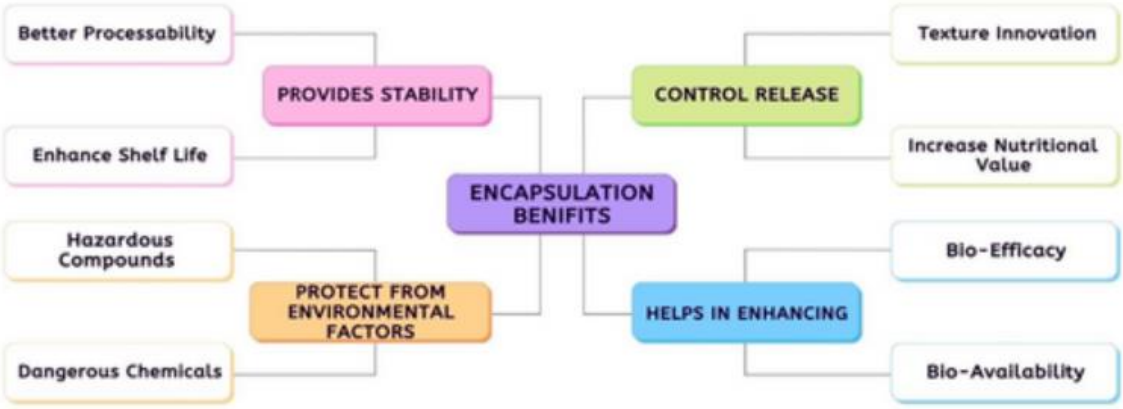

Fig 1-4. Visual depiction of the benefits of encapsulation (Islam et al., 2023)

1.5.4. Hordein applications

The unique properties of hordein have gained attention from researchers to developed hordein nanoparticles for many widely used applications such as emulsifying agents, and nanocarriers for bioactive compounds. Boostani et. al (2020) studied the physical stability and rheological properties of Pickering emulsions stabilized by hordein nanoparticles (Boostani et al., 2020). The physical stability using static multiple light scattering (MLS) revealed three destabilization profiles of foam-like, emulsion-foam, and gel-like structures using hordein as an emulsion stabilizer. Their study showed the potential of hordein to be applied as food foams in a variety of food products such as meringues, whipped cream, cakes, and mousses. As mentioned previously, the amino acid profile of hordein allows its potential as a nanocarrier for both hydrophobic and hydrophilic bioactive compounds. One study used barley protein nanoparticles to improve the absorption of β-carotene using *in vitro* Caco-2 cell and *ex-vivo* small intestine models. Low cytotoxicity was observed in their Caco-2 cell monolayer model and greater uptake was observed for encapsulated β-carotene in barley nanoparticles (15%) compared to free β-carotene (2.6%) (Liu et al., 2019).

1.6. Pectin overview

Pectin is a water-soluble anionic polysaccharide found in the cell wall of plants and in the middle lamella of higher plants. It has gained attention in the food, pharmaceutical, and biomedical industry with the global pectin market, estimated at $1 billion in 2019 and expected to reach $1.5 billion in 2025 (Freitas et al., 2021). Pectin is one of the most widely used plant polysaccharides in the food industry due to their versatile gelling properties which can be used in the making of jellies, jams, marmalades, fruit beverages, and confectionary products (Gawkowska et al., 2018). Its versatility allows its application as a functional ingredient in the health and medical field due to its high soluble fiber content which has shown beneficial health benefits to modulate the gut microbiota (Elshahed et al., 2021; Shtriker et al., 2018). The following sections will highlight the structure of pectin, its unique functionalities owing to its applications in various fields.

1.6.1. Pectin structure

The structure of pectin is composed of three main well-characterized polysaccharide motifs: homogalacturonan (HG), rhamnogalacturonan I (RG-I) and rhamnogalacturonan II (RG-II) (**Fig 1-5**). Among the three, HG is the most abundant (~ 65% of pectin) and represents the backbone chain of the pectin molecule, and contains α-1, 4-linked D-galacturonic acid (GalA) residues, which can be methyl-esterified at C-6 and/or acetylated on O-2 and O-3 (Chen et al., 2015). RG-I consists of repeating residues of GalA and α-1,2-L-rhamnose, in which rhamnose can be branched with neutral side chains at the C-4 position comprising of arabinose or galactose (Zhang et al., 2022). There is an assumption that HG and RG-I are covalently linked and cannot be separated with a chain-cleavage for example, enzymes such as endopolygalacturonase, or chromatographic fractionation methods (Gawkowska et al., 2018). The backbone of RG-II is

composed of 7-9 GalA residues branched with 4 side chains at the C-2 and C-3 position which consists of galactose, arabinose, apiose, fucose, rhamnose, aceric acid, glucuronic acid, galacturonic acid, 2-O-methyl-xylose, 2-O-methyl-fucose, 3-deoxy-lyxo-2-heptulosaric acid (DHA), and 3-deoxy-manno-2-octulosonic acid (KDO) (Gawkowska et al., 2018). Xylogalacturonic acid (XGA) is a small fraction in the backbone of pectin which contains xylose residues attached to O-3 of some GalA units (Schols et al., 1995). Modifications of these units in pectin's structure have a significant role in its functionalities and will be discussed in the next section.

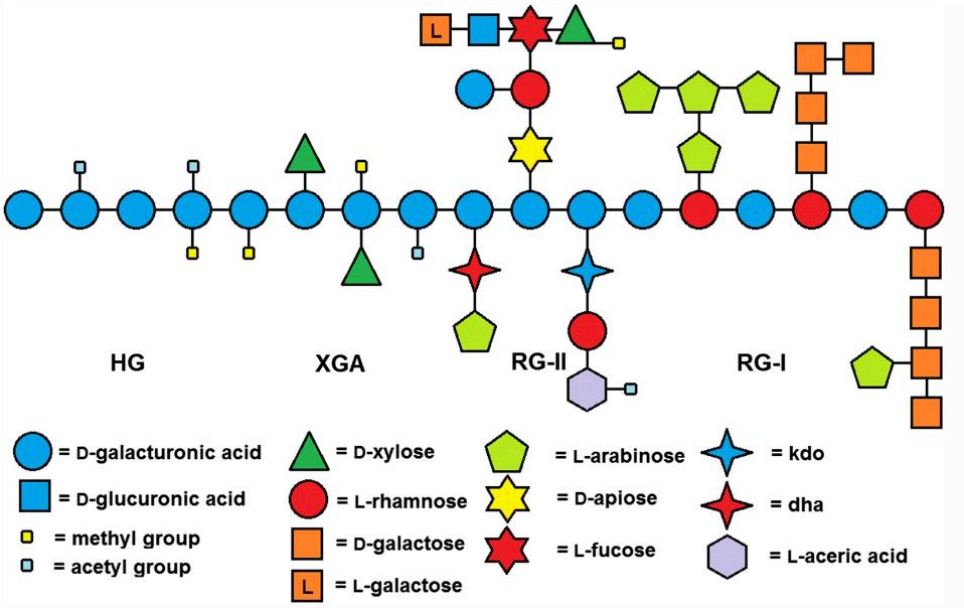

Fig 1-5. Structure of pectin polymers homogalacturonan (HG), xylogalacturonan (XGA), rhamnogalacturonan II (RG-II), and rhamnogalacturonan I (RG-I) (Kuivanen et al., 2015)).

1.6.2. Degree of esterification and amidation

The unique gelling capacity of pectin is correlated to its degree of esterification (DE) and the degree of amidation (DA), which is defined as the percentage of esterified or amidated carboxyl groups of GalA residues relative to the total number of GalA residues in the molecule

(cite). High methoxyl (HM) pectin is defined as have a DE > 50% while low methoxyl (LM) pectin has a DE < 50% (Chen et al., 2015). The DE/DA of pectin has been shown to affect their functional properties. For instance, HM pectin are often used in the food industry as gelling agents due to the higher proportion of hydrophobic methyl groups better equipped to form gels while LM are often used in lower-calorie food products since no sugars are required for gelation (Zhao et al., 2022). The gel formation of HM and LM pectin are different from one another thus it is important to discuss the following parameters that influence their gelling capacity.

HM pectin

HM pectin can form gels at pH < 3.5 and at high sugar concentrations (>55%). The gel formation at acidic media is a result in the dissolution of the carboxyl groups in the GalA residues which results in lower electrostatic repulsive forces (Van Buren, 1991). Combinations of hydrogen bonding and hydrophobic bonding also have an impact on HM pectin's ability to gel. One study by Oakenfull and Scott (1984) investigated the role of hydrophobic interactions on the gelling properties of HM pectin (Oakenfull & Scott, 1984). It was indicated that the gelling of HM pectin is stabilized by a combination of both hydrogen and hydrophobic bonds. The contribution of hydrophobic interactions to the free energy of developed junction jones was half that from hydrogen bonding but is required since hydrogen bonding is insufficient in stabilizing gelation alone. The pH of the aqueous media and DE also have an influence on the gelling properties of HM pectin. For instance, the gel strength of HM pectin gels increases with increasing DE, as well as the rate of gelation, however, as the DE is lowered, lower pH is required for gelation (BeMiller, 1986). This is attributed to the fact that as the DE is lowered, the pH required to product a given percentage of carboxyl groups in the carboxylic acid form increases due to an increase in the pKa, and the number of contiguous carboxylate groups must

be increased and converted to unionized carboxylic acid groups before chain association can occur (BeMiller, 1986). This results in a greater percentage of carboxylate groups that must be converted into free carboxylate groups to influence its gelling properties, as the DE of HM pectin is lowered.

LM Pectin

LM pectin can form gels in the presence of divalent cations (Ca^{2+}) at a pH range of pH 2-6 without the presence of sugars. The mechanism behind LM pectin's ability to gel is related to the "egg-box" model which also has been used to describe the binding of Ca^{2+} by alginates (Cao et al., 2020). Junction jones are developed by binding between Ca^{2+} and non-esterified GalA units via the oxygen atoms in the carboxyl groups of the pectin chain. The DE for LM pectin also influences the parameters necessary for its gelling capacity. For instance, lower DE pectin requires higher gelling temperatures and greater requirement for divalent cations (cross-linking) (BeMiller, 1986). Also, the distribution of the carboxyl groups affects the gelling properties where pectins with blocks of methyl ester and carboxyl groups (as opposed to random distribution) generally produce weaker gels and greater need for divalent cations (BeMiller, 1986). One of the sparking interesting in using LM pectin gels in the food industry is due to their low calorie and low sugar contents (Broomes & Badrie, 2010).

1.6.3. Pectin applications

Food

Pectin has been widely used in the food industry as gelling, thickening, stabilizing, and emulsifying agent. Hydrogels are mainly used as thickeners and stabilizers and must be derived from plant-based biopolymers such as polysaccharides and proteins for applications in the food industry (Ishwarya S & Nisha, 2022). The gelation capability of pectin was coined by Henry

Braconnot, a French chemist, to signify a colloidal substance that he found responsible for the gelation of heated mixture of fruits, water, and sugar upon cooling (Ishwarya S & Nisha, 2022). Due to the antioxidant ability of pectin, its application as a functional ingredient has also emerged due to its ability to chelate toxic metal ions which has been shown to be dependent on its structure. It is predicted that the hydroxyl groups on pectin can show good antioxidant activity when the viscosity is not too high (Wathoni et al., 2019). Pectin has shown higher DPPH radical scavenging activity compared to other polysaccharides (Ro et al., 2013). This is attributed to the high abundance of hydroxyl groups which can donate hydrogen or electrons to free radicals. Active films derived from pectin sources have been shown to provide antioxidant capacity while retaining physical properties by acting as a light barrier and preventing photooxidation (Eça et al., 2015). Recent interest has been in the development of food packaging materials derived from pectin due to its biodegradability, low-cost, and excellent mechanical properties which makes it an ideal candidate.

Biomedical

As a biocompatible and biodegradable natural polymer, pectin stands out as an ideal candidate for developing innovative strategies to improve health in the biomedical field. This stems from pectin's ability to easily form gels in acidic media, mucosal adhesion, easy dissolution in basic media, non-toxicity, and the possibility to easily modify its functional groups (i.e., -COOH, -OH) (Freitas et al., 2021). These properties are ideal for the administration of different drugs or compounds. For instance, the muco-adhesive properties of pectin can be utilized to target and control the administration of some compounds to the nasal or gastric environment because of its resistance to proteases and amylases (Martău et al., 2019). Pectin gels have also been considered as capsules for the delivery or weight reduction and obesity

medications (Jitpukdeebodintra & Jangwang, 2009). The ability of pectin gels to swell under acidic environments allows the gels to adhere to the stomach walls long before digestion, leading to prolonged non-appetite sensation.

1.7. Bioactive compounds

A consensus in a review by Bielsalski et. al (2009) described the term "bioactive compound" as "*Essential and non-essential compounds (e.g., vitamins or polyphenols) that occur in nature, are part of the food chain, and can be shown to have an effect on human health" (Biesalski et al., 2009).* Bioactive compounds are secondary metabolites abundant in plants and can be considered essential ingredients for the promotion of human health. Growing interest in bioactive compounds is correlated to their effectiveness as antioxidants, antimicrobials, anti-inflammatory agents, and mitigating the risks of cardiovascular disease, diabetes, and etc. (Campos, 2018). Bioactive compounds such as phytochemicals (phenolics, flavonoids, and carotenoids), vitamins (vitamin C, folate, and provitamin A), minerals (potassium, calcium, and magnesium), and fibers can be found in a wide variety of fruits and vegetables. The incorporation of bioactive compounds into food matrices as functional foods has gained attention to provide health benefits in which these bioactive compounds target specific sites in the human body to manage, prevent, and/or treat certain diseases. Both lutein and carvacrol are bioactive compounds with a range of health benefits and applications and will be discussed in the next few sections.

1.7.1. Lutein

Lutein is a carotenoid compound mainly present in Marigold flowers, egg products, leafy greens, and vegetables such as corn and potatoes (Abdel-Aal et al., 2013). Lutein can be classified as a xanthophyll, which is a member of the carotenoid family. However, in contrast to

carotenes, xanthophylls contain additional hydroxyl groups. Lutein is reported to have anti-inflammatory properties, with particular interest in its beneficial effects on eye health (Adib A et al., 2009; Johnson, 2014; Koushan et al., 2013). Other research has also observed beneficial effects of lutein on cognitive functions, cardiovascular disease (CVD), reduced cancer risk, and other systemic and metabolic effects. Lutein is considered safe, with no study reporting its toxicity, either in acute or chronic lutein supplementation (EFSA, 2012; Nidhi & Baskaran, 2013). Since humans are unable to synthesize carotenoids, diet related interventions or nutritional interventions are required for lutein absorption. Although there are many foods that contain lutein, it has low water solubility which reduces its bioaccessibility in the gastrointestinal tract (Steiner et al., 2018). Lutein is also susceptible to degradation when exposed to environmental stress (such as pH, heat, and light) which could limit its application as a functional food ingredient. However, encapsulation systems incorporating lutein have shown positive effects in overcoming some of these limitations (H. Li et al., 2020; S. Li et al., 2018; C. Zhao et al., 2018).

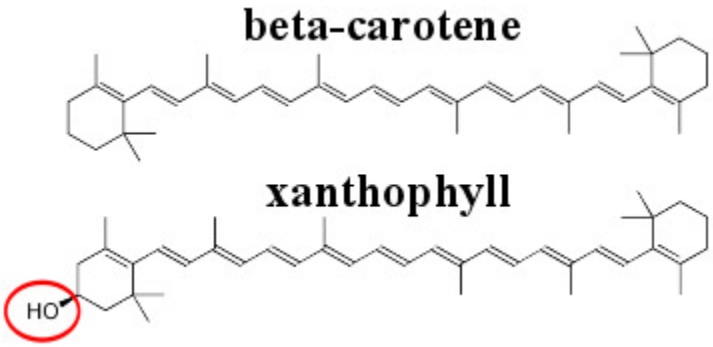

Fig 1-6. Chemical structure of beta-carotene and xanthophyll (Zarekarizi et al., 2019)

1.7.2. Carvacrol

Carvacrol (**Fig. 1-7**) is a phenolic monoterpenoid, present in the essential oil of oregano (*Origanum vulgare*), thyme (*Thymus vulgaris*), powerwort (*Lepidium flavum*), wild bergamot (*Citrus aurantium* var. *bergamia* Loisel), and other plants (Sharifi-Rad et al., 2018). Studies have indicated the various benefits of carvacrol such as its antimicrobial (Nostro & Papalia, 2012), antitumor (Khan et al., 2018), anti-inflammatory (Ezz-Eldin et al., 2020), anti-cancer (Ahmad et al., 2021), and other beneficial properties. Carvacrol has been approved by the Federal Drug Administration (FDA) for its uses in food to control the growth of microorganisms, as feed supplementation, and a natural preservative (Suntres et al., 2015). There is limited information on the toxicology of carvacrol. Suntres et al. (2015) reviews information on carvacrol that reports that the mean lethal dose of carvacrol in rats is 810 mg/kg of body weight when administered orally (Suntres et al., 2015). The estimated lethal dose when administered intravenously or intraperitoneally in mice was around 80 and 73.3 mg/kg body weight, respectively. Nonspecific effects such as depression, were seen at a dose of 50 mg/kg, while slight ataxia at higher doses (110-233.3 mg/kg carvacrol) in mice were seen. The LD_{50} in rabbits (dermal application) was estimated at 2700 mg/kg while the LD_{50} following subcutaneous administration in mice was around 680 mg/kg (Suntres et al., 2015). The lethal dose of carvacrol administered intravenously in dogs was 0.31 mg/kg (Suntres et al., 2015). Nanoencapsulation systems offer a promising way of mitigating some of the toxicological effects of essential oil bioactive compounds. One proposed mechanism is that nanoencapsulation systems can lower the concentration of the essential oil bioactive compound by slowing its release rate from the nanoencapsulation matrix. However, there are still challenges concerning carvacrol's application in the food industry. For instance, its low water-solubility, high volatility, strong odor, low bioavailability, and susceptibility to environmental conditions (heat and acidic pH) limits its use. However, colloidal

delivery systems can provide an advantage since carvacrol can be engineered through a variety of preparation methods which can improve its properties and expand its applications (Wang & Wu, 2021).

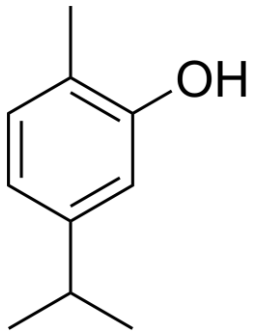

Fig 1-7. Chemical structure of carvacrol (Wikepedia, 2007)

1.8. Hypothesis and objectives

1.8.1. Summary of rationale for this research

The overall rationale for this research is to contribute to the scientific community in developing novel structures in promoting human health. The advantages of utilizing food biopolymers compared to synthetic materials for the fabrication of nanomaterials are due to their non-toxicity, biodegradability, biocompatibility, and can be easily manipulated as compared to inorganic materials. Nanoencapsulation of bioactive compounds has gained interest in the food, pharmaceutical, and medicinal fields and can overcome some of the limitations of bioactive compounds as functional ingredients. Proteins are excellent nanocarriers for bioactive compounds due to their unique amino acid structures and their hydrophobic nature allows the incorporation of hydrophobic bioactive compounds into their matrix. However, the chemical instability of protein nanoparticles stems from their instability to aggregate against environmental degradation (such as pH, temperature, salt) limits their applications in delivery of

the bioactive compounds to targeted sites in the human body. Polysaccharides have the potential to protect the bioactive compounds encapsulated into protein nanoparticles in the gastrointestinal tract (GIT) and are expected to control their releases during digestion. Protein-polysaccharide nanoparticles have been widely studied in the encapsulation of bioactive compounds, however the development of nanoparticles utilizing hordein and pectin has not been investigated.

1.8.2. Hypothesis

Hypothesis 1: Pectin will act as a protective coating for hordein nanoparticles against environmental stresses such as pH, temperature, and ionic concentration.

Hypothesis 2: Incorporation of pectin onto the surface of lutein encapsulated into hordein nanoparticle will have a protective effect against environmental stress (pH, salt, and heat) and improve the dispersibility of lutein in an aqueous solution and enhance the bioaccessibility of lutein under *in vitro* digestion.

Hypothesis 3: The addition of pectin coating onto hordein nanoparticles encapsulated with carvacrol essential oil will improve the dispersibility of carvacrol in an aqueous solution while still retaining its antimicrobial activity.

1.9.3. Objectives

The overall objective of this research project is to develop a hordein-pectin nanoparticle complex for the encapsulation of lutein and carvacrol to enhance their functionalities such as solubility and bioavailability. Special focus will be on the effect of a polysaccharide coating on the stability of the core-shell formation developed from hordein and the bioactive compound of interest.

Chapter 2: Fabrication and characterization of hordein-pectin nanoparticle complex

2.1. Abstract

A biopolymer nanoparticle complex was synthesized using anionic pectin to coat the surface of cationic hordein. The particles were prepared by an anti-solvent precipitation method (pH 4). The resulting nanoparticles were spherical with a smooth surface, and relatively small diameter (246 nm). Fourier transform infrared spectroscopy (FTIR) indicated that hordein interacted with pectin mainly through newly formed hydrogen bonds and electrostatic deposition as indicated by the surface charge (-16 mV). The application of pectin coating onto the surface of hordein nanoparticles (HNP) illustrated a protective effect with no significant changes in particle size at various pH values (pH 3.0-9.0) especially close to the isoelectric point (pI) of hordein (pH 5.0-6.0). Reduction in stability was observed against salt concentration (0-100 μM) likely caused by salt screening effects reducing the electrostatic repulsion between molecules. Longer duration of heat treatment (80 °C for 120 mins) resulted in the formation of larger particles however hordein-pectin nanoparticle complex (HP-NPC) was able to maintain its particle size distribution from 0-90 mins (80 °C). When re-dispersed into an aqueous medium post-lyophilization, both HNP and HP-NPC significantly increased in particle size but the particle size of HNP was drastically larger ($p < 0.05$) compared to HP-NPC. No changes in surface charge were observed for HP-NPC which indicates the lyoprotective effect of pectin as a coating material. This study highlights some of the importance of applying coating materials onto the surface of protein nanoparticles. Future work will highlight the encapsulation potential of HP-NPC to enhance the bioavailability of bioactive compounds.

2.2. Introduction

Food nanotechnology focuses on the characterization, fabrication, and manipulation of food-grade materials in the nanoscale (1-1000 nm) and can help improve their physical properties and enhance functionalities. The production of nanomaterials and fabrication of nanostructures can be achieved by two preferred approaches (i.e., top-down, and bottom-up). The top-down approach breaks or disassembles bulk solids into finer particles with the utilization of processing technology but can be time-consuming and costly due to the higher amounts of energy required. Thus, the bottom-up approach is preferred since it involves the coalescences of atoms and is more economical due to the lower use of synthetic materials during synthesis (Kumar et al., 2020). Important parameters such as pH, temperature, and ionic concentration play a critical role in controlling the properties of nanoparticles formed by the bottom-up approach (Moraru et al., 2003). However, the benefits of synthesizing colloidal nanoparticles from food-grade materials are due to their generally recognized as safe (GRAS) status, biodegradability, and environmental sustainability.

Barley is considered the fourth most cultivated cereal grains in the world, followed by wheat, rice, and corn (Bamdad et al., 2011). Hordein is the major storage protein in barley grains accounting for 40-45% of the crude protein content and consists of four main fractions depending on their solubility: A-, B-, C-, and D-hordein (Wang et al., 2010). Hordein is considered a prolamin due to its large proportion of proline and glutamine and contains an abundance of non-polar amino acids (~40%) such as proline, leucine, and valine (Zhao et al., 2010) but is not considered a complete protein due to the low amounts of essential amino acids present (He et al., 2020). Thus, due to the unique amino acid profile of hordein, it is generally soluble in 65-85% aqueous-ethanol solutions. This property of hordein makes it a suitable

material to encapsulate hydrophobic bioactive molecules (Liu et al., 2019), form films with low water permeability (S. Li et al., 2020), and an emulsion stabilizer (Boostani et al., 2020). However, prolamin proteins often have poor stability to aggregate when exposed to environmental conditions especially in food and pharmaceutical products, such as pH (approaching isoelectric point), salt concentration, and thermal processing. Thus, researchers have illustrated that the incorporation of a polysaccharide coating on the surface of protein nanoparticles can improve its stability and prevent aggregation under certain conditions (Li & de Vries, 2018). Li et al. (2021) prepared a Pickering emulsion stabilized by hordein-chitosan complex particles (Li et al., 2021). Although the addition of chitosan to hordein nanoparticles led to an increase in particle size, excellent wettability was achieved at a hordein to chitosan mass ratio of 2:1. It was also confirmed that hydrogen bonds and hydrophobic interactions were the main driving forces between hordein and chitosan interaction.

Pectin is a non-toxic and biodegradable natural anionic polysaccharide extracted from the cell walls of citrus fruits and consists of (1→4)-α-D-galacturonic acid (Gal A) residues. It is considered as a functional ingredient, gelling/thickening agent and stabilizer in the food industry due to its ability to form aqueous gels and has been utilized in jams and jellies, fruit preparation, fruit drink concentrates, fruit juices, desserts, and fermented dairy products (Chen et al., 2015). The gelling ability of pectin is correlated to the content of methylated carboxyl groups and is referred to as its degree of esterification (DE). DE is defined as the ratio of esterified GalA groups to total GalA groups and depending on the DE, pectin can be classed into two groups: high methoxyl (HM) (DE < 50) and low methoxyl (LM) pectin (DE > 50) (**Fig. 2-1**) (Chen et al., 2015). Hu et. al (2015) fabricated zein-pectin nanoparticles for the encapsulation of curcumin, in which the core-shell biopolymer nanoparticles were formed by electrostatic deposition (Hu et al.,

2015). The particles were spherical with relatively small size (~250 nm). However, the application of a pectin coating on hordein nanoparticles has not been investigated.

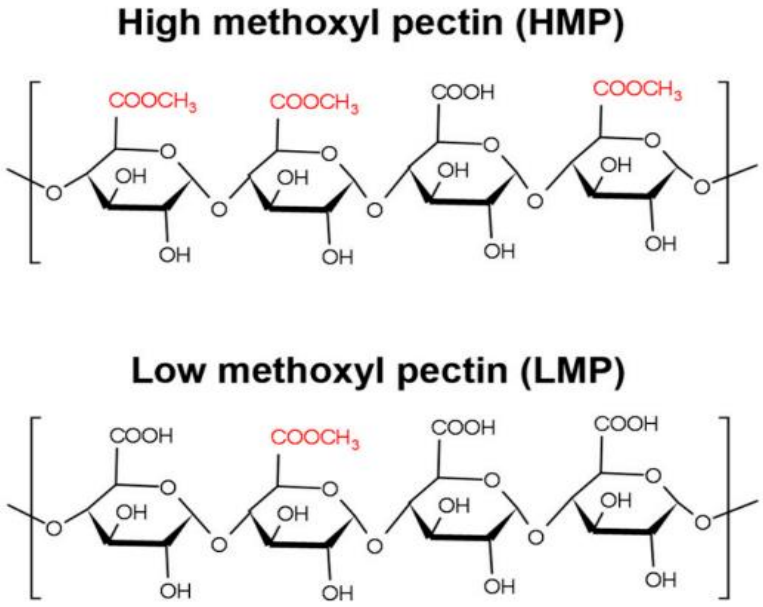

Fig. 2-1. Scheme of the chemical structure of pectin indicating differences in the degree of esterification (DE) (Steigerwald et al., 2021)

Therefore, the purpose of this study is to focus on the utilization of anionic pectin to coat cationic hordein nanoparticles using an anti-solvent precipitation method. The stability of hordein-pectin nanoparticle complex (HP-NPC) will be determined under various environmental conditions such as pH, salt concentration, and thermal treatment and compared to the stability of hordein nanoparticles (HNP) without a polysaccharide coating.

2.3. Material and methods

2.3.1. Materials

Dried hulled barley grains were purchased from Barry Farm (Wapakoneta, Ohio, USA). Pectin (DE=71%) was purchased from MP Biomedicals (Santa Ana, California, USA). Other

chemicals such as hexane, ASP/USP grade ethanol alcohol, hydrochloric acid, sodium hydroxide, and sodium chloride were purchased from VWR International (Ranchor, Pennsylvania, USA). Deionized (DI) water was made in the laboratory.

2.3.2. Extraction of hordein

The extraction and preparation of hordein nanoparticles was developed using the methods described by Boostani et al. (2019) with slight modifications (Boostani et al., 2019). Hulled barley grains were first grinded to a fine powder using a MagicBullet grinder for 30-60 seconds (Los Angeles, California, USA). Barley powder was then defatted at 23°C using hexane at a barley-to-hexane mixing ratio of 1:6 under continuous stirring (600 rpm) for 2 hours followed by centrifugation (Avanti® J-E Centrifuge, Beckman Coulter, USA) at 8500 g for 15 mins at 23°C. The defatted barley powder was then left to air dry overnight (~10 hours) to remove any excess hexane. The obtained barley flour was then dispersed (1:6) in 0.1 M NaCl to remove any salt-soluble fractions followed by dispersion into DI water to remove water-soluble fractions, followed by centrifugation (8500 g, 15 mins, 23°C). To isolate the hordein fraction, the treated residue was continuously stirred in a 75% ethanol solution at with a mixing speed of 600 rpm for 2 hours at 23°C followed by centrifugation (8500 g, 15 mins, 23°C). The supernatant that was obtained was evaporated using a rotary evaporator (Rotavapor R II, Buchi, Switzerland) followed by cold precipitation overnight (~12 hours) at 4°C to complete the isolation. The obtained diluted precipitates underwent dialysis under stirring against DI water (at 23°C for 48 hours) to remove any excess salts and lyophilized (HarvestRight, Salt Lake City, Utah, USA). Protein content was obtained by determining nitrogen content (Rapid N Exceed, Elementar, Ronkonkoma, New York, USA) with a protein factor 6.25. To determine which fractions of hordein were present, the molecular weight of the lyophilized powders was determined using

matrix-assisted laser desorption/ionization-time of flight (MALDI-TOF) (Bruker Autoflex Speed, Billerica, MA, USA).

2.3.3. Pectin stock

Pectin powder was dispersed in DI water at a concentration of 0.05% (w/v) and continuously stirred (650 rpm) at room temperature until fully dissolved followed by centrifugation (10,000 rpm, 10 mins, 23°C) to remove any insoluble aggregates.

2.3.4. Hordein nanoparticle synthesis

The synthesis of hordein nanoparticles (HNP) was carried out using an anti-solvent precipitation method similar to Hu et al. (2015) with slight modifications (Hu et al., 2015). 100 mg of hordein powder was dispersed in 10 mL 75% aqueous ethanol solution with continuous stirring at 800 rpm for 1 hour. The dispersion was then centrifuged (10,000 rpm, 23°C, 5 mins) to remove any insoluble components. The supernatant was then added to 4 parts DI water pre-adjusted to pH 4 using a controlled syringe pump (Model 200 Series, kd Scientific, Holliston, MA, USA) (0.8 mL/min) and continuously stirred (650 rpm) for 5 mins. Ethanol was removed using a rotary evaporator and then DI water (pH 4) was added to compensate for the ethanol removed to achieve a final volume of 50 mL. The dispersion was then centrifuged (10,000 rpm, 23°C, 5 mins) and stored at 3 °C for further analysis.

2.3.5. Preparation of hordein-pectin nanoparticle complex

The preparation of hordein-pectin nanoparticle complex (HP-NPC) was carried out with the same procedure for the HNP synthesis (**section 2.3.4**). However, 15 mL of the HNP dispersion was added to 15 mL of the pectin stock solution (0.05% w/v) pre-adjusted to pH 4 at a fixed ratio of 1:1 and continuously stirred at 900 rpm for 10 mins followed by centrifugation

(10,000 rpm) for 5 mins to remove the insoluble components. The freshly prepared HNP and HP-NPC dispersions were then lyophilized, and the dried powders were stored in sealed bags and stored at room temperature.

2.3.6. Particle size and ζ-potential

The particle size distribution and electrical characteristics (ζ-potential) of freshly synthesized colloidal dispersion was measured using a zetasizer equipped with dynamic light scattering (DLS) (Zetasizer Advanced Series, Malvern Panalytical, Westborough, MA, USA). Samples were diluted 50x with DI water (pH 4) prior to measurements to avoid multiple scattering effects.

2.3.7. Fourier transform infrared spectroscopy (FTIR)

FTIR spectra of hordein, pectin, HNP, and HP-NPC were performed using a Fourier transform spectrophotometer (Jasco FT/IR-4100, Easton, MD, USA). The spectrum range was from 550 to 4000 cm^{-1} with 32 scans with a 4.0 cm^{-1} resolution.

2.3.8. Scanning electron microscopy (SEM)

The surface morphology of hordein, pectin, HNP and HP-NPC was investigated using a scanning electron microscope (SU-70, Hitachi, Japan) at an accelerating voltage of 10 kV. Samples were coated with a gold layer using a compact coating unit (CCU-010, Safematic, Switzerland) to avoid charging under the electron beam.

2.3.9. Dispersibility characterization

The water-dispersibility of lyophilized HNP and HP-NPC was determined by dispersing 5 mg of the powdered nanoparticles in 25 mL DI water with constant stirring (600 rpm) for 2 hours. The particle size distribution was measured by DLS.

2.3.10. Effect of pH

Freshly prepared nanoparticle dispersions were added to DI water pre-adjusted to various pH values (pH 3.0, 5.0, 7.0, and 9.0) to determine the effect of pH on the particle size distribution and ζ-potential of the colloidal dispersions. If necessary, the pH of the samples was adjusted using either 0.1M of HCl or 0.1M NaOH. Samples were diluted 50x to avoid multiple scattering effects.

2.3.11. Effect of heat

Colloidal dispersions were prepared at pH 4.0 and heated at 80 °C using a heated water bath (Thermo Scientific, Waltham, MA, USA) for different times (0, 30, 60, 90, 120 mins) to determine the effect of heat treatment on the particle size of freshly prepared nanoparticle dispersions. At each time interval, samples were cooled to room temperature before analysis.

2.3.12. Effect of salt concentration

Different amounts of sodium chloride (0, 20, 40, 60, 80, 100 μM) were added to freshly prepared nanoparticle dispersions to determine the effect of salt concentration on the particle size of freshly synthesized nanoparticles.

2.3.13. Data analysis

The statistical analysis was performed using RStudio 2022.12.0 software (RStudio, Boston, MA, USA). Statistical differences were evaluated using one-way Analysis of Variance (ANOVA) between different groups using Tukey's post-hoc test with a statistical significance level of $p < 0.05$ for all comparisons. In certain conditions, Student's t-test assuming unequal variance was performed with a significance level of $p < 0.05$. All measured values were expressed as mean ± standard deviation of three independent replicate trials.

2.4. Results and discussion

2.4.1. Protein content and MALDI-TOF

The visual representation of freeze-dried extracted hordein powders is illustrated in **Fig 2-2**. The purity of the extracted hordein powder was around 87%, as determined by its nitrogen content and protein factor of 6.25. Hordein can be classified into 4 subunits based on their solubility and molecular weight. Matrix-assisted laser desorption/ionization-time of flight (MALDI-TOF) was used to better understand which fraction of hordein was extracted by determining its molecular weight. As depicted in **Fig 2-3**, a major intensity peak was observed at 38 kDA which indicates the strong presence of B-hordein. B-hordein (30-50 kDA) are considered sulfur-rich (S-rich) and accounts for 70-80% of the total protein content (Bamdad et al., 2011). Sharp peaks were also observed around 13 kDA which represents the low molecular weight A-hordeins (<15 kDA) that are a group of salt-soluble hydrophobic proteins rather than a storage protein (Wang et al., 2010).

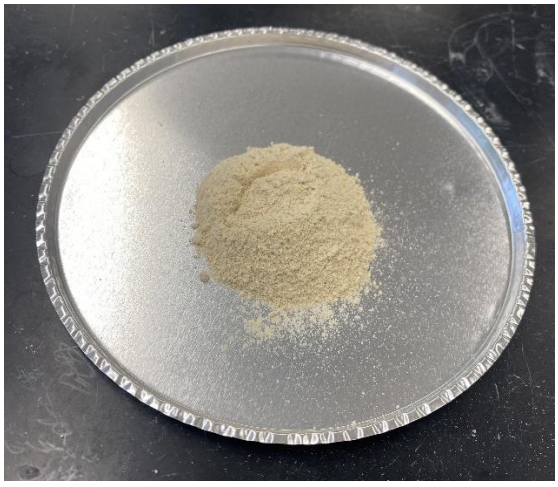

Fig. 2-2. Visual representation of freeze-dried extracted hordein powder.

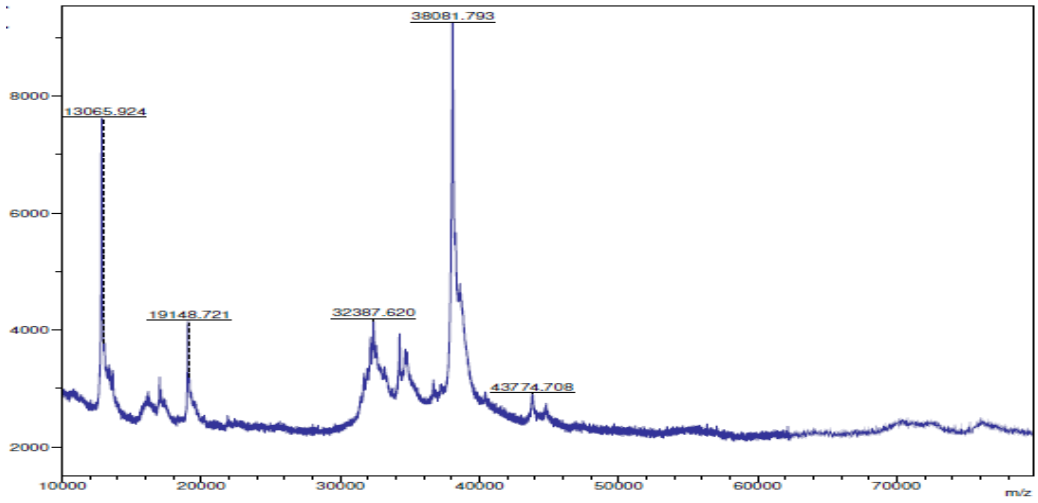

Fig. 2-3. The molecular weight (DA) of extracted hordein depicted by MALDI-TOF.

2.4.2. Particle size and ζ-potential

Visual representation of freshly prepared hordein nanoparticle (HNP) and hordein-pectin nanoparticle complex (HP-NPC) dispersions are shown in **Fig 2-4**, respectively. Both HNP and HP-NPC were synthesized using an anti-solvent precipitation method. The mean particle size, polydispersity index (PDI) and ζ-potential of freshly prepared HNP and HP-NPC can be shown in **Table 2-1**. The mean particle diameter of HP-NPC (246 ± 11 nm) was significantly larger ($p < 0.05$) compared to hordein nanoparticles (HNP) alone (180 ± 3 nm). However, the difference in particle size may be attributed to the electrostatic deposition method at pH 4. The carboxyl groups on pectin are reported to have a dissociation constant (pKa) around pH 3.5 (Opanasopit et al., 2008). Therefore, at pH values at and around pH 3.5, the electrostatic repulsive forces in pectin are decreased, which would increase the particle-particle interactions, resulting in the increase in particle size due to aggregation. The negative net charge (-16 ± 6 mV) indicates that HP-NPC was formed through electrostatic interactions because of the absorbance of anionic pectin molecules onto the surfaces of cationic hordein molecules. The isoelectric point (pI) of hordein has been reported around pH 5-6 (Yalçın & Çelik, 2007). Therefore, at pH 4.0, hordein

should carry a net positive charge and pectin should carry a net negative charge. The net negative charge of HP-NPC at pH 4.0 is similar to the results of Hu et al who developed zein-pectin nanoparticles for the encapsulation of curcumin (Hu et al., 2015). The absorption of pectin molecules to the hordein particle surface was attributed to electrostatic attraction between the two biopolymers at this pH.

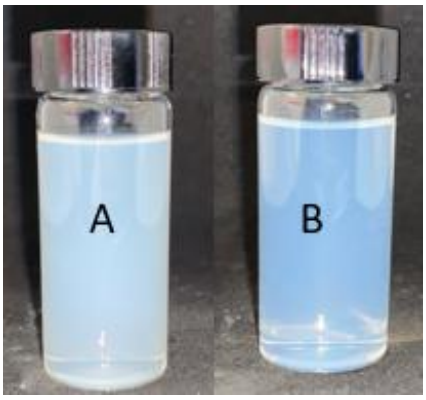

Fig. 2-4. Visual representation of A.) freshly prepared hordein nanoparticle (HNP) dispersion and B.) freshly prepared hordein-pectin nanoparticle complex (HP-NPC) dispersion

	Particle Size (nm)	**PDI**	**ζ-potential (mV)**
HNP	180 ± 3^{a}	0.32 ± 0.01	33 ± 4^{a}
HP-NPC	246 ± 11^{b}	0.26 ± 0.02	-16 ± 6^{b}

Table 2-1. Average particle size, PDI, and ζ-potential of hordein nanoparticles (HNP) and hordein-pectin nanoparticle complex (HP-NPC). Different superscripts in each column represents significance differences ($p < 0.05$) between the two samples. Values are represented as the mean ± standard deviation of three replicates.

2.4.3. FTIR

Fourier transform infrared spectroscopy (FTIR) measurements were applied to provide information about the intermolecular interaction between the two biopolymers. FTIR spectra of hordein, pectin, HNP, and HP-NPC are provided in **Fig 2-5A-D**. Pure hordein (**Fig 2-5A**) exhibited a broad characteristic peak at ~3280 cm^{-1} which shows existence of hydrogen bonds in the hordein molecule. There was also an appearance of two major characteristic peaks of pure hordein at 1640 and 1530 cm^{-1} which correspond to amide I (1700-1600 cm^{-1}) and amide II bands (1600-1500 cm^{-1}), respectively (Miller et al., 2013). In comparison to the hordein nanoparticle spectrum (**Fig 2-5C**), there was a shift from 3280 cm^{-1} for pure hordein to 3292 cm^{-1} for HNP in the -OH region, suggesting that new hydrogen bonds may have been formed because of the anti-solvent precipitation method in the fabrication of HNP. In the pectin spectrum (**Fig 2-5B**), there were vibrations ~3100-3620 cm^{-1} which correspond to strong vibrations of -OH stretching. Due to the higher degree of esterification (DE > 50%) of the pectin powder used in this study, a sharp peak was observed at 1745 cm^{-1} which corresponds to the carbonyl group stretching of the ester groups. Peaks observed at 1010 and 1059 cm^{-1} represent the C-O stretching in -COOH and O-H bending (Kamble et al., 2017; Sivam et al., 2012), respectively. Comparing the FTIR spectra of HNP (**Fig 2-5C**) and HP-NPC (**Fig 2-5D**), it could be observed that the absorption peak at 3292 cm^{-1} corresponding to the hydrogen bonds of H-NP shifted to 3279 cm^{-1} with the addition of the pectin coating for HP-NPC, which may indicate the presence of newly formed hydrogen bonds. The results of this study are similar to the FTIR spectrum of Song et al. (2022), in which the addition of chitosan into hordein nanoparticles caused a red shift in the spectrum due to newly formed hydrogen bonds between chitosan and hordein molecules (Song et al., 2022). Hydrophobic interactions may have also occurred between the C-O Studies

have indicated that polysaccharides can interact with the outer layer of proteins through electrostatic attraction, hydrogen bonding, or van der Waals forces (Abd Elgadir et al., 2015).

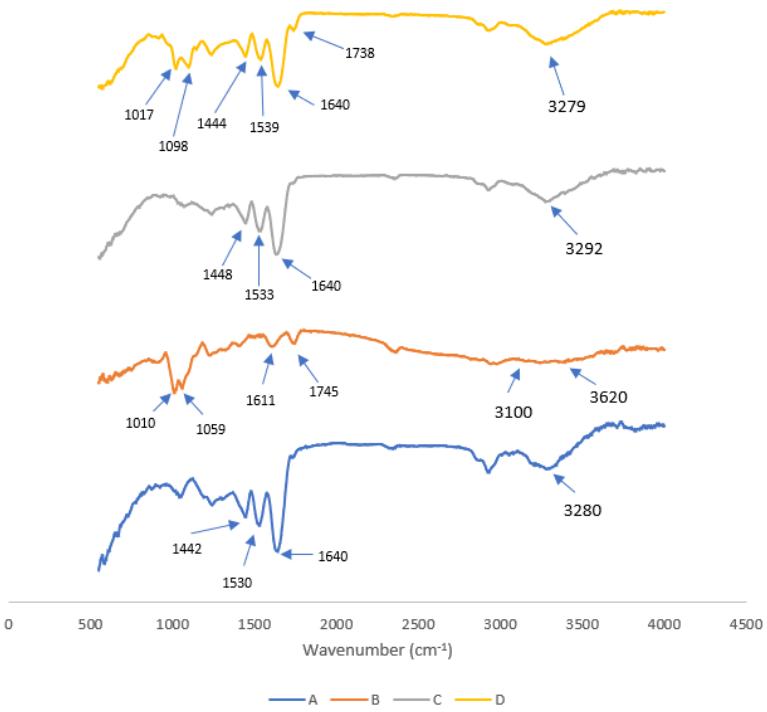

Fig. 2-5. FTIR spectra of A.) hordein; B.) pectin; C.) hordein nanoparticle (HNP); D.) hordein-pectin nanoparticle complex (HP-NPC)

2.4.4. SEM

Scanning electron microscopy (SEM) was used to investigate the surface morphology of pure hordein, pectin, HNP, and HP-NPC (**Fig 2-6A-D**). Morphology by SEM illustrated a globular particle arrangement and stacked flaky structure for pure hordein (**Fig 2-6A**) similar to the results of Rani et. al (2021), who characterized gliadin, secalin, and hordein fractions with various analytical techniques in their study (Rani et al., 2021). The SEM morphology of pure pectin **(Fig 2-6B**) revealed a spherical granular structure in its surface morphology. The surface

morphology of pectin displayed larger particle size compared to pure hordein, which may be a result of the high molecular weight of pectin in comparison to hordein. SEM morphology of HNP (**Fig 2-6C**) showed a smooth amorphous structure similar to Liu et. al (2017) who revealed smooth shaped spheres in their SEM morphology for zein nanoparticles. It was suggested in their study that the procedure for the zein nanoparticle formation may have altered the self-assembly of zein molecules, leading to a more smooth and spherical morphology compared to pure zein (Liu et al., 2017). SEM morphological image of HP-NPC is displayed in **Fig 2-6D**. The SEM morphology of HP-NPC confirmed its spherical nature and smooth surface with uniform particle distribution and corresponds to our reported polydispersity index (PDI) (~0.26). The results of this study are similar to Thankappan et. al (2020) who fabricated zein-pectin nanoparticles with SEM morphology confirming the smooth and spherical nature of their synthesized nanoparticles (Thankappan et al., 2020).

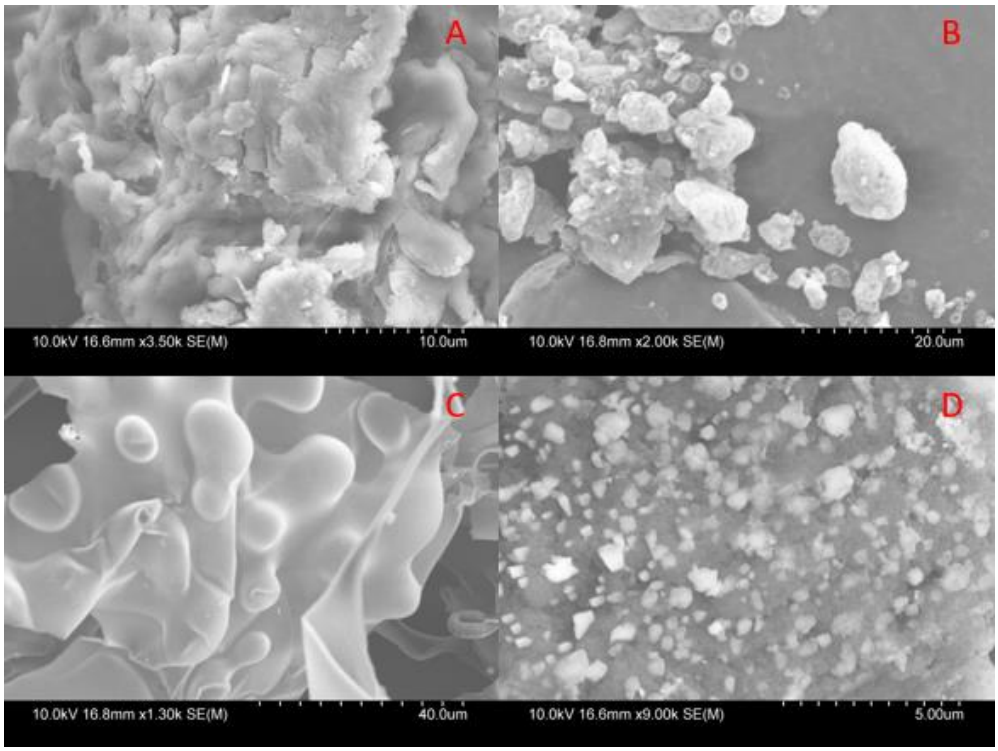

Fig. 2-6. SEM images of A.) hordein, B.) pectin, C.) hordein nanoparticles (HNP), and D.) hordein-pectin nanoparticle complex (HP-NPC)

2.4.5. Dispersibility of nanoparticles

The process of freeze-drying and rehydration are essential processing steps especially for the utilization of nanoparticles as powdered functional ingredients in foods and beverages (Hu et al., 2015). Thus, the effect of freeze-drying followed by rehydration on the particle size and ζ-potential of hordein nanoparticles and hordein-pectin nanoparticles was investigated. As shown in **Table 2-2**, there were significant differences ($p < 0.05$) in the particle size between HNP and HP-NPC post-lyophilization. However, significant increase ($p < 0.05$) was shown in both the particle size of HNP (440 ± 38 nm) and HP-NPC (295 ± 12 nm) post-lyophilization compared to their particle size prior to the freeze-drying step. The increase in the particle size of both HNP and HP-NPC is mainly attributed to particle aggregation which may occur due to a decrease in the particle's stability because of the freeze-drying procedure. There are several mechanisms as to how the freeze-drying process may negatively affect the stability of biopolymer nanoparticles: 1.) Changes during the freezing step can rapidly increase the concentration of all compounds in the remaining liquid fraction and facilitate particle-particle interactions as attractive forces, overcoming repulsive forces resulting in particle aggregation. 2.) Phase separation may also lead to liquid-liquid separation causing a destabilizing effect between the molecules in the nanoparticles. 3.) Sublimation may occur during the primary drying of the frozen liquid and residual adsorbed water becomes desorbed during the secondary drying step. Dehydration can lead to a disruption of the repulsive electrostatic forces (Trenkenschuh & Friess, 2021). For HNP, there was a significant decrease ($p < 0.05$) in the ζ-potential from 33 ± 4 mV to 15 ± 4 mV post-freeze drying. This may be attributed to the freeze-drying process influencing some conformational changes in the hordein structure. It is possible that the freeze-drying process led

to irreversible changes in the hordein molecule such as the unfolding of its protein chain, leading to the exposure of the charged hydrophobic residues which were buried in the native structure (Roy & Gupta, 2004). For HP-NPC, no significant differences ($p > 0.05$) were observed in the zeta potential (-17 ± 1 mV) after freeze-drying which indicates that pectin coating had a protective effect on the destabilization of the hordein molecules during the freeze-drying process. This result may be attributed to pectin forming new hydrogen bonds with the hordein molecules, preventing inter-droplet protein interactions (Mun et al., 2008).

	Particle size (nm)		ζ-potential (mV)	
	Before	After	Before	After
HNP	180 ± 3^{a}	440 ± 38^{b}	33 ± 4^{a}	15 ± 4^{b}
HP-NPC	246 ± 11^{a}	295 ± 12^{b}	-16 ± 6^{a}	-17 ± 1^{a}

Table 2-2. Average particle size (nm) and ζ-potential (mV) of hordein nanoparticles (HNP) and hordein-pectin nanoparticle complex (HP-NPC) before and after lyophilization. Different superscripts in each column represent statistical differences ($p < 0.05$) prior and post-lyophilization for each respective sample. Values are represented as mean ± standard deviation of three replicates.

2.4.6. Effect of pH

The stability of nanoparticles against aggregation was investigated from pH 3.0 to 9.0. Proteins are highly susceptible to pH changes and tend to aggregate around their isoelectric point (pI), where they carry a neutral net charge. Thus, the effect of an anionic pectin coating on the surface of the hordein nanoparticles to prevent aggregation at hordein's pI (~pH 5.0-6.0) was investigated. As expected, the particle size of HNP (977 ± 11 nm) was significantly larger compared to HP-NPC (267 ± 5 nm) at pH 5.0 **(Table 2-3)**. The decreased stability of HNP at pH

5.0 may be attributed to a low surface charge relative to the pI of the hordein molecule, limiting repulsive interactions between the nanoparticles within aqueous dispersions (Cheng & Jones, 2017). The ability of pectin coating on the surface of the hordein molecule is mainly attributed to the electrostatic and steric stabilization between the pectin and hordein molecules (Wagoner et al., 2016). The ζ-potential values for HNP and HP-NPC at pH 5.0 was around +1 and -36 mV, respectively. The stability of HP-NPC may likely be attributed to the adsorption of pectin molecules to the surface of hordein, reducing their positive charge, thereby decreasing the electrostatic repulsion between particles (Joye et al., 2015). The ζ-potential value (-5 ± 1 mV) at pH 3.0 of HP-NPC was expected due to the occurrence of partial protonation of the carboxyl groups around and below their pKa value (pH ~ 3.5) (Jones et al., 2010). No significant changes ($p > 0.05$) in particle size were observed from pH 3.0-9.0 for HP-NPC which indicates that pectin coating provided a protective coating around HNP due to strong electrostatic repulsion and possible lack of available cationic sites for bridging flocculation to occur.

	Particle size (nm)		**PDI**		**ζ-potential**	
	HNP	HP-NPC	HNP	HP-NPC	HNP	HP-NPC
pH 3	318 ± 11^{c}	246 ± 22^{a}	0.37 ± 0.01	0.30 ± 0.07	19 ± 2^{d}	-5 ± 1^{b}
pH 5	977 ± 11^{a}	267 ± 5^{a}	0.32 ± 0.01	0.30 ± 0.08	1 ± 2^{c}	-36 ± 2^{a}
pH 7	453 ± 16^{b}	243 ± 21^{a}	0.35 ± 0.04	0.31 ± 0.05	-21 ± 0^{b}	-38 ± 1^{a}
pH 9	177 ± 8^{d}	267 ± 75^{a}	0.27 ± 0.02	0.36 ± 0.09	-32 ± 3^{a}	-33 ± 5^{a}

Table 2-3. Effect of pH on the particle size (nm), polydispersity index, and ζ-potential of hordein nanoparticles (HNP) and hordein-pectin nanoparticle complex (HP-NPC). Different superscripts in each column represent statistical differences ($p < 0.05$) at different pH values for each respective sample. Values are represented as mean ± standard deviation of three replicates.

2.4.7. Effect of heat

Proteins have complex structures with numerous levels including primary, secondary, tertiary, and quaternary structures. Partial or total denaturation can occur during heating, in which partial or total unraveling of the protein changes through the hydrogen bonding and defines the higher-order native structure of the protein (Bischof & He, 2006). Heat denaturation of proteins is generally considered irreversible, and the term denaturation can refer to aggregation, coagulation, and gelation. Thermal treatment is an important processing step during food formulation, thus the effect of pectin coating on the stability of HNP subjected to thermal treatment (80 °C) for 0-120 mins was investigated (**Table 2-4**). The effect of pectin had a major impact on maintaining the particle size of HP-NPC against thermal treatment (80 °C) from 30-90 mins in which no significant differences ($p > 0.05$) in size were observed. However, there was a significant difference ($p < 0.05$) when the colloidal dispersions were heated at 120 mins compared to no heat treatment (0 mins). For hordein nanoparticles, significant increase ($p < 0.05$) in particle size was observed from 0 to 30 mins with significant decrease ($p < 0.05$) in size observed from 30 to 120 mins. The increase in the particle size from 0 to 30 mins may have been attributed to the changes in the primary structure and decreased alpha-helix content of the secondary structure (Pascoli et al., 2018). These results are comparable to the results of Selling et. al (2007), who investigated the effects of temperature (25-70 °C) on the secondary and tertiary structures of zein (Selling et al., 2007). The alterations of the structure of heat treated

zein were reversed when temperatures returned to 25 °C. In this study, the particle size of the freshly prepared heat-treated nanoparticle dispersions was measured after cooling to room temperature. It is possible that heat treatment for 30 mins on HNP may have led to partial denaturation of the protein structure, however the changes were reversible when exposed to ambient conditions. In the case of particle size for HNP, there were significant differences ($p < 0.05$) in particle size from 60 (165 ± 1 nm) and 90 minutes (154 ± 5 nm) of heat treatment when compared to no heat treatment (181 ± 3 nm). The decrease in particle size observed (60 and 90 mins) may be attributed to the breakdown of the disulfide bonds within the hordein molecules after thermal treatment resulting in a more compact structure (Song et al., 2021). In comparison, the particle size of HNP heated at 120 mins was significantly larger ($p < 0.05$) compared to 30-60 mins. Longer durations of heat treatment times can result in the formation of larger particles similar to the results of Sun et al. (2016) who found that extended heat-treated times for zein nanoparticles lead to the complete unfolding of zein molecules which formed protein aggregates (Sun et al., 2016). However, the changes in the structure of hordein after thermal treatment was not investigated in this study.

	0 mins	**30 mins**	**60 mins**	**90 mins**	**120 mins**
HNP	181 ± 3^{a}	270 ± 2^{b}	165 ± 1^{c}	154 ± 5^{d}	185 ± 6^{a}
HP-NPC	246 ± 11^{a}	259 ± 5^{ab}	260 ± 1^{ab}	266 ± 9^{ab}	276 ± 11^{b}

Table 2-4. Effect of thermal treatment (80 °C) for 0-120 mins on the particle size of hordein nanoparticles (HNP) and hordein-pectin nanoparticle complex (HP-NPC). Different superscripts in each row represents significant differences ($p < 0.05$) in particle size at different heating times

for each respective sample. Values are expressed as mean ± standard deviation of three replicates.

2.4.8. Effect of salt concentration

Biopolymer nanoparticles may be exposed to different ionic environments in various food systems and during digestion in the gastrointestinal tract. For this reason, the impact of salt concentration (0-100 μM) on the stability of HNP and HP-NPC was investigated. Proteins are susceptible to high salt environments because of the reduction of electrostatic interactions thus leading to the aggregation of the protein molecules (Chi et al., 2003). As expected, the particle size of HNP was significantly increased ($p < 0.05$) when exposed to higher concentrations from 0 to 100 μM (**Table 2-5**). In the case of HP-NPC, although the particle size was still relatively small when compared to HNP ($p < 0.05$), the particle size was significantly increased ($p < 0.05$) with the increase in salt concentration (20-100 μM). This increase in particle size may be attributed to a slight reduction in the repulsive forces between them. This is similar to the results of Liang et al. (2021), who fabricated tannic acid-fortified zein-pectin nanoparticles (Liang et al., 2021). The particle size of their synthesized nanoparticles increased from 166 to 280 nm when NaCl concentration was raised from 0 to 25 mM. Like their results, it is likely that the reduction in stability may have occurred because of two reasons: 1.) salt screening effects reduced the electrostatic repulsion between the molecules: 2.) salt screening effects reduced the electrostatic attraction between the pectin and hordein molecules, thereby causing some of the pectin to be desorbed (Liang et al., 2021).

	0 μM	**20 μM**	**40 μM**	**60 μM**	**80 μM**	**100 μM**

HNP	181 ± 3[a]	341 ± 8[b]	633 ± 17[c]	919 ± 78[d]	1005 ± 46[e]	1031 ± 5[e]
HP-NPC	246 ± 11[a]	286 ± 6[b]	293 ± 3[b]	300 ± 1[b]	313 ± 3[b]	341 ± 2[c]

Table 2-5. Effect of salt concentration (0-100 μM) on the particle size (nm) of hordein nanoparticles (HNP) and hordein-pectin nanoparticle complex (HP-NPC). Different superscripts in each row represents significant differences ($p < 0.05$) in particle size at salt concentrations for respective samples. Values are expressed as mean ± standard deviation of three replicates.

2.5. Conclusion

In this study, hordein-pectin nanoparticle complex was synthesized using an anti-solvent precipitation method and the effect of pectin onto the surface of hordein nanoparticles was determined. The resulting nanoparticle complex was smooth and spherical with relatively small particle size (~246 nm). Pectin coating was able to effectively stabilize HNP when exposed to different pH conditions (pH 3.0-9.0) and no significant change observed even at the isoelectric point (pH ~ 5.0-6.0). In addition, heat treatment (0-120 mins, 80°C) on freshly prepared HP-NPC dispersions had limited influence on the particle size and the particles remained relatively small when exposed to increasing salt concentration (0-120 μM). It was shown that hordein and pectin interacted with each other primarily through hydrogen bonding and electrostatic interactions. The biopolymer nanoparticle complex fabricated in this study indicates the significance of applying coating materials onto the surfaces of protein nanoparticles to enhance their stability and functionalities. Further research will be conducted on the encapsulation of hydrophobic bioactive compounds into the hordein-pectin nanoparticle complex. The next chapter will focus on the

effect of pectin coating to enhance the functionalities of the bioactive component such as solubility, loading capacity and encapsulation efficiency, release, bioaccessibility, stability, and absorption throughout the gastrointestinal tract.

Chapter 3: Encapsulation of lutein into hordein-pectin nanoparticle complex for improved functionalities

3.1. Abstract

Lutein has effectively been shown to be beneficial for eye health and inhibit the development of age-related macular degeneration (AMD), however its poor water-solubility and chemical instability limits its applications as a nutraceutical. In this work, a hordein/pectin nanoparticle complex was fabricated using an anti-solvent precipitation and electrostatic deposition method (pH 4) to encapsulate lutein. The freshly synthesized lutein-hordein/pectin nanoparticle complex (L-HP-NPC) displayed an irregular and smooth morphology with relatively small particle size (369 nm) and ζ-potential of around -22 mV. The dispersibility of L-HP-NPC post-lyophilization was determined since functional food ingredients may be subjected to freeze-drying and no significant change ($p < 0.05$) in particle size and ζ-potential was observed which indicates that pectin acting as a lyoprotectant during the process. *In vitro* digestion resulted in a higher bioavailability of lutein into the simulated intestinal fluid (SIF) when encapsulated into the hordein/pectin nanoparticle complex (~22.3%) when compared to lutein encapsulated into hordein nanoparticles (~9%). This was a result of pectin's gelling ability in acidic media (SGF) which acted as a protective coating against gastric enzymes that can degrade both hordein and lutein. This study highlights the benefits to utilizing pectin as a protective coating for the delivery and controlled release of bioactive compounds in the gastrointestinal tract and future studies can be implemented to understand it's incorporation into a real-life food matrix.

3.2. Introduction

Due to the increasing awareness of consumers focus on nutrition and health, there is much demand in the field of functional foods supplemented with bioactive compounds to promote health beneficial products. However, direct application of bioactive compounds into food products is often limited due to their low solubility, chemical instability, and may also diminish the quality of products such as negative effects on color, texture, flavor, and appearance (Mohammadian et al., 2020).

Xanthophylls are a class of carotenoids consisting of a hydrocarbon structure, however in contrast to carotenes, they also contain hydroxyl groups. Lutein (**Fig 3-1**) is a member of the xanthophyll class and is mainly found in Marigold flowers, egg products, leafy greens, and cereal grains such as corn. (Steiner et al., 2018). Cataracts is one of the leading causes of preventable blindness worldwide, with evidence showing that it accounts for 10.8 million out of 32.4 million blind individuals, and that 35.1 million out of 191 million people with impaired vision globally are affected by this disease (Khairallah et al., 2015). Age-related macular degeneration (AMD) is a considerable health problem and is a significant cause of central visual loss, affecting 10% of people older than 65 years and more than 25% of people older than 75 years (Al-Zamil & Yassin, 2017). Lutein has been shown to effectively inhibit the development of AMD due to its ability to aid the activation of nuclear factor erythroid 2-related factor 2 target genes in the human retinal pigment epithelial cells (Frede et al., 2017). It is suggested that an intake of 6 mg per day of lutein in men and women has been suggested to reduce the risk of AMD, however studies have found that the typical daily intake of lutein per day for men and women was around 2.7 mg and 3.09 mg per day, respectively. Lutein has also shown benefits in preventing osteoporosis (Yamaguchi, 2012), effectiveness in wound healing (Y. Li et al., 2018), antiplasmodial effects (Vishwanathan et al., 2011), and cardioprotective effects (Maria et al.,

2015). Therefore, effective diet-based strategies have been implemented to reduce the risks of developing AMD. Although many foods naturally contain high levels of lutein, its low water solubility limits its absorption in the gastrointestinal tract (GIT), reducing its bioavailability (Steiner et al., 2018). Lutein is often prone to degradation when exposed to environmental stresses (such a pH, heat, and light) due to its conjugated double bonds (Sant'Anna et al., 2013). Therefore, encapsulation systems can be developed to overcome these limitations and can help facilitate the delivery of these poorly bioavailable compounds by increasing their absorption into cellular structures through favorable particle properties (Bazana et al., 2019).

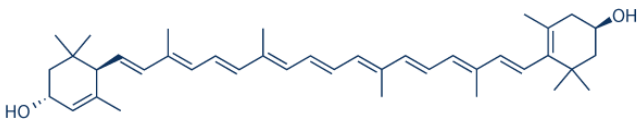

Fig. 3-1. Chemical structure of lutein (Selleckchem).

Cereal storage protein-based nanoparticles are good candidates for the encapsulation of lipophilic bioactive compounds due to their hydrophobicity, non-toxicity, biodegradability, and environmental sustainability. Hordein is the major storage protein in whole barley grain and is considered a prolamin due to its large proportion of Pro and Glu. The unique solubility of hordein (65-85% aqueous-alcohol solutions) is related to its large abundance of non-polar amino acids, accounting for ~40% of its amino acid composition (Zhao et al., 2010). Because of this, hordein nanoparticles can be developed as encapsulation systems suitable for the controlled

release of hydrophobic and amphiphilic bioactive compounds (Hong et al., 2020). However, applications of protein-based nanoparticle delivery systems as functional food ingredients are often limited due to the low-solubility of proteins in aqueous solutions, chemical instability against environmental stresses (pH, heat, and high salt concentration), as well as enzymatic changes throughout the gastrointestinal tract.

Recent interest has shifted towards modifications of protein-nanoparticle delivery systems coated with polysaccharide biopolymers to enhance their stability and functionalities (Li et al., 2022; Wei & Huang, 2019). Electrostatic interactions play a dominant role in the stability of protein-polysaccharide nanoparticles, while hydrophobic interactions and hydrogen bonds may also be involved (Li et al., 2022). Polysaccharides are beneficial materials as surface coatings of protein nanoparticles because of their non-toxicity, biocompatibility, abundance in nature, and environmental sustainability. Pectin, a widely sourced and inexpensive anionic polysaccharide has been used as a coating material for the encapsulation of hydrophobic bioactive compounds into protein-based nanoparticles. One study by Huang et. al (2019) developed core-shell zein/pectin nanoparticles for the encapsulation of resveratrol (Huang et al., 2019). The core-shell nanoparticles fabricated using anti-solvent precipitation and electrostatic deposition methods exhibited stability against aggregation from pH 2 to 7, good heat stability (80 °C), and enhanced bioaccessibility and antioxidant capacity compared to that of free resveratrol. Another study investigated the stability and bioactivity of curcumin encapsulated into casein-pectin nanocomplexes as an oral delivery system (Hua et al., 2021). The nanocomplexes revealed monodispersed spherical nanoparticles (~266.4 nm), and the *in vitro* release behaviors indicated that the surface coating of pectin hindered the release of curcumin in simulated gastric fluid, and the controlled release was enhanced in the simulated gastric fluid. However, the effect of pectin

coating on the surface of hordein nanoparticles to encapsulate lutein has not yet been investigated.

Therefore, the purpose of this study is to: 1. determine the effect of pectin coating on the environmental stability of lutein encapsulated into hordein nanoparticles and 2. characterize the bioaccessibility and bioavailability of lutein encapsulated into hordein-pectin nanoparticles.

3.3. Materials and method

3.3.1. Materials

Hulled barley grains were purchased from Barry Farm (Wapakoneta, Ohio, USA). Pectin (DE=71%) was purchased from MP Biomedicals (Santa Ana, California, USA). Lutein (~90%) was purchased from Thermo Fisher Scientific (Waltham, Massachusetts, USA) and both simulated gastric fluid (SGF) (without pepsin) and simulated intestinal fluid (SIF) were purchased from Ricca Chemical Company (Arlington, Texas, USA). Pepsin 1:3000 was also purchased from Spectrum Chemical Mfg. Corp. (New Brunswick, New Jersey, USA). ASP/USP grade ethanol alcohol, hydrochloric acid, sodium hydroxide, and sodium chloride, dimethyl sulfoxide (DMSO) were purchased from VWR International (Ranchor, Pennsylvania, USA).

3.3.2. Pectin stock

0.05% (w/v) stock of pectin was prepared by dispersing 30 mg of pectin powder into 60 mL of DI water with continuous stirring (1 h, 600 rpm, 23 °C) until fully dissolved. Afterwards, the dispersion was filled through a 12.5 cm filter paper (VWR, Radnor, Pennsylvania, USA) to remove any insoluble aggregates.

3.3.3. Lutein-hordein nanoparticle synthesis

The fabrication of lutein-hordein nanoparticles (L-HNP) was carried out using an anti-solvent precipitation method. Briefly, 100 mg of hordein powder was dissolved in 10 mL of a 75% aqueous-ethanol solution and continuously stirred (800 rpm) for 30 mins at room temperature to achieve a concentration of 0.1% (w/v). After 30 mins, lutein was added to the hordein stock solution at different mass ratios of hordein-to-lutein (100:0,10:1, 5:1, and 1:1) and stirred for an additional 30 mins followed by centrifugation (Avanti® J-E Centrifuge, Beckman Coulter, USA) (10,000 rpm, 10 mins, 23 °C) to remove any insoluble aggregates. Hordein-lutein stock solution was then added to 4 parts DI water (pre-adjusted to pH 4) using a controlled syringe pump (Model 200 Series, kd Scientific, Holliston, MA, USA) at a dropping speed of 0.8 mL/min followed by continuous stirring for an additional 5 mins (650 rpm). Ethanol was removed using a rotary evaporator (Rotavapor R II, Buchi, Switzerland) (45 °C). To compensate for the lost ethanol during the rotary evaporation, DI water pre-adjusted to pH 4 was added to reach a final volume of 50 mL.

3.3.4. Fabrication of lutein-hordein/pectin nanoparticle complex

Lutein-hordein/pectin nanoparticles complex (L-HP-NPC) was fabricated using the same procedure as mentioned in **section 3.3.3**. However, for the incorporation of pectin as the wall material, 15 mL of freshly prepared L-HNP dispersion was added to 15 mL of the 0.05 (w/v) pectin stock (pre-adjusted to pH 4) at fixed ratio of 1:1. The following dispersion was continuously stirred (800 rpm) for 10 minutes and centrifuged at 10,000 rpm for 5 mins to remove any insoluble aggregates. Afterwards, the freshly prepared L-HNP and L-HP-NPC dispersions were lyophilized, and the dried nanoparticle powders were stored at 3 °C with limited exposure to sunlight for further analysis.

3.3.5. Particle size and ζ-potential

The particle size distribution and electrical characteristics (ζ-potential) of the synthesized colloidal dispersion was measured at pH 4 using a zetasizer equipped with dynamic light scattering (DLS) (Zetasizer Advanced Series, Malvern Panalytical, Westborough, MA, USA). Samples were diluted 50x with DI water prior to measurements to avoid multiple scattering effects.

3.3.6. Fourier transform infrared spectroscopy (FTIR)

FTIR spectra of lutein, L-HNP, and L-HP-NPC were performed using a Fourier transform spectrophotometer (Jasco FT/IR-4100, Easton, MD, USA). The spectrum range was from 550 to 4000 cm-1 with 32 scans with a 4.0 cm-1 resolution.

3.3.7. Scanning electron microscopy (SEM)

The surface morphology of lutein, L-HNP, and L-HP-NPC was investigated using a scanning electron microscope (SU-70, Hitachi, Japan) at an accelerating voltage of 10 kV. Samples were coated with a gold layer using a compact coating unit (CCU-010, Safematic, Switzerland) to avoid charging under the electron beam.

3.3.8. Dispersibility

The water-dispersibility of lyophilized L-HNP and L-HP-NPC was determined by dispersing 5 mg of the powdered nanoparticles in 25 mL DI water with constant stirring (600 rpm) for 2 hours and determining the particle size distribution.

3.3.9. Determination of lutein content

The determination of lutein content inside L-HNP and L-HP-NPC was carried out using a protocol similar to Ma et. al (2021) with slight modifications (Ma et al., 2021). The content of

lutein was determined using an ultraviolet spectrophotometer (Life Science UV/Vis Spectrophotometer, Beckman Coulter, Brea, CA, USA). 10 mg of pure lutein was added to 10 mL of DMSO until fully dissolved and centrifuged at 10,000 rpm for 30 minutes at 23 °C. Then the supernatant was diluted 10x with DMSO and standard solutions (0-10 µg/mL) were used to obtain a calibration curve against an DMSO blank. The linear equation was y=0.1425x + 0.0057, where y was the absorbance value (A), and x was the concentration of the sample (C, µg/mL), R^2 (regression coefficient) was 0.9981.

3.3.10. Loading capacity (LC) and encapsulation efficiency (EE)

To determine the loading capacity (LC) and encapsulation efficiency (EE) of lutein into L-HNP and L-HP-NPC, briefly, 1 mg of either freeze-dried L-HNP and L-HP-NPC samples were vigorously mixed with 5 mL of DMSO, and the mixture was then centrifuged (3000 rpm, 5 mins). The lutein content in the supernatant was then diluted 10x and the absorbance was determined to quantify the concentration.

The particle yield and lutein leading efficiency was calculated using the obtained concentration from **section 3.9.9**:

$$\textbf{LC (\%)} = \frac{encapsulated\ lutein\ (mg)}{total\ weight\ of\ lutein,hordein,and\ pectin\ (mg)}\ X\ 100\%$$

$$\textbf{E.E (\%)} = \frac{lutein\ in\ nanoparticles}{total\ lutein\ input}\ X\ 100\%$$

3.3.11. Effect of pH

Freshly prepared nanoparticle dispersions were added to DI water pre-adjusted to various pH values (pH 3.0, 5.0, and 7.0) to determine the effect of pH on the particle size, PDI, and zeta potential of the colloidal dispersions. If necessary, the pH of the samples was adjusted using

either 0.1M of HCl or 0.1M NaOH. Samples were diluted 50x prior to analysis to avoid multiple scattering effects.

3.3.12. Effect of salt concentration

Different amounts of sodium chloride (0, 20, 40, 60, 80, 100 μM) were added to freshly prepared nanoparticle dispersions to determine the effect of salt concentration on the particle size of synthesized nanoparticles.

3.3.13. Effect of heat

Colloidal dispersions were prepared at pH 4.0 and heated at 80 °C using a heated water bath (Thermo Scientific, Waltham, MA, USA) for different times (0, 30, 60, 90, 120 mins) to determine the effect of heat treatment on the particle size of freshly prepared nanoparticle dispersions. At each time interval, samples were cooled to room temperature and then particle size was measured using DLS.

3.3.14. *In vitro* digestion

The determination of the bioaccessibility of lutein during in vitro digestion was carried out using a procedure similar to Li et. al (2020) with slight modifications (H. Li et al., 2020). 10 mL of L-HNP, and L-HP-NPC at a lutein-to-hordein mass ratio of 1:1 (dissolved in absolute ethanol) was vortexed with 10 mL simulated gastric fluid (SGF) with 5 mg of added pepsin. 10 mL of free lutein was also dissolved in absolute ethanol as the control. The 20 mL mixtures were then adjusted to pH 3.0 with hydrochloric acid and then shaken continuously using an orbital shaking incubator (Orbital Shaker, Forma Scientific, Waltham, MA, USA) set at 140 rpm and 37 °C for 2 hours to stimulate stomach digestion. Afterwards, the 15 mL mixtures were transferred to the intestinal phase and mixed with 15 mL simulated intestinal fluids (SIF). The 30 mL mixtures

were then adjusted to pH 7.0 using sodium hydroxide and shaken for 2 hours using a stomacher to simulate intestinal digestion. Following gastric and intestinal digestion, the samples were centrifuged at 10,000 rpm for 40 min at 10 °C. Subsequently, the supernatant of the SGF and SIF was filtered using a controlled syringe pump equipped with a 0.1 μ filter at a dropping rate of 1 mL/min. The amount of lutein was determined according to (**Section 3.3.9**.). The in vitro bioaccessibility of lutein was determined using the following equation:

Bioaccessibility of lutein: $\frac{Soluble\ lutein\ in\ gastrointestinal\ fluids}{Total\ lutein\ input}$ x 100%

3.3.15. Data analysis

The statistical analysis was performed using RStudio 2022.12.0 software (RStudio, Boston, MA, USA). Statistical differences were evaluated using one-way Analysis of Variance (ANOVA) between separate groups using Tukey's post-hoc test with a statistical significance level of $p < 0.05$ for all comparisons. In certain conditions, Student's t-test assuming unequal variance was performed with a significance level of $p < 0.05$. All measured values were expressed as mean ± standard deviation of three independent replicates.

3.4. Results and Discussion

3.4.1. Particle size and ζ-potential

Visual representation of freshly prepared L-HNP and L-HP-NPC were shown in **Fig 3-2**, respectively. Both nanoparticle dispersions were prepared using an anti-solvent precipitation method. The mean particle diameter (369 ± 21 nm), polydispersity index (0.52 ± 0.05), and ζ-potential (-22 ± 1 mV) of freshly prepared HP-NPC was measured at pH 4 (**Table 3-1**). The mean particle diameter of HP-NPC showed no significant differences ($p > 0.05$) compared to lutein-hordein nanoparticles (L-HNP) (343 ± 25 nm) indicating that pectin had no effect on the

particle size of L-HNP as a protective coating. The negative charge of HP-NPC is a result of the absorption of anionic pectin coating onto the surface of cationic L-HNP. As indicated, the ζ-potential of HP-NPC was around -22 mV compared to L-HNP which was around +26 mV. The result of the negative charge on HP-NPC can be attributed to electrostatic interactions between the two biopolymers at this pH since pectin carries a net negative charge at pH 4, while hordein carries a net positive charge.

Fig 3-2. Visual representation of A.) freshly prepared lutein-hordein nanoparticle (L-HNP) dispersion and B.) freshly prepared lutein-hordein/pectin nanoparticle (L-HP-NPC) dispersion

	Particle size (nm)	**PDI**	**ζ-potential (mV)**
L-HNP	343 ± 25^{a}	0.55 ± 0.02	26 ± 3^{a}
L-HP-NPC	369 ± 21^{a}	0.52 ± 0.05	-22 ± 1^{b}

Table 3-1. Average particle size, polydispersity index (PDI), and ζ-potential of lutein-hordein nanoparticles (L-HNP) and lutein-hordein/pectin nanoparticle complex (L-HP-NPC). Different superscripts in each column represents significant differences ($p < 0.05$) between the two samples. Values are represented as the mean ± standard deviation of three replicates.

3.4.2. Effect of mass ratio of hordein-to-lutein

The effects of the hordein-to-lutein mass ratio (100:0, 10:1, 5:1, and 1:1) on the particle size, PDI, and ζ-potential of L-HNP and L-HP-NPC was measured (**Table 3-2**). Both L-HNP and L-HP-HPC at hordein-to-lutein mass ratios of 10:1 and 1:1 exhibited significant increase ($p < 0.05$) in particle size when compared to non-encapsulated nanoparticles (100:0). However, at a mass ratio of 5:1, both nanoparticles showed no significant increase ($p > 0.05$) in particle size when compared to a mass ratio of 100:0. This suggests that the presence of lutein may have interfered with the nanoparticle formation during the antisolvent precipitation procedure at those two concentrations. When comparing the polydispersity index (PDI) of both nanoparticles, L-HNP exhibited a much more polydisperse particle distribution compared to L-HP-NPC at mass ratio values of 100:0 and 5:1 suggesting that some nanoparticle aggregation occurred. This is similar to the results of Liang et. al (2021) who developed zein/pectin nanoparticles for the encapsulation of tannic acid (TA) (Liang et al., 2021). As the mass ratio of Zein-to-TA increased to 5:1, there were significant increases in both particle size and PDI. This suggests that pectin as a coating material had some protective effect in maintaining a more uniform distribution of particles during the antisolvent precipitation procedure. No significant changes occurred in ζ-potential when measured for both L-HNP and L-HP-NPC as the mass ratio values increased, suggesting that lutein concentration did not interfere with the surface potential of both nanoparticles.

Mass Ratio (hordein:lutein)	**Particle size (nm)**		**PDI**		**ζ-potential (mV)**	
	A	**B**	**A**	**B**	**A**	**B**

100:0	180 ± 3[b]	246 ± 11[c]	0.32 ± 0.01	0.26 ± 0.02	33 ± 4[a]	-16 ± 6[a]
10:1	279 ± 43[a]	297 ± 6[b]	0.66 ± 0.12	0.37 ± 0.01	31 ± 4[a]	-18 ± 1[a]
5:1	184 ± 10[b]	246 ± 9[c]	0.75 ± 0.01	0.32 ± 0.04	29 ± 1[a]	-21 ± 1[a]
1:1	343 ± 25[a]	369 ± 21[a]	0.55 ± 0.03	0.52 ± 0.05	26 ± 3[a]	-22 ± 1[a]

Table 3-2. Effect of mass ratio (hordein-to-lutein) on particle size, polydispersity index (PDI), and ζ-potential of A.) lutein-hordein nanoparticles (L-HNP) and B.) lutein-hordein/pectin nanoparticle complex (L-HP-NPC). Different superscripts in each column represents significance ($p < 0.05$) between mass ratios of respective samples. Values are represented as mean ± standard deviation of three replicates.

3.4.3. FTIR

The FTIR spectra of lutein, L-HNP, and L-HP-NPC are provided in **Fig 3-3** to provide information about the intermolecular interactions between the following biopolymers. In the pure lutein spectra (**Fig 3-3A**), peaks at 2865 cm^{-1} represent asymmetric and symmetric stretching vibrations of CH_2 and CH_3. Characteristic peaks were also observed at 1352 cm^{-1} and 955 cm^{-1} representing the dimethyl group splitting and trans conjugated alkene (-CH=CH-) out of plane deformation, respectively (do Prado Silva et al., 2017). As expected, peak broad intensity peaks were observed in the -OH region (3200-2700 cm^{-1}) for lutein due to the limited amounts of -OH groups present in its structure. For the L-HNP spectrum (**Fig 3-3B**), the two characteristic peaks of hordein at 1649 cm^{-1} and 1527 cm^{-1} corresponded to the amide I (1700-1600 cm^{-1}) and amide II (1600-1500 cm^{-1}) bands, respectively. Peaks were observed at 1740 and 1030 cm^{-1} in the L-HP-NPC spectrum (**Fig 3-3C**), which was characteristic of the carbonyl group stretching of the

ester groups and C-O stretching in -COOH for pectin, respectively (Singthong et al., 2004). The sharp peak at 3293 cm^{-1} represents the -OH region which is attributed to the inter- and intra-molecular hydrogen bonding of the galacturonic acid (GalA) backbone of pectin (Singthong et al., 2004). The FTIR spectra for both L-HNP and L-HP-NPC (**Fig 3-3C-D**) were both similar in peaks, however for L-HP-NPC there were peaks observed at 1030 and 1100 cm^{-1} representing the C-O stretching in -COOH and O-H bending, respectively, which is a result of the incorporation of pectin as a coating (Kamble et al., 2017). Interestingly, FTIR spectroscopy revealed no characteristic peaks of lutein in either the L-HNP, and L-HP-NPC spectra, may have indicated that no chemical reaction had occurred between lutein and neither hordein nor pectin. This may imply that the encapsulation procedure had little obvious effects on the structural conformation of hordein and pectin. This is similar to the results of Zhao et. al (2018) who developed lutein-loaded sodium caseinate (NaCas) microparticles (T. Zhao et al., 2018). Their results indicated that the no obvious differences between NaCas and lutein-loaded microcapsules may have been due to the relatively low concentrations of nutraceuticals and interactions with the surrounding matrix. However, with the shift from 3292 cm^{-1} for L-HNP to 3272 cm^{-1} for L-HP-NPC in both spectrums in the -OH region, it is possible that pectin also interacted with both hordein and lutein through newly formed hydrogen bonds.

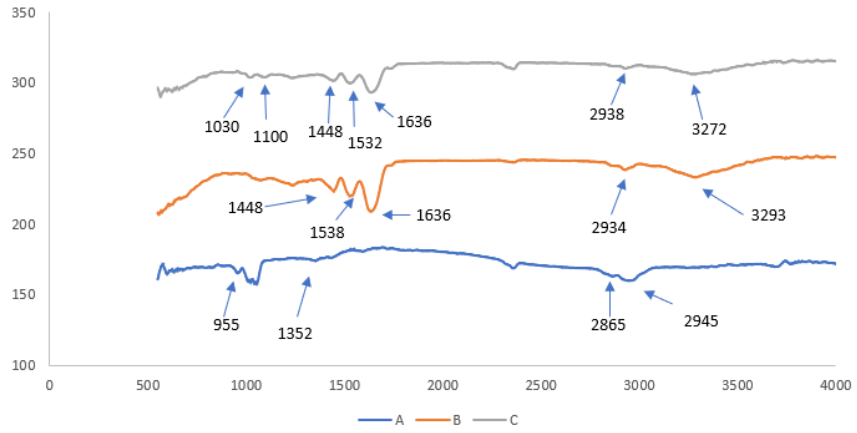

Fig 3-3. FTIR spectra of A.) lutein; B.) lutein-hordein nanoparticles (L-HNP); C.) lutein-hordein/pectin nanoparticles (L-HP-NPC)

3.4.4. SEM

The SEM morphology of lutein, L-HNP, and L-HP-NPC is shown in **Fig 3-4**. Pure lutein showed an irregular morphological appearance with a rigid and hardened shape, while L-HNP and L-HP-NPC still revealed an irregular appearance with a smoother shape. When comparing the SEM morphology of L-HNP and L-HP-NPC to unencapsulated HNP and HP-NPC (**Ch. 2, Fig 2-6**), incorporating of lutein into the nanoparticle matrix appeared to influence its morphology. Both unencapsulated HNP and HP-NPC revealed more smooth and spherical morphologies compared to the irregular appearance of L-HNP and L-HP-NPC and showed similar appearances to pure lutein which indicates that lutein was successfully encapsulated into the nanoparticle matrix.

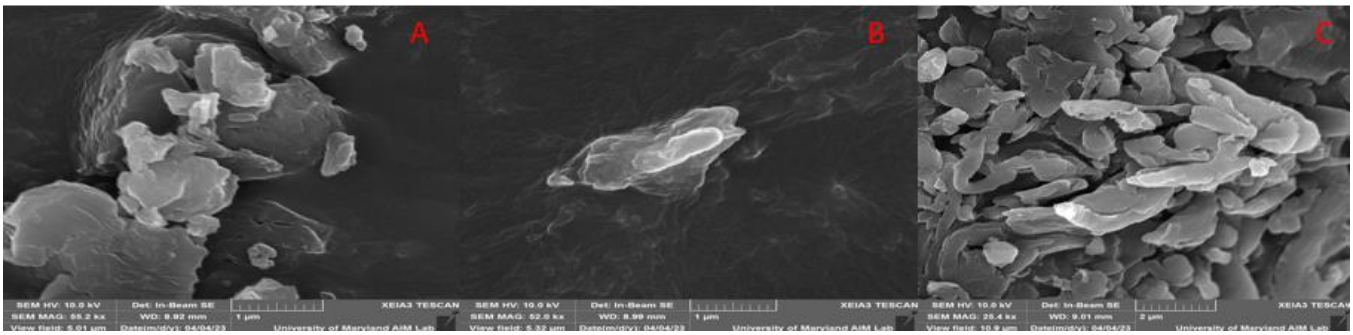

Fig 3-4. SEM images of A.) Lutein; B.) lutein-hordein nanoparticles (L-HNP); and C.) Lutein-hordein/pectin nanoparticle complex (L-HP-NPC)

3.4.5. Dispersibility

The particle size, PDI, and ζ-potential of re-dispersed lyophilized L-HNP and L-HP-NPC was measured to determine the effect of freeze-drying on freshly prepared nanoparticle dispersions (**Table 3-3**). Freeze-drying is an important process during the incorporation of functional food ingredients into beverages, thus the effect of freeze-drying followed by re-dispersion into an aqueous medium on the stability of L-HNP and L-HP-NPC was determined. Both L-HNP and L-HP-NPC displayed no significant changes in particle size and PDI indicating that the freeze-drying process followed by re-dispersion into an aqueous media had no effect. However, the significant changes ($p < 0.05$) in ζ-potential were observed in L-HNP following the freeze-drying and re-dispersion process. The ζ-potential of freshly prepared nanoparticle dispersions of L-HNP was around +26 mV while the ζ-potential of freeze-dried and re-dispersed L-HNP was around -7 mV. The change in the ζ-potential of L-HNP after freeze-drying could be explained by the changes in the physiochemical characteristics of proteins during lyophilization. The drying procedure may have influenced the structural integrity of the hordein molecule since extending drying time (~ 24 hours) was required to obtain a fully dried powder. Extended heat treatment at higher temperatures can cause irreversible changes in the hordein molecule which

may have caused structural changes such as the unfolding of protein chains that were buried in the native structure (Roy & Gupta, 2004). It is possible that the structural changes during the unfolding of the hordein chains during the drying process may have exposed some of those negatively charged amino acids such as aspartic acid (Asp) or glutamic acid (Glu) which led to the negative surface charge (-7 mV). However, no significant change ($p > 0.05$) in the ζ-potential for L-HP-NPC occurred indicating that the addition of pectin as a coating material acted as a lyoprotectant during the freeze-drying process. Numerous compounds such as sugars, amino acids, amines, polyols, and some salts have been shown to act as lyoprotective agents during the freeze-drying of proteins (Roy & Gupta, 2004). FTIR spectroscopy used by Carpenter and Crowe (1998) have shown that certain carbohydrates protect proteins by hydrogen bonding, a role displayed by water molecules which are removed during drying (Carpenter & Crowe, 1988). Pectin is a biopolymer rich in GalA residues, which have been shown to act as lyoprotective agents. One study by Chen et. al (2006) determined the effect of carbohydrates as lyoprotective agents on the survival of microorganisms on kefir (Chen et al., 2005). Their results indicated that the addition of 10% lyoprotective agents which included galatose, maltose, sucrose, and trehalose significantly improved the viability of lactic acid bacteria and yeasts after freeze-drying.

	Particle size (nm)		**PDI**		**ζ-potential**	
	Before	**After**	**Before**	**After**	**Before**	**After**
L-HNP	343 ± 25^{a}	372 ± 21^{a}	0.55 ± 0.02	0.53 ± 0.07	26 ± 3^{a}	-7 ± 3^{b}
L-HP-NPC	369 ± 21^{a}	371 ± 25^{a}	0.52 ± 0.05	0.40 ± 0.01	-22 ± 1^{a}	-20 ± 0^{b}

Table 3-3. Average particle size (nm), polydispersity index (PDI), and ζ-potential of lutein-hordein nanoparticles (L-HNP) and lutein-hordein/pectin nanoparticle complex (L-HP-NPC) before and after lyophilization. Different superscripts in each column represents significant differences ($p < 0.05$) before and after lyophilization for each respective sample.

3.4.6. LC and EE

Loading capacity (LC) and encapsulation efficiency (EE) are important characteristics when developing delivery vehicles, thus the LC and EE of L-HNP and L-HP-NPC was determined when the mass ratio of hordein-to-lutein was 1:1 (**Table 3-4)**. Both L-HNP (81% ± 3) and L-HP-NPC (82% ± 1) exhibited similar results in their EE indicating that hordein played a dominant role in the encapsulation of lutein, and the addition of pectin did not have a significant contribution to encapsulate lutein. The LC of both L-HNP (16% ± 3) and L-HP-NPC (16% ± 1) also showed similar trends and no significant differences ($p > 0.05$) were observed. Although the LC and EE of hordein-to-pectin of different mass ratios was not investigated, it is assumed that decreasing the mass ratios would result in a higher EE. This is due to the possibility of less lutein available to saturate the nanoparticle system. This is similar to the results of Li et. al (2020) who developed zein/soluble soybean polysaccharide composite nanoparticles for the encapsulation and delivery of lutein (H. Li et al., 2020). Their results exhibited no significant changes in the LC of lutein, even with the addition of soluble soybean. However, as the mass ratios of zein-to-lutein increased, the EE decreased due to the saturation of lutein within their systems.

	LC (%)	**EE (%)**
L-HNP	16 ± 3^{a}	81 ± 3^{a}

L-HP-NPC	16 ± 2^{a}	82 ± 1^{a}

Table 3-4. Loading capacity (LC) and encapsulation efficiency (E.E) of lutein-hordein nanoparticle complex (L-HNP) and lutein-hordein/pectin nanoparticle complex (L-HP-NPC). Different superscripts represent significance ($p < 0.05$) between both samples. Values are represented as the mean ± standard deviation of three replicates.

3.4.7. Effect of pH

Applied functional food ingredients may be exposed to a variety of food or beverage products that differ in pH, thus the effect of pH (pH 3-7) on the particle size, PDI, and ζ-potential (mV) of L-HNP and L-HP-NPC was investigated (**Table 3-5**). L-HP-NPC exhibited a significantly larger particle size ($p < 0.05$) compared to L-HNP at all pH values. It was expected that the particle size of L-HP-NPC would be larger compared to L-HNP at pH 3 since high methoxy pectin (HMP) (DE = 71%) was used in the study. HMPs can form gels at pH < 3.5 and at high sugar concentrations (> 55%) due to the pKa value of pectin reported at pH 3.5 (Gawkowska et al., 2018). At pH > 3.5, the carboxyl groups of the GalA groups in pectin become dissociated lowering the electrostatic repulsive forces between the pectin chains. This also attributes to the results of the ζ-potential of L-HP-NPC at pH 3 (-6 mV), in which the lowering of the electrostatic repulsive forces between the pectin chain was a result of the dissociation of the carboxyl groups. The significant increase in particle size from pH 3 to pH 5-7 can be attributed to the fact that the adsorbed pectin molecules impacted the effective size of the core-shell particles. Although it was not investigated in this study, the effect of pectin on the approximate thickness of the shell may have impacted the particle diameter of L-HP-NPC. Like Huang et al.

(2016), larger particle sizes of their zein-pectin nanoparticles increased from pH 5-7 (Huang et al., 2016). Their results suggested that the increase in particle size was attributed to the radius of hydration of pectin molecules in their solution which was dependent on pH. L-HNP were still able to maintain a relatively small particle size compared to L-HP-NPC ($p < 0.05$). The significant increase in particle size from pH 5 (229 ± 19 nm) to pH 7 (320 ± 2 nm) indicates the susceptibility of protein aggregation when exposed to its pI. This correlates to the change in ζ-potential for L-HNP which transitioned from a positive to a negative charge from pH 3 to 7 due to the low surface charge of hordein at it pI, which was between pH 5-7 in this study. The significant increase in ζ-potential for L-HP-NPC as the pH increased from pH 3 to pH 7 is a result of highly charged pectin strongly bound to the surfaces of cationic hordein through electrostatic attractions.

	Particle Size (nm)		**PDI**		**ζ-potential (mV)**	
	A	**B**	**A**	**B**	**A**	**B**
pH 3	3201 ± 23^{aB}	389 ± 23^{bA}	0.59 ± 0.03	0.42 ± 0.06	23 ± 0^{a}	-6 ± 0^{b}
pH 5	229 ± 19^{bA}	444 ± 16^{aB}	0.49 ± 0.03	0.45 ± 0.05	15 ± 1^{b}	-34 ± 0^{a}
pH 7	320 ± 2^{aB}	517 ± 29^{aA}	0.37 ± 0.05	0.50 ± 0.02	-5 ± 0^{c}	-35 ± 1^{a}

Table 3-5. Effect of pH (3-7) on the average particle size, polydispersity index (PDI), and ζ-potential of A.) lutein-hordein nanoparticles (L-HNP) and B.) lutein-hordein/pectin nanoparticle complex (L-HP-NPC). Different uppercase superscripts represent significant differences ($p <$

0.05) between both samples while different lowercase superscripts in each column represents significance ($p < 0.05$) between mass ratios of respective samples. Values are represented as mean ± standard deviation of three replicates.

3.4.8. Effect of heat

The effect of heat treatment (80 °C for 0-120 mins) on the mean particle size and PDI of L-HNP and L-HP-NPC was investigated (**Table 3-6**). L-HP-NPC was able to maintain no significant ($p > 0.05$) increase in particle size when heated at 0-60 mins. However, aggregation of the L-HP-NPC particles were shown when heated at 90-120 mins. The PDI of L-HP-NPC was significantly decreased ($p < 0.05$) at 30-120 mins compared to non-heat-treated samples, indicating that heat treatment had a significant impact on creating a more uniform particle distribution. In contrast, L-HNP showed a trend in the increase in particle size when the heat treatment was extended from 0-120 mins indicating the aggregation of the particles. Proteins are generally unstable to heat treatment as illustrated in another study by Hu and McClements (2015) who developed zein-alginate core/shell nanoparticles) (Hu & McClements, 2015). The increase in particle size suggests the possibility of heat treatment affecting the reorganization of the hordein structure thus causing the aggregation of the hordein molecules within the nanocomposite. These results suggest that the incorporation of pectin as a coating material on the surface of bioactive-encapsulated protein materials may prevent their aggregation during thermal processing such as pasteurization, sterilization, and cooking.

	Particle size (nm)		**PDI**	
Heating time (mins)	**A**	**B**	**A**	**B**
0	343 ± 25^{d}	369 ± 21^{b}	0.55 ± 0.03^{a}	0.52 ± 0.05^{a}

30	*534 ± 15^{c}	398 ± 22^{b}	*0.44 ± 0.05^{b}	0.37 ± 0.03^{b}
60	436 ± 42^{bc}	389 ± 9^{b}	*0.59 ± 0.06^{a}	0.39 ± 0.03^{b}
90	567 ± 58^{b}	556 ± 28^{a}	0.45 ± 0.05^{b}	0.36 ± 0.02^{b}
120	*1035 ± 77^{a}	609 ± 30^{a}	0.36 ± 0.02^{b}	0.33 ± 0.02^{b}

Table 3-6. Effect of heat treatment (80 °C) at various times (0-120 mins) on the average particle size and polydispersity index (PDI) of A.) lutein-hordein nanoparticles (L-HNP) and B.) lutein-hordein/pectin nanoparticle complex (L-HP-NPC). Asterisks (*) represent significant differences ($p < 0.05$) between both samples while different superscripts in each column represents significance ($p < 0.05$) between mass ratios of respective samples. Values are represented as mean ± standard deviation of three replicates.

3.4.9. Effect of salt concentration

Salt is a major component of a variety of food products, thus the effect of salt concentration (0-100 μM) on the particle size and PDI of L-HNP and L-HP-NPC was determined (**Table. 3-7**). As expected, the particle size of L-HNP dramatically increased as the salt concentration increased from 0-100 μM. This is a result of protein susceptibility with the addition of salt, which can promote particle aggregation through an electrostatic screening effect (Li et al., 2019). L-HP-NPC was able to maintain its particle size from 0-60 μM NaCl and significant increase in particle size ($p < 0.05$) was observed with the addition of 80-100 μM NaCl. This can be attributed to the weakening of electrostatic repulsion between hordein and pectin molecules at these salt levels, which would result in particle increase due to aggregation (Yao et al., 2018). However, pectin was able to exhibit a protective effect when exposed to salt

(0-60 µM) which favors its applications as a coating material for bioactive compounds as well as proteins.

	Particle size (nm)		PDI	
Salt concentration (µM)	**A**	**B**	**A**	**B**
0	343 ± 25^{f}	369 ± 21^{b}	0.55 ± 0.03	0.52 ± 0.05
20	*1328 ± 45^{e}	370 ± 36^{b}	0.47 ± 0.07	0.43 ± 0.04
40	*1612 ± 26^{d}	408 ± 90^{b}	0.51 ± 0.04	0.56 ± 0.11
60	*2861 ± 98^{a}	415 ± 21^{b}	0.34 ± 0.02	0.46 ± 0.03
80	*2434 ± 30^{b}	621 ± 22^{a}	0.35 ± 0.07	0.45 ± 0.02
100	*1946 ± 228^{c}	678 ± 17^{a}	0.41 ± 0.11	0.52 ± 0.05

Table 3.7. Effect of salt concentration (0-100 µM) on the average particle size and polydispersity index (PDI) of A.) lutein-hordein nanoparticles (L-HNP) and B.) lutein-hordein/pectin nanoparticle complex (L-HP-NPC). Different superscripts in each column represents significance ($p < 0.05$) between the particle size of respective samples. Values are represented as mean ± standard deviation of three replicates.

3.4.10. *In vitro* digestion

The *in vitro* bioaccessibility of unencapsulated lutein and encapsulated lutein into L-HNP and L-HP-NPC is depicted in **Fig 3-5**. Bioaccessibility of lutein was determined by measuring the percentage of lutein released and solubilized after two digestion phases (SGF and SIF) (H. Li et al., 2020). Focus on the effect of pectin as a nanoparticle coating on enhancing the

bioaccessibility of lutein was highlighted. Around 7.6% of non-encapsulated lutein was released and solubilized in the SGF which showed similar trends with no significant differences observed ($p > 0.05$) compared to L-HNP and L-HP-NPC, where only around 7.9% and 9.0% were available, respectively. Bioaccessibility of lutein was dramatically enhanced when encapsulated in L-HP-NPC (~22.3%) which showed higher bioaccessibility compared to L-HNP (~13.1%). This could be a result of the addition of a pectin coating which could act as a protectant against digestive enzymes which can easily hydrolyze proteins like hordein and the harsh digestive conditions. These results can be due to pectin's ability to produce gels in acidic media which favors its application as a carrier for bioactive compounds. The gastric environment is around pH 1.5-3.5, which is ideal for the formation of pectin gels. However, pectin gels are known to swell in aqueous media which could explain the higher amounts of lutein released into the SIF (Munarin et al., 2012). The bioaccessibility of lutein for L-HNP in the SIF was significant lower compared to L-HP-NPC ($p < 0.05$). The low amount of lutein released into the SIF could be a result of the hydrolysis effect of proteases. Pepsin was added to the SIF to replicate actual digestion in the gastrointestinal tract. However, the bioaccessibility of L-HNP and LP-HP-NPC in SIF without pepsin was not investigated in this study.

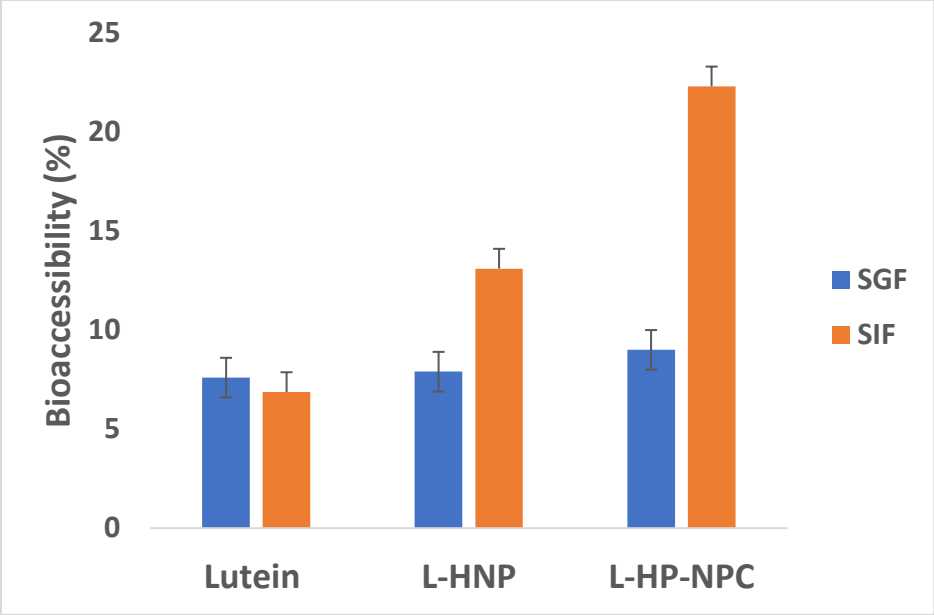

Fig 3-5. In Vitro bioaccessibility of non-encapsulated lutein and lutein-hordein nanoparticles (L-HNP) and lutein-hordein/pectin nanoparticle complex (L-HP-NPC) in simulated digestive fluids (SGF and SIF)

3.5. Conclusion

For this objective, lutein-hordein/pectin nanoparticle complex was synthesized using an anti-solvent precipitation with electrostatic deposition method. The mean particle diameter of the freshly prepared dispersions was still relatively small (369 nm), and the irregular morphology of pure lutein was shown in the morphology of L-HP-NPC but with a smoother shape. Lutein interacted with hordein mainly through newly formed hydrogen bonds and had no obvious effects on the structural conformation of hordein and pectin. Pectin as a coating material on the outer surface of hordein encapsulated with lutein showed improved resistance to aggregation against heat and salt concentration, but the particle size increased as the pH of the media became less acidic. This could have been a result of the greater adsorption of pectin molecules to onto both hordein and lutein which may have contributed to the effective size of the core-shell

particles. Pectin did not have a significant role in the encapsulation efficiency (EE) and loading capacity (EE) of lutein with no significant differences observed between L-HNP and L-HP-NPC, which indicates that hordein had a dominant role in the encapsulation procedure. Pectin was able to enhance the bioaccessibility of lutein in the simulated intestinal fluid (SIF) compared to L-HNP. The gelling capability of pectin was able to protect lutein from the digestive enzymes in the simulated gastric fluid (SGF) and enhance its bioavailability in the small intestines. This study illustrates the important properties of pectin which allows its applications in the food and pharmaceutical industry for the control delivery and release of bioactive components. The next objective will focus on the encapsulation of carvacrol into hordein-pectin nanoparticles. Special focus will be on the addition of pectin to enhance carvacrol's solubility and determine the antimicrobial activity of encapsulated carvacrol.

Chapter 4: Antimicrobial properties and solubility of carvacrol essential oil encapsulated into hordein-pectin nanoparticle complex.

4.1. Abstract

Carvacrol is a phenolic monoterpene known for its antimicrobial and anti-inflammatory properties, however its poor water-solubility, strong odor, and high volatility limits its applications in the food industry. In this work, a hordein/pectin nanoparticle complex was developed using an anti-solvent precipitation and electrostatic deposition method (pH 4) to encapsulate carvacrol. The optimal mass ratio of hordein-to-carvacrol was achieved at 5:1 with small particle diameter (183 nm), polydispersity index (PDI) of 0.25 and surface charge (ζ-potential) around -18 mV. A gel-like structure was shown as illustrated by scanning electron microscopy (SEM) which may have been attributed to newly formed hydrogen bonds and hydrophobic-hydrophobic interactions that favor the gel formation of high methoxyl (HM) pectin molecules. CA-HP-NPC was able to still maintain a relatively small particle size (207 nm) when dispersed into an aqueous media post-lyophilization and pectin was able to act as a lyoprotectant for hordein and carvacrol as indicated by no significant changes in its ζ-potential. The antimicrobial activity of CA-HP-NPC was investigated against non-pathogenic gram-positive *L. innocua* and gram-negative *E. coli K12*. However, no antimicrobial activity was shown against both bacteria. This study illustrates that bioactive compounds like carvacrol can be successfully encapsulated into food biopolymer nanoparticles, however further studies need to be investigated on their release properties to further enhance their applications.

4.2. Introduction

Since ancient times, essential oils (EOs) have been utilized in various cultures for medicinal and health purposes owing to their antibacterial (Moleyar & Narasimham, 1992), antiviral (Astani et al., 2010), antifungal (Nazzaro et al., 2017), anticarcinogenic, antimutagenic (Jeena et al., 2014), anti-inflammatory (Miguel, 2010), and antioxidant properties (Lammari et al., 2020). The European Pharmacopoeia (Uerpmann-Wittzack, 2017) defines an EO as an "odorous product, usually of complex composition, obtained from a botanically defined plant raw material by steam distillation, dry distillation, or a suitable mechanical process without heating". EOs can be obtained from a variety of sources such include flowers, leaves, seeds, rhizomes, fruits, woods, and so on. The vast properties of essential oils allow their applications in the food industry to enhance food quality, food preservation, and overall food safety. However, their applications are often masked by their low water solubility, high volatility, and strong odor (Amaral & Bhargava, 2015).

Carvacrol (5-isopropyl-2-methylphenol) (**Fig 1-7**), is a phenolic monoterpene listed by the Food and Drug Administration (FDA) as food additives, flavoring agent and as a natural food preservative (Shinde et al., 2020). Carvacrol can be found in a variety of natural sources such as oregano, thyme, sweet basil, and sweet cumin (Rathod et al., 2021). The therapeutic (Imran et al., 2022), anti-cancerous (Yazici et al., 2021), antimicrobial (Nostro & Papalia, 2012), and anti-inflammatory properties (da Silva Lima et al., 2013) of carvacrol demonstrate its potential application in the food and pharmaceutical industry. However, its low water solubility, susceptibility to oxidation, strong odor and volatilization are some of the limitations that can interfere with its application. Nano-based delivery systems offer a promising approach to mediate some of these limitations due to their small size, large surface area, biocompatibility, and

biodegradability which can improve the bioavailability, and organoleptic properties of carvacrol (de Souza et al., 2022). Nano-scaled encapsulation of bioactive compounds such as EOs can also increase their concentration in food components where microorganisms thrive, such as water-rich phases or liquid-solid interfaces (Weiss et al., 2009).

Hordein, a prolamin protein found in barley grains is rich in non-polar amino acids (~ 40%) and is soluble in 65-85% aqueous-ethanol solutions. Due to its unique solubility, liquid-liquid dispersion methods allow the encapsulation of EOs that can co-dissolve in the aqueous-ethanol solution along with hordein (Wu et al., 2012). Hordein also possesses unique functional properties which include but not limited to, greater adhesion, extensibility, and gelation, which are all characteristics necessary for preparing nanoparticles as carriers for controlling the release of hydrophobic compounds such as EOs (He et al., 2020). However, the hydrophobic nature of most prolamin proteins limits their solubility into aqueous solutions. This problem can be mitigated by incorporating a polysaccharide molecule as a coating because of their ability to modulate electrostatic and steric repulsion between the particles.

Therefore, the objective of this study is to encapsulate carvacrol into a hordein/pectin nanoparticle complex using an antisolvent precipitation and electrostatic deposition method (pH 4). The antimicrobial properties and dispersibility of the fabricated nanoparticles will be determined. The hypothesis of the study is that the encapsulated carvacrol into the nanoparticle complex will have enhanced solubility in an aqueous media and potentially be used as a functional food ingredient to enhance its shelf-life as well while providing some of the beneficial properties of carvacrol.

4.3. Materials and methods

4.3.1. Materials

Hordein was previously extracted from (**Ch. 2, Section 1.3.2**) and pectin (DE = 71%) was purchased from MP Biomedicals (Santa Ana, California, USA). Carvacrol was purchased from Sigma Aldrich (St. Louis, Missouri, USA). For the antimicrobial experiment, gram-negative *E. coli K12 (*ATCC 10798) and gram-positive *Listeria innocua* (ATCC 11262) were cultured overnight from frozen stock cultures. Nutrient agar, nutrient broth, peptone water, and tryptic soy broth were purchased from Difco Laboratories Incorporated (Franklin Lakes, New Jersey, USA). Other chemicals such as ASP/USP grade ethanol alcohol, hydrochloric acid, sodium hydroxide, and sodium chloride were purchased from VWR International (Ranchor, Pennsylvania, USA).

4.3.2. Pectin stock

0.05% (w/v) stock of pectin was prepared by dispersing 30 mg of pectin powder into 60 mL of DI water with continuous stirring (1 h, 600 rpm, 23 °C) until fully dissolved. Afterwards, the dispersion was filled through a 12.5 cm filter paper (VWR, Radnor, Pennsylvania, USA) to remove any insoluble aggregates.

4.3.3. CA-hordein nanoparticle fabrication

The fabrication of carvacrol-loaded hordein nanoparticle (CA-HNP) was carried out using an anti-solvent precipitation method. Briefly, hordein powder (extracted from Ch. 3) and carvacrol oil at various hordein-to-carvacrol ratios (20:1, 10:1, and 5:1) were dissolved in 10 mL of a 75% aqueous-ethanol solution and continuously stirred (800 rpm) for 1 hour at room temperature. The resulting dispersion was then centrifuged (Avanti® J-E Centrifuge, Beckman Coulter, USA) at 10,000 rpm for 10 minutes at 23 °C to remove any insoluble aggregates. The

supernatant was then added to 4 parts DI water (pre-adjusted to pH 4) using a controlled syringe pump (Model 200 Series, kd Scientific, Holliston, MA, USA) at a dropping speed of 0.8 mL/min followed by continuous stirring for an additional 5 mins (600 rpm). Ethanol was then removed using a rotary evaporator (Rotavapor R II, Buchi, Switzerland) (55 °C).

4.3.4. CA-hordein/pectin nanoparticle complex fabrication

The carvacrol-hordein/pectin nanoparticle complex was synthesized using the same procedure as in section **2.1.1**. After rotary evaporation, CA-HNP dispersion was added to the 0.05% w/v pectin stock at a fixed ratio of 1:1. The mixture was continuously stirred at 900 rpm for 10 mins, followed by centrifugation (10,000 rpm, 5 mins, 23°C). Afterwards, freshly prepared CA-HNP and CA-HP-NPC dispersions were lyophilized, and the dried nanoparticle powders were stored at 3 °C for further analysis.

4.3.5. Effect of mass ratio of hordein-to-carvacrol

The particle size distribution and electric characteristics (ζ-potential) of freshly prepared CA-HNP and CA-HP-NPC dispersions with different hordein-to-carvacrol mass ratios (20:1, 10:1, and 5:1) was measured at pH 4 using a zetasizer equipped with dynamic light scattering (DLS) (Zetasizer Advanced Series, Malvern Panalytical, Westborough, MA, USA). Samples were diluted 50x with DI water prior to measurements to avoid multiple scattering effects.

4.3.6. Fourier transform infrared spectroscopy (FTIR)

FTIR spectra of non-encapsulated HNP, HP-NPC, CA-HNP and CA-HP-NPC were performed using a Fourier transform spectrophotometer (Jasco FT/IR-4100, Easton, MD, USA). The spectrum range was from 550 to 4000 cm-1 with 32 scans with a 4.0 cm-1 resolution.

4.3.7. Scanning electron microscopy (SEM)

The surface morphology of non-encapsulated HNP, HP-NPC, CA-HNP and CA-HP-NPC was investigated using a scanning electron microscope (SU-70, Hitachi, Japan) at an accelerating voltage of 10 kV. Samples were coated with a gold layer using a compact coating unit (CCU-010, Safematic, Switzerland) to avoid charging under the electron beam.

4.3.8. Encapsulation efficiency (EE)

The encapsulation efficiency (EE) of the carvacrol into HP-NPC at different mass ratios (20:1, 10:1, and 5:1) was carried out according to a method similar to Zheng et. al (2022), with slight modifications (Zheng et al., 2022). A standard curve was first established by dissolving carvacrol into absolute ethanol at different concentrations (0-20 µg/mL). The content of carvacrol was measured using an ultraviolet spectrophotometer (Life Science UV/Vis Spectrophotometer, Beckman Coulter, Brea, CA, USA) was used to measure the absorbance at a wavelength of 276 nm. The linear equation was $y = 0.033x + 0.0073$, where y was the absorbance value (A) and x was the concentration of the sample (C, µg/mL), R^2 (regression coefficient) was 0.9684.

To determine the amount of carvacrol loaded into the nanoparticle complex, 10 mg of dried CA-HP-NPC powders were dissolved in absolute ethanol and then rotary evaporated at 10,000 rpm for 10 mins. The supernatant was then diluted 10x using ethanol, and the absorbance was measured at 276 nm and ethanol was used as a blank. The encapsulation efficiency was calculated using the following formula:

$$\text{EE (\%)} = \frac{m1-m2}{m1} \text{ x } 100\%$$

Where m1 represents the total mass of CA in the nanoparticles, and m2 represents the dissociative mass of CA.

4.3.9. Dispersibility characterization

The water dispersibility of carvacrol, CA-HNP, and CA-HP-NPC was determined by dispersing 5 mg of carvacrol or powered nanoparticles into 25 mL DI water with constant stirring (600 rpm) for 2 hours. The particle size and PDI were determined by DLS.

4.3.10. Antimicrobial activity

The antimicrobial activity of CA-loaded nanoparticles was determined against non-pathogenic gram-negative *E. coli K12* and gram-positive *L. innocua.* Briefly, each bacterial was cultured from frozen stock into tryptic soy broth (TSB) overnight for 18-22 hours at 37 °C. The bacterial count was estimated to be around 10^7-10^8 CFU/mL. Afterwards, sterile nutrient broth mediums (10 mL) were seeded with bacterial strains (~10^6 CFU/mL) and each treatment was added at a concentration of 8% v/v. The nutrient broths containing the respective bacterial strains of *E. coli k12* and *L. innocua*, with the different treatments were placed in an orbital shaker (Orbital Shaker, Forma Scientific, Waltham, MA, USA) set at 130 rpm, 23°C for 24 hours. 100 µL samples of the test strains were plated onto nutrient agar at various time intervals (0, 12, and 24 hours) and colony counts were observed after 22-24 hours. Unencapsulated carvacrol was used as a positive control and compared to the various treatments which included: Hordein nanoparticles (HNP), hordein-pectin nanoparticle complex (HP-NPC), carvacrol-hordein nanoparticles (CA-HNP), and carvacrol-hordein/pectin nanoparticles (CA-HP-NPC).

4.3.11. Statistical analysis

The statistical analysis was performed using RStudio 2022.12.0 software (RStudio, Boston, MA, USA). Statistical differences were evaluated using one-way Analysis of Variance (ANOVA) between different groups using Tukey's post-hoc test with a statistical significance level of $p < 0.05$ for all comparisons. In certain conditions, Student's t-test assuming unequal variance was performed with a significance level of $p < 0.05$. All measured values were expressed as mean ± standard deviation of three independent replicates.

4.4. Results and Discussion

4.4.1. Effect of mass ratio of hordein-to-carvacrol

The effect of the mass ratio of hordein-to-carvacrol (20:1, 10,1, and 5:1) on the particle size, PDI, and ζ-potential of freshly prepared CA-HNP and CA-HP-NPC are shown in **Table 4-1**. The optimal mass ratio was seen at 5:1, where the smallest mean particle size was observed for both CA-HNP (136 ± 2 nm) and CA-HP-NPC (183 ± 2 nm). The largest particle size of around 231 and 231 nm was seen at a 10:1 mass ratio for CA-HNP and CA-HP-NPC, respectively. This increase in particle size may likely be attributed to the decreased absorption of carvacrol into the hordein matrix, which would have caused the leakage of carvacrol within the nanoparticle systems. No significant change ($p > 0.05$) in ζ-potential was observed at all mass ratios which indicates that increasing the concentration of carvacrol had no significant impact on the stability of the prepared nanoparticles.

Mass ratio of hordein-to-carvacrol	**Particle size (nm)**		**PDI**		**ζ-potential (mV)**	
	A	**B**	**A**	**B**	**A**	**B**

20:1	197 ± 2[b]	196 ± 9[b]	0.39 ± 0.02	0.30 ± 0.04	32 ± 1[a]	-17 ± 1[a]
10:1	231 ± 3[a]	231 ± 3[a]	0.33 ± 0.01	0.36 ± 0.01	34 ± 1[a]	-20 ± 4[a]
5:1	136 ± 2[c]	183 ± 2[c]	0.27 ± 0.02	0.25 ± 0.02	32 ± 3[a]	-18 ± 2[a]

Table 4-1. Effect of mass ratio of hordein-to-lutein (20:1, 10:1, 5:1) on the particle size, polydispersity index, and ζ-potential of A.) carvacrol-hordein nanoparticles (CA-HNP) and B.) carvacrol-hordein/pectin nanoparticle complex (CA-HP-NPC). Different superscripts in each column represent significance ($p < 0.05$) within each sample, respectively.

4.4.2. FTIR

The FTIR spectra of CA-HNP and CA-HP-NPC was compared to the spectra of unencapsulated HNP and HP-NPC to better understand the intermolecular interactions between the molecules (**Fig 4-1**). For unencapsulated HNP, major characteristic peaks were observed at 1640 cm^{-1} and 1533 cm^{-1} which correspond to amide I (1700-1600 cm^{-1}) and amide II bands (1600-1500 cm^{-1}), respectively (Miller et al., 2013). Strong vibrations were observed in the -OH region (~3279 cm^{-1}) for HP-NPC and a sharp peak observed at 1738 cm^{-1} correspond to the carbonyl group stretching of the ester groups present on pectin's galacturonic acid (GalA) residues (Sivam et al., 2012). Peaks observed at 1017 cm^{-1} and 1098 cm^{-1} in the HP-NPC spectra correspond to the C-O stretching in -COOH and O-H bending, respectively (Kamble et al., 2017). The carvacrol FTIR spectrum was not included in the study due to the difficulty of obtaining a powdered form, thus, the CA-HNP and CA-HP-NPC spectra were compared with results from other studies. For the CA-HNP spectra, peaks were observed at 813 cm^{-1} and 860 cm^{-1} which corresponds to the aromatic C-H bond associated with carvacrol's aromatic ring

structure (Shinde et al., 2020). For the CA-HP-NPC spectra, there was a shift in the -OH region from 3292 cm^{-1} (HP-NPC) to 3257 cm^{-1} (CA-HP-NPC) which may indicate the presence of newly formed hydrogen bonds. Hydrogen bonds could be generated between the amide groups of hordein's amino acid residues, hydroxyl groups of pectin, as well as the phenolic hydroxyl groups of carvacrol, as indicated by Shinde et. al (2020) (Shinde et al., 2020).

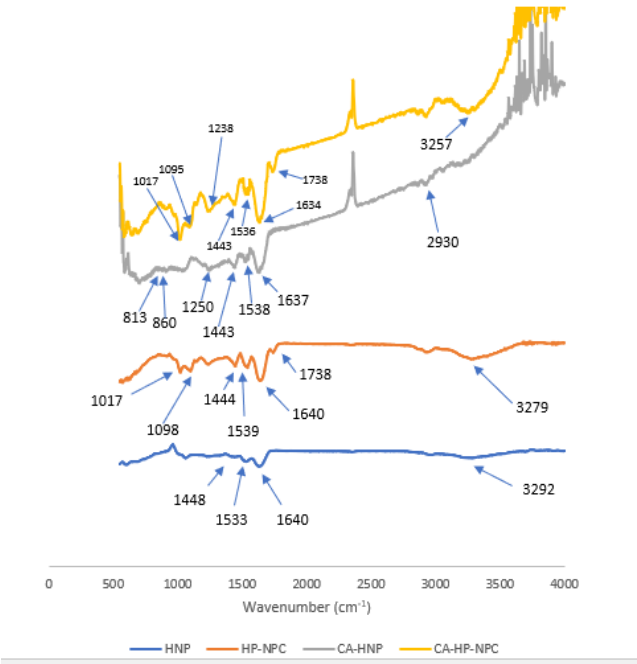

Fig 4-1. FTIR spectra of hordein nanoparticles (HNP), hordein-pectin nanoparticle complex (HP-NPC), carvacrol-hordein nanoparticles (CA-HNP), and carvacrol-hordein/pectin nanoparticle complex (CA-HP-NPC)

4.4.3. SEM

The SEM morphology of CA-HNP and CA-HP-NPC is shown in **Fig 4-2**. For CA-HNP, the distribution of the particles was compact but appeared smooth and spherical. The compactness of the particles can be a result of aggregation due to the drying process during the lyophilization process prior to SEM analysis. Proteins tend to aggregate during extended heat treatment times due to the structural changes causing the unfolding of the protein chains during heat treatment (Roy & Gupta, 2004). For CA-HP-NPC the morphology depicts an interconnected gel-like network containing irregular pore cavities. One proposed mechanism behind the gel-like network may be due to hydrogen bonds and hydrophobic interactions which have an influence on pectin's gel formation. High methoxyl HM) pectin was used in this study and they have been

shown to form junction zones by cross-linking of the homogalacturonan (HG) region by hydrogen bridges and hydrophobic forces between methoxyl groups, both favoring high sugar concentration and low pH in its gel formation (Gawkowska et al., 2018). Although sugar was not utilized as a cross-linking agent in this study, the nanoparticle dispersions were prepared using electrostatic deposition (pH 4). It is possible that the newly formed hydrogen bonds and hydrophobic-hydrophobic interactions between the molecules created a small gel-like network (Willats et al., 2006). However, further studies would need to be carried out to determine whether a gel-like network indeed developed, such as understanding its viscosity and mechanical strength.

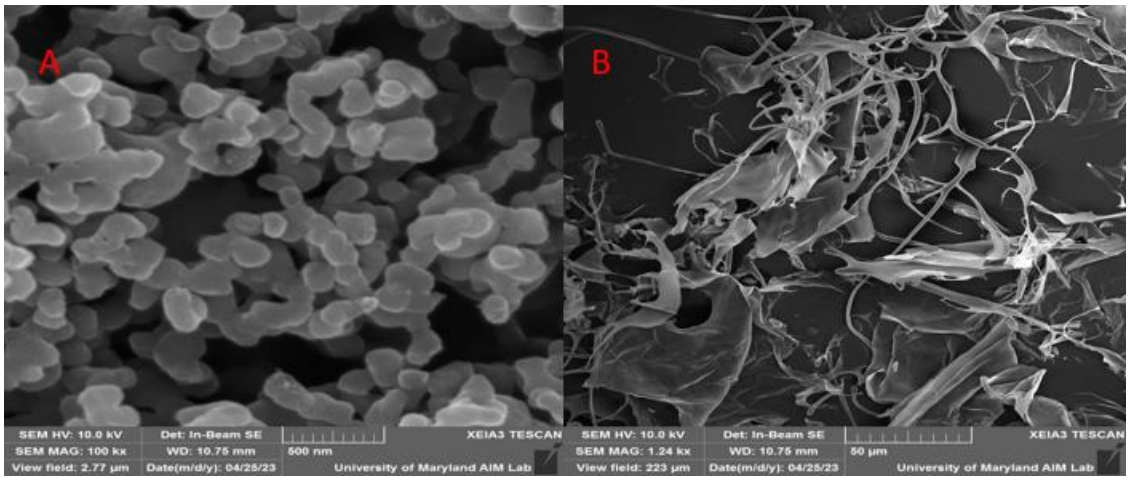

Fig 4-2. SEM images of A.) carvacrol-hordein nanoparticles (CA-HNP) and B.) carvacrol-hordein/pectin nanoparticle complex (CA-HP-NPC)

4.4.4. EE

The encapsulation efficiency (EE %) of CA-HNP and CA-HP-NPC at various mass ratios of hordein-to-carvacrol are shown in **Table 4-2**. The high encapsulation for both CA-HNP (71% ± 2) and CA-HP-NPC (70% ± 0) was shown at a hordein-to-carvacrol mass ratio of 5:1. No

differences ($p > 0.05$) were observed between CA-HNP and CA-HP-NPC at all mass ratios which indicates that hordein was the main force behind the encapsulation of carvacrol. This is similar to results obtained in chapter 2, where lutein was encapsulated into hordein/pectin nanoparticle complex. The incorporation of a pectin coating did not influence the encapsulation of lutein. Since hordein is abundant in hydrophobic amino acids, the encapsulation efficiency should not be influenced by pectin due to the strong affinity of carvacrol to interact with hordein through hydrophobic-hydrophobic interactions.

Mass Ratio (hordein:carvacrol)	**Encapsulation efficiency (%)**	
	A	**B**
20:1	70 ± 4^{aA}	70 ± 1^{aA}
10:1	63 ± 6^{bA}	62 ± 4^{bA}
5:1	71 ± 2^{aA}	70 ± 2^{bA}

Table 4-2. Encapsulation efficiency (%) of A.) carvacrol-hordein nanoparticles (CA-HNP) and B.) carvacrol-hordein/pectin nanoparticle complex (CA-HP-NPC). Different lowercase superscripts in each column represent statistical differences ($p < 0.05$) in encapsulation efficiency at different mass ratios for each respective sample. Different uppercase superscripts represent significant differences between each sample at the respective mass ratio. Values are represented as the mean ± standard deviation of at least three replicates.

4.4.5. Dispersibility

Dispersibility is an important characteristic of powders, and freeze drying is an essential step in food processing which can influence the stability and physical properties of functional ingredients (Zheng et al., 2022). Thus, the dispersibility of CA-HNP and CA-HP-NPC in an aqueous media after lyophilization was investigated (**Table 4-3**). Both CA-HNP (282 nm) and CA-HP-NPC (207 nm) showed significant increases ($p < 0.05$) in particle size post-lyophilization, compared to their dispersibility pre-lyophilization (~ 138 and 183 nm, respectively). This agrees with the results obtained showing increase in polydispersity index (PDI) for both CA-HNP (~ 0.34) and CA-HP-NPC (~ 0.30) in which the particle size distribution became more polydisperse due to aggregation. The surface charge (ζ-potential) of CA-HP-NPC (-17 mV) was not affected by the lyophilization process compared ($p > 0.05$) to CA-HNP (+16 mV). The change in ζ-potential for CA-HNP post-lyophilization could be explained by the physiochemical changes of proteins subjected to various processing techniques. Increased temperatures during the drying process may have caused irreversible changes in the hordein molecule which can cause the structural changes such as the unfolding of protein chains that were buried in the native structure (Roy & Gupta, 2004). However, the ζ-potential CA-HP-NPC was not affected by lyophilization which could indicate that the pectin coating acting as a lyoprotectant. Pectin contains neural sugars such as arabinose, galactose, and rhamnose in its rhamnogalacturonan I (RG-I) and rhamnogalacturonan II (RG-II) regions. Carpenter and Crow (1998) indicate that carbohydrates can protect proteins by hydrogen bonding, a role displayed by water molecules which are removed during drying (Carpenter & Crowe, 1988).

	Particle size (nm)		**PDI**		**ζ-potential**	
	Before	**After**	**Before**	**After**	**Before**	**After**
CA-HNP	136 ± 2^{a}	282 ± 3^{b}	0.27 ± 0.02	0.34 ± 0	32 ± 3^{a}	$16 + 2^{b}$

CA-HP-NPC	183 ± 2[a]	207 ± 8[b]	0.25 ± 0.02	0.30 ± 0	-18 ± 2[a]	-17 ± 2[b]

Table 4-3. Average particle size (nm), polydispersity index (PDI), and ζ-potential of carvacrol-hordein nanoparticles (CA-HNP) and carvacrol-hordein/pectin nanoparticle complex (CA-HP-NPC) before and after lyophilization. Different superscripts in each column represents significant differences ($p < 0.05$) before and after lyophilization for respective samples.

4.4.6. Antimicrobial activity

The antimicrobial activity of carvacrol, HNP, HP-NPC, CA-HNP, and CA-HP-NPC was investigated against gram-positive *L. innocua* and gram-negative *E. coli K12* and the colony counts were determined at various time intervals (0, 12, and 24 hours) (**Table 4-4**). Carvacrol was used as the control due to its antimicrobial activity which is explained by the interaction of lipophilic carvacrol which can cause dramatic changes to the phospholipid membrane components of microorganisms (Wu et al., 2012). However, after 12 and 24 hours, the plates were too numerous to count (TNTC), and lawn streaks were observed for all treatments (**Fig 4-3**) (except carvacrol). No observed antimicrobial effects were shown with the various treatments which might be due to the entrapment of carvacrol into the nanoparticle matrix which slowed its release rate. Although the release kinetics of carvacrol from the fabricated nanoparticles was not investigated, it's possible its slow-release rate in this study led to no antimicrobial activity after 24 hours. One study by Oliveira et. al (2014) developed alginate/cashew gum nanoparticles for the encapsulation of *Lippia siodoides* (LS), an essential oil primarily composed of thymol (50-70%). Their results indicated that the maximal release (plateau) of the LS oil from the nanoparticles was achieved at around 30-50 hours (de Oliveira et al., 2014).

Another proposed mechanism behind the lack of antimicrobial activity may be because no real conditions were met to allow the carvacrol oil to release from the nanoparticle matrix. In this study, zones of inhibition of the various treatments were also investigated (**Fig 4-4**) and no zone of inhibition was observed which could be the lack of carvacrol escaping the nanoparticle matrices. The release of encapsulated bioactive compounds from nanoparticles usually occurs due to environmental stress (pH, heat, or salt) or enzymatic or physical changes that would cause the nanoparticle matrix to swell or aggregate, causing the release of the bioactive compound (Martínez-Ballesta et al., 2018). In this study, although the treatments were subjected to physical stress, the stress imposed was very little (~ 130 rpm) which could explain the slow/lack of release of carvacrol. Further studies will need to be conducted to determine the release of carvacrol from both hordein and hordein/pectin nanoparticles to enhance its applications.

Treatments	***E. coli K12* (log 10 cfu/ml)**			***L. innocua* (log 10 cfu/ml)**		
	Time (h)					
	0	**12**	**24**	**0**	**12**	**24**
A	0	0	0	0	0	0
B	0	0	0	0	0	0
C	4.2	TNTC	TNTC	TNTC	TNTC	TNTC
D	3.6	TNTC	TNTC	TNTC	TNTC	TNTC
E	4.1	TNTC	TNTC	TNTC	TNTC	TNTC
F	3.6	TNTC	TNTC	TNTC	TNTC	TNTC

G	3.8	TNTC	TNTC	TNTC	TNTC	TNTC
H	3.4	TNTC	TNTC	TNTC	TNTC	TNTC
I	4.2	TNTC	TNTC	TNTC	TNTC	TNTC
J	3.5	TNTC	TNTC	TNTC	TNTC	TNTC

Table 4-4. Total colony counts of E. coli K12 and L. innocua after subjected to various treatments. The following letters represent the different treatments which are: A.) Carvacrol (control) + E. coli K12; B.) Carvacrol (control) + L. innocua; C.) hordein nanoparticle (HNP) + E. coli K12; D.) hordein nanoparticle (HNP) + L. innocua; E.) hordein-pectin nanoparticle complex (HP-NPC) + E. coli K12; F.) hordein-pectin nanoparticle complex (HP-NPC) + L. innocua; G.) carvacrol-hordein nanoparticles (CA-HNP) + E. coli K12; H.) carvacrol-hordein nanoparticles (CA-HNP) + L. innocua; I.) carvacrol-hordein/pectin nanoparticle complex (CA-HP-NPC) + E. coli K12; and J.) carvacrol-hordein/pectin nanoparticle complex (CA-HP-NPC) + L. innocua

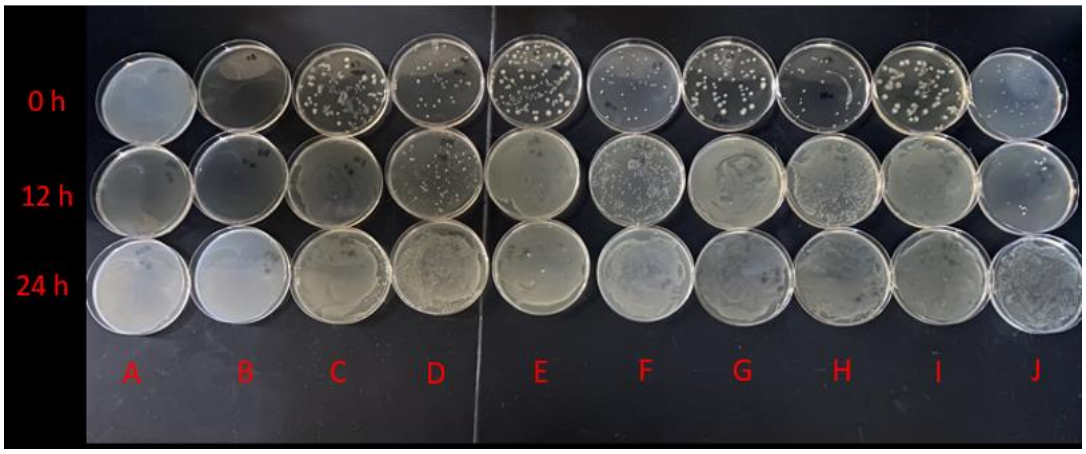

Fig 4-3. Visual representation of nutrient agars inoculated with E. coli K12, L. innocua and various treatments. The different time intervals (0, 12, and 24 hours) are represented from top to bottom in that respective order. The bacteria with different treatments are represented from left to right where: A.) Carvacrol (control) + E. coli K12; B.) Carvacrol (control) + L. innocua; C.) hordein nanoparticle (HNP) + E. coli K12; D.) hordein nanoparticle (HNP) + L. innocua; E.) hordein-pectin nanoparticle complex (HP-NPC) + E. coli K12; F.) hordein-pectin nanoparticle complex (HP-NPC) + L. innocua; G.) carvacrol-hordein nanoparticles (CA-HNP) + E. coli K12; H.) carvacrol-hordein nanoparticles (CA-HNP) + L. innocua; I.) carvacrol-hordein/pectin nanoparticle complex (CA-HP-NPC) + E. coli K12; and J.) carvacrol-hordein/pectin nanoparticle complex (CA-HP-NPC) + L. innocua

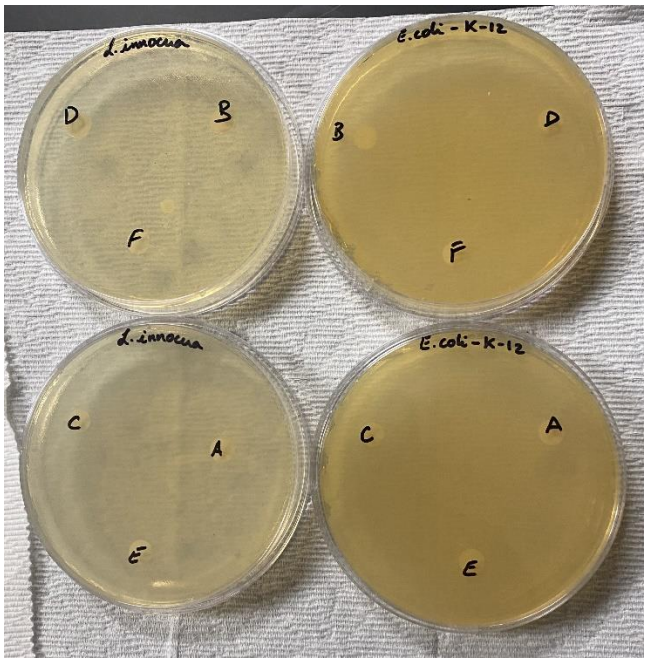

Fig 4-4. Visual representation of the zone of inhibition against gram-positive L. innocua and gram-negative E. coli K12. The following treatments are represented as: A.) DI water; B.) 0.1% peptone water; C.) hordein nanoparticles (HNP); D.) hordein-pectin

nanoparticle complex (HP-NPC); E; carvacrol-hordein nanoparticles (CA-HNP); and F.) carvacrol-hordein/pectin nanoparticle complex (CA-HP-NPC)

4.5. Conclusion

In this objective, carvacrol-hordein/pectin nanoparticle complex was synthesized using an anti-solvent precipitation with electrostatic deposition method (pH 4). The encapsulated nanoparticle complex was prepared at various mass ratios of hordein-to-carvacrol. The optimal ratio to obtain the smallest particle size (183 nm) was observed at a hordein-to-carvacrol mass ratio of 5:1. It was indicated that hydrogen bonding was the driving force behind the intermolecular interaction between pectin, hordein, and carvacrol. The Pectin coating was able to enhance the solubility of carvacrol in an aqueous, while still maintaining a relatively small particle size (207 nm) post-lyophilization. However, there are a few limitations to the study that need to be addressed. First off, carvacrol was not able to be released into the nutrient broth containing either *E. coli K12* or *L. innocua*, which limits its applications as a functional ingredient for enhanced anti-microbial activity. It is proposed that carvacrol was still trapped inside the nanoparticle matrix with no means of escaping. Further studies would have to be conducted to better understand the release kinetics of carvacrol from the nanoparticle matrix and whether certain stresses (pH, temperature, salt, physical, or enzymatic changes) can enhance its release rate. Also in this study, the carvacrol-encapsulated nanoparticles were not applied to actual foods which may also limit its real-life applications. Further studies such developing emulsions which are widely applied to the food industry or developing active films using carvacrol-hordein/pectin nanoparticles will better highlight its functionalities. In the future, further studies can also be done to highlight many benefits of carvacrol such as its antioxidant, anticancer, and anti-inflammatory properties.

Chapter 5. Summary and future perspectives

Food nanotechnology is a promising field with projected market growth for its various applications in the food industry. The small particle size, high surface-to-volume ratio and pore-interconnectivity are beneficial to its wide applications in the food industry. Food polymers are gaining interest due to their easy manipulation, non-toxicity, low-cost, biodegradability, and environmental sustainability.

The low cost of using food polymers is due to their wide abundance in nature and their non-toxic nature makes it suitable for consumer preferences. The fortification of food products has gained attention due to consumer awareness of diets high in nutritional value. Many foods contain essential nutrients and vitamins, however, many of those compounds are not absorbed into the GIT due to their low-solubility and susceptibility to enzymatic degradation.

Encapsulation systems utilizing food polymers are popular because the bioavailability and solubility of the encapsulated bioactive compound may be mitigated by the properties of food polymers because of their easy manipulation which gives them unique functionalities for encapsulation purposes. The benefits of using food polymers are mainly attributed to their non-toxicity as compared to non-organic materials. However, food polymers such as proteins are often susceptible to aggregation at their pI which makes their applications limited. Polysaccharides can be used as coating materials in the fabrication of nanoparticles. Polysaccharides such as pectin, can develop gels in acidic media or with divalent cations (Ca^{2+}) depending on their degree of DE. The ability to develop gels is beneficial for the controlled release of bioactive compounds into target sites in the body.

When developing nanoparticles from food polymers, it is important to understand the properties of the food polymers, as well as the parameters to fabricate nanoparticles derived from them. One of the essential factors in developing a delivery system is to understand the release kinetics which will allow the bioactive compound to achieve its functional properties. It is essential to promote healthy beneficial foods in a world that is increasing in population. With the increase in climate change and deterioration of the environment, we as humans need to figure out a way to create healthier food options, while creating a more sustainable environment.

Bibliography

Abd Elgadir, M., Uddin, M. S., Ferdosh, S., Adam, A., Chowdhury, A. J. K., & Sarker, M. Z. I. (2015). Impact of chitosan composites and chitosan nanoparticle composites on various drug delivery systems: A review. *Journal of food and drug analysis*, *23*(4), 619-629.

Abdel-Aal, E.-S. M., Akhtar, H., Zaheer, K., & Ali, R. (2013). Dietary sources of lutein and zeaxanthin carotenoids and their role in eye health. *Nutrients*, *5*(4), 1169-1185.

Abid, N., Khan, A. M., Shujait, S., Chaudhary, K., Ikram, M., Imran, M., . . . Maqbool, M. (2022). Synthesis of nanomaterials using various top-down and bottom-up approaches, influencing factors, advantages, and disadvantages: A review. *Advances in Colloid and Interface Science*, *300*, 102597.

Adib A, M., Riad A, B., & Florence N, F. (2009). Xanthophylls and eye health of infants and adults.

Ahmad, A., Saeed, M., & Ansari, I. A. (2021). Molecular insights on chemopreventive and anticancer potential of carvacrol: Implications from solid carcinomas. *Journal of Food Biochemistry*, *45*(12), e14010.

Al-Zamil, W. M., & Yassin, S. A. (2017). Recent developments in age-related macular degeneration: a review. *Clinical interventions in aging*, 1313-1330.

Aman Mohammadi, M., Dakhili, S., Mirza Alizadeh, A., Kooki, S., Hassanzadazar, H., Alizadeh-Sani, M., & McClements, D. J. (2022). New perspectives on electrospun nanofiber applications in smart and active food packaging materials. *Critical Reviews in Food Science and Nutrition*, 1-17.

Amaral, D. F., & Bhargava, K. (2015). Essential oil nanoemulsions and food applications. *Adv Food Technol Nutr Sci Open J*, *1*(4), 84-87.

Anderson, O. D. (2013). The B-hordein prolamin family of barley. *Genome*, *56*(3), 179-185.

Anusha, R., & Priya, S. (2022). Dietary Exosome-Like Nanoparticles: An Updated Review on Their Pharmacological and Drug Delivery Applications. *Molecular Nutrition & Food Research*, *66*(14), 2200142.

Arole, V., & Munde, S. (2014). Fabrication of nanomaterials by top-down and bottom-up approaches-an overview. *J. Mater. Sci*, *1*, 89-93.

Astani, A., Reichling, J., & Schnitzler, P. (2010). Comparative study on the antiviral activity of selected monoterpenes derived from essential oils. *Phytotherapy Research: An International Journal Devoted to Pharmacological and Toxicological Evaluation of Natural Product Derivatives*, *24*(5), 673-679.

Aswathanarayan, J. B., & Vittal, R. R. (2019). Nanoemulsions and their potential applications in food industry. *Frontiers in Sustainable Food Systems*, *3*, 95.

Bamdad, F., Wu, J., & Chen, L. (2011). Effects of enzymatic hydrolysis on molecular structure and antioxidant activity of barley hordein. *Journal of Cereal Science*, *54*(1), 20-28.

Bazana, M. T., Codevilla, C. F., & de Menezes, C. R. (2019). Nanoencapsulation of bioactive compounds: Challenges and perspectives. *Current opinion in food science*, *26*, 47-56.

BeMiller, J. N. (1986). An introduction to pectins: structure and properties. In. ACS Publications.

Biesalski, H.-K., Dragsted, L. O., Elmadfa, I., Grossklaus, R., Müller, M., Schrenk, D., . . . Weber, P. (2009). Bioactive compounds: Definition and assessment of activity. *Nutrition*, *25*(11-12), 1202-1205.

Bischof, J. C., & He, X. (2006). Thermal stability of proteins. *Annals of the New York Academy of Sciences*, *1066*(1), 12-33.

Bondu, C., & Yen, F. T. (2022). Nanoliposomes, from food industry to nutraceuticals: Interests and uses. *Innovative Food Science & Emerging Technologies*, 103140.

Boostani, S., Hosseini, S. M. H., Golmakani, M.-T., Marefati, A., Hadi, N. B. A., & Rayner, M. (2020). The influence of emulsion parameters on physical stability and rheological properties of Pickering emulsions stabilized by hordein nanoparticles. *Food Hydrocolloids*, *101*, 105520.

Boostani, S., Hosseini, S. M. H., Yousefi, G., Riazi, M., Tamaddon, A.-M., & Van der Meeren, P. (2019). The stability of triphasic oil-in-water Pickering emulsions can be improved by physical modification of hordein-and secalin-based submicron particles. *Food Hydrocolloids*, *89*, 649-660.
Brandt, A., Montembault, A., Cameron-Mills, V., & Rasmussen, S. K. (1985). Primary structure of a B1 hordein gene from barley. *Carlsberg research communications*, *50*, 333-345.
Broomes, J., & Badrie, N. (2010). Effects of low-methoxyl pectin on physicochemical and sensory properties of reduced-calorie sorrel/roselle (Hibiscus sabdariffa L.) jams. *The Open Food Science Journal*, *4*(1).
Bulman, P., Zarkadas, C. G., & Smith, D. L. (1994). Nitrogen fertilizer affects amino acid composition and quality of spring barley grain. *Crop Science*, *34*(5), 1341-1346.
Calzolai, L., Gilliland, D., & Rossi, F. (2012). Measuring nanoparticles size distribution in food and consumer products: a review. *Food Additives & Contaminants: Part A*, *29*(8), 1183-1193.
Campos, M. R. S. (2018). *Bioactive compounds: health benefits and potential applications*. Woodhead Publishing.
Cao, L., Lu, W., Mata, A., Nishinari, K., & Fang, Y. (2020). Egg-box model-based gelation of alginate and pectin: A review. *Carbohydrate polymers*, *242*, 116389.
Carpenter, J. F., & Crowe, J. H. (1988). The mechanism of cryoprotection of proteins by solutes. *Cryobiology*, *25*(3), 244-255.
Celebioglu, A., Yildiz, Z. I., & Uyar, T. (2018). Thymol/cyclodextrin inclusion complex nanofibrous webs: Enhanced water solubility, high thermal stability and antioxidant property of thymol. *Food research international*, *106*, 280-290.
Chau, C.-F., Wu, S.-H., & Yen, G.-C. (2007). The development of regulations for food nanotechnology. *Trends in Food Science & Technology*, *18*(5), 269-280.
Chen, H.-C., Lin, C.-W., & Chen, M.-J. (2005). The effects of freeze drying and rehydration on survival of microorganisms in kefir. *Asian-australasian journal of animal sciences*, *19*(1), 126-130.
Chen, J., Liu, W., Liu, C.-M., Li, T., Liang, R.-H., & Luo, S.-J. (2015). Pectin modifications: a review. *Critical reviews in food science and nutrition*, *55*(12), 1684-1698.
Cheng, C. J., & Jones, O. G. (2017). Stabilizing zein nanoparticle dispersions with ι-carrageenan. *Food Hydrocolloids*, *69*, 28-35.
Chi, E. Y., Krishnan, S., Randolph, T. W., & Carpenter, J. F. (2003). Physical stability of proteins in aqueous solution: mechanism and driving forces in nonnative protein aggregation. *Pharmaceutical research*, *20*, 1325-1336.
Cho, S.-Y., & Rhee, C. (2009). Functional and film-forming properties of fractionated barley proteins. *Food Science and Biotechnology*, *18*(4), 889-894.
Coupland, J. N., Shaw, N. B., Monahan, F. J., O'Riordan, E. D., & O'Sullivan, M. (2000). Modeling the effect of glycerol on the moisture sorption behavior of whey protein edible films. *Journal of food engineering*, *43*(1), 25-30.
da Silva Lima, M., Quintans-Junior, L. J., de Santana, W. A., Kaneto, C. M., Soares, M. B. P., & Villarreal, C. F. (2013). Anti-inflammatory effects of carvacrol: evidence for a key role of interleukin-10. *European journal of pharmacology*, *699*(1-3), 112-117.
Dasgupta, N., Ranjan, S., & Gandhi, M. (2019). Nanoemulsions in food: Market demand. *Environmental Chemistry Letters*, *17*, 1003-1009.
de Oliveira, E. F., Paula, H. C., & de Paula, R. C. (2014). Alginate/cashew gum nanoparticles for essential oil encapsulation. *Colloids and Surfaces B: Biointerfaces*, *113*, 146-151.
de Oliveira Mallia, J., Galea, R., Nag, R., Cummins, E., Gatt, R., & Valdramidis, V. (2022). Nanoparticle food applications and their toxicity: current trends and needs in risk assessment strategies. *Journal of Food Protection*, *85*(2), 355-372.
De Queiroz, J. L. C., Costa, R. O. D. A., Matias, L. L. R., De Medeiros, A. F., Gomes, A. F. T., Pais, T. D. S., . . . Morais, A. H. D. A. (2018). Chitosan-whey protein nanoparticles improve encapsulation efficiency and stability of a trypsin inhibitor isolated from Tamarindus indica L. *Food Hydrocolloids*, *84*, 247-256.

de Ruiter, J., & Karl, D. (2001). The influence of nitrogen and sulphur fertiliser on amino acid composition of wheat and barley grain. 31st Joint NZIAS/NZSHS Annual Conference Conference Location CANTERBURY, NEW ZEALAND,

de Souza, R. L., Dantas, A. G. B., de Oliveira Melo, C., Felício, I. M., & Oliveira, E. E. (2022). Nanotechnology as a tool to improve the biological activity of carvacrol: A review. *Journal of Drug Delivery Science and Technology*, 103834.

do Prado Silva, J. T., da Silva, A. C., Geiss, J. M. T., de Araújo, P. H. H., Becker, D., Bracht, L., . . . Gonçalves, O. H. (2017). Analytical validation of an ultraviolet–visible procedure for determining lutein concentration and application to lutein-loaded nanoparticles. *Food chemistry*, *230*, 336-342.

Duclairoir, C., Orecchioni, A., Depraetere, P., & Nakache, E. (2002). α-Tocopherol encapsulation and in vitro release from wheat gliadin nanoparticles. *Journal of microencapsulation*, *19*(1), 53-60.

EFSA, A. (2012). Panel (EFSA Panel on Food Additives and Nutrient Sources added to Food), 2012. *Guidance for submission for food additive evaluations. EFSA Journal*, *10*(7), 2760.

Elshahed, M. S., Miron, A., Aprotosoaie, A. C., & Farag, M. A. (2021). Pectin in diet: Interactions with the human microbiome, role in gut homeostasis, and nutrient-drug interactions. *Carbohydrate Polymers*, *255*, 117388.

Ezz-Eldin, Y. M., Aboseif, A. A., & Khalaf, M. M. (2020). Potential anti-inflammatory and immunomodulatory effects of carvacrol against ovalbumin-induced asthma in rats. *Life sciences*, *242*, 117222.

Eça, K. S., Machado, M. T., Hubinger, M. D., & Menegalli, F. C. (2015). Development of active films from pectin and fruit extracts: Light protection, antioxidant capacity, and compounds stability. *Journal of food science*, *80*(11), C2389-C2396.

Forde, B. G., Kreis, M., Williamson, M. S., Fry, R. P., Pywell, J., Shewry, P. R., . . . Miflin, B. J. (1985). Short tandem repeats shared by B-and C-hordein cDNAs suggest a common evolutionary origin for two groups of cereal storage protein genes. *The EMBO Journal*, *4*(1), 9-15.

Frede, K., Ebert, F., Kipp, A. P., Schwerdtle, T., & Baldermann, S. (2017). Lutein activates the transcription factor Nrf2 in human retinal pigment epithelial cells. *Journal of Agricultural and Food Chemistry*, *65*(29), 5944-5952.

Freitas, C. M. P., Coimbra, J. S. R., Souza, V. G. L., & Sousa, R. C. S. (2021). Structure and applications of pectin in food, biomedical, and pharmaceutical industry: A review. *Coatings*, *11*(8), 922.

Gawkowska, D., Cybulska, J., & Zdunek, A. (2018). Structure-related gelling of pectins and linking with other natural compounds: A review. *Polymers*, *10*(7), 762.

Gentile, L. (2020). Protein–polysaccharide interactions and aggregates in food formulations. *Current Opinion in Colloid & Interface Science*, *48*, 18-27.

Giroux, H. J., & Britten, M. (2011). Encapsulation of hydrophobic aroma in whey protein nanoparticles. *Journal of Microencapsulation*, *28*(5), 337-343.

Goswami, P., & Mathur, J. (2019). Positive and negative effects of nanoparticles on plants and their applications in agriculture. *Plant Science Today*, *6*(2), 232-242.

He, A., Guan, X., Song, H., Li, S., & Huang, K. (2020). Encapsulation of (−)-epigallocatechin-gallate (EGCG) in hordein nanoparticles. *Food Bioscience*, *37*, 100727.

Hong, S., Choi, D. W., Kim, H. N., Park, C. G., Lee, W., & Park, H. H. (2020). Protein-based nanoparticles as drug delivery systems. *Pharmaceutics*, *12*(7), 604.

Hu, K., Huang, X., Gao, Y., Huang, X., Xiao, H., & McClements, D. J. (2015). Core–shell biopolymer nanoparticle delivery systems: Synthesis and characterization of curcumin fortified zein–pectin nanoparticles. *Food chemistry*, *182*, 275-281.

Hu, K., & McClements, D. J. (2015). Fabrication of biopolymer nanoparticles by antisolvent precipitation and electrostatic deposition: Zein-alginate core/shell nanoparticles. *Food Hydrocolloids*, *44*, 101-108.

Hua, C., Yu, W., Yang, M., Cai, Q., Gao, T., Zhang, S., . . . Liu, Y. (2021). Casein-pectin nanocomplexes as a potential oral delivery system for improving stability and bioactivity of curcumin. *Colloid and Polymer Science*, *299*, 1557-1566.

Huang, X., Huang, X., Gong, Y., Xiao, H., McClements, D. J., & Hu, K. (2016). Enhancement of curcumin water dispersibility and antioxidant activity using core–shell protein–polysaccharide nanoparticles. *Food Research International*, *87*, 1-9.

Huang, X., Liu, Y., Zou, Y., Liang, X., Peng, Y., McClements, D. J., & Hu, K. (2019). Encapsulation of resveratrol in zein/pectin core-shell nanoparticles: Stability, bioaccessibility, and antioxidant capacity after simulated gastrointestinal digestion. *Food Hydrocolloids*, *93*, 261-269.

Imran, M., Aslam, M., Alsagaby, S. A., Saeed, F., Ahmad, I., Afzaal, M., . . . Khames, A. (2022). Therapeutic application of carvacrol: A comprehensive review. *Food Science & Nutrition*, *10*(11), 3544-3561.

Ishwarya S, P., & Nisha, P. (2022). Advances and prospects in the food applications of pectin hydrogels. *Critical reviews in food science and nutrition*, *62*(16), 4393-4417.

Islam, F., Amer Ali, Y., Imran, A., Afzaal, M., Zahra, S. M., Fatima, M., . . . Mehta, S. (2023). Vegetable proteins as encapsulating agents: Recent updates and future perspectives. *Food Science & Nutrition*.

Jaeger, A., Zannini, E., Sahin, A. W., & Arendt, E. K. (2021). Barley protein properties, extraction and applications, with a focus on brewers' spent grain protein. *Foods*, *10*(6), 1389.

Jamali, S. N., Assadpour, E., & Jafari, S. M. (2020). Formulation and application of nanoemulsions for nutraceuticals and phytochemicals. *Current Medicinal Chemistry*, *27*(18), 3079-3095.

Jeena, K., Liju, V. B., Viswanathan, R., & Kuttan, R. (2014). Antimutagenic potential and modulation of carcinogen-metabolizing enzymes by ginger essential oil. *Phytotherapy Research*, *28*(6), 849-855.

Jitpukdeebodintra, S., & Jangwang, A. (2009). Instant noodles with pectin for weight reduction. *Journal of Food, Agriculture & Environment*, *7*(3-4), 126-129.

Johnson, E. J. (2014). Role of lutein and zeaxanthin in visual and cognitive function throughout the lifespan. *Nutrition reviews*, *72*(9), 605-612.

Jones, O. G., Decker, E. A., & McClements, D. J. (2010). Comparison of protein–polysaccharide nanoparticle fabrication methods: Impact of biopolymer complexation before or after particle formation. *Journal of Colloid and Interface Science*, *344*(1), 21-29.

Joye, I. J., & McClements, D. J. (2014). Biopolymer-based nanoparticles and microparticles: Fabrication, characterization, and application. *Current opinion in colloid & interface science*, *19*(5), 417-427.

Joye, I. J., Nelis, V. A., & McClements, D. J. (2015). Gliadin-based nanoparticles: Stabilization by post-production polysaccharide coating. *Food Hydrocolloids*, *43*, 236-242.

Kalita, P., Singh, J., Kumar Singh, M., Solanki, P. R., Sumana, G., & Malhotra, B. (2012). Ring like self assembled Ni nanoparticles based biosensor for food toxin detection. *Applied physics letters*, *100*(9), 093702.

Kamble, P. B., Gawande, S., & Patil, T. S. (2017). Extraction of pectin from unripe banana peel. *International Research Journal of Engineering and Technology*, *4*(7), 2259-2264.

Kapp, G. R., & Bamforth, C. W. (2002). The foaming properties of proteins isolated from barley. *Journal of the Science of Food and Agriculture*, *82*(11), 1276-1281.

Kaya-Celiker, H., & Mallikarjunan, K. (2012). Better nutrients and therapeutics delivery in food through nanotechnology. *Food engineering reviews*, *4*, 114-123.

Khairallah, M., Kahloun, R., Bourne, R., Limburg, H., Flaxman, S. R., Jonas, J. B., . . . Pesudovs, K. (2015). Number of people blind or visually impaired by cataract worldwide and in world regions, 1990 to 2010. *Investigative ophthalmology & visual science*, *56*(11), 6762-6769.

Khan, I., Bahuguna, A., Kumar, P., Bajpai, V. K., & Kang, S. C. (2018). In vitro and in vivo antitumor potential of carvacrol nanoemulsion against human lung adenocarcinoma A549 cells via mitochondrial mediated apoptosis. *Scientific reports*, *8*(1), 1-15.

Kocira, A., Kozłowicz, K., Panasiewicz, K., Staniak, M., Szpunar-Krok, E., & Hortyńska, P. (2021). Polysaccharides as edible films and coatings: Characteristics and influence on fruit and vegetable quality—A review. *Agronomy*, *11*(5), 813.

Koushan, K., Rusovici, R., Li, W., Ferguson, L. R., & Chalam, K. V. (2013). The role of lutein in eye-related disease. *Nutrients*, *5*(5), 1823-1839.

Kuivanen, J., Penttilä, M., & Richard, P. (2015). Metabolic engineering of the fungal D-galacturonate pathway for L-ascorbic acid production. *Microbial Cell Factories*, *14*(1), 1-9.

Kumar, P., Mahajan, P., Kaur, R., & Gautam, S. (2020). Nanotechnology and its challenges in the food sector: A review. *Materials Today Chemistry*, *17*, 100332.

Kumar, T. S. M., Kumar, K. S., Rajini, N., Siengchin, S., Ayrilmis, N., & Rajulu, A. V. (2019). A comprehensive review of electrospun nanofibers: Food and packaging perspective. *Composites Part B: Engineering*, *175*, 107074.

Kuznetcova, D. V., Linder, M., Jeandel, C., Paris, C., Desor, F., Baranenko, D. A., . . . Yen, F. T. (2020). Nanoliposomes and nanoemulsions based on chia seed lipids: Preparation and characterization. *International Journal of Molecular Sciences*, *21*(23), 9079.

Lammari, N., Louaer, O., Meniai, A. H., & Elaissari, A. (2020). Encapsulation of essential oils via nanoprecipitation process: Overview, progress, challenges and prospects. *Pharmaceutics*, *12*(5), 431.

Li, D., Zhang, R., Liu, G., Kang, Y., & Wu, J. (2020). Redox-responsive self-assembled nanoparticles for cancer therapy. *Advanced healthcare materials*, *9*(20), 2000605.

Li, F., Li, X., Huang, K., Luo, Y., & Mei, X. (2021). Preparation and characterization of pickering emulsion stabilized by hordein-chitosan complex particles. *Journal of Food Engineering*, *292*, 110275.

Li, H., Wang, D., Liu, C., Zhu, J., Fan, M., Sun, X., . . . Cao, Y. (2019). Fabrication of stable zein nanoparticles coated with soluble soybean polysaccharide for encapsulation of quercetin. *Food Hydrocolloids*, *87*, 342-351.

Li, H., Wang, T., Hu, Y., Wu, J., & Van der Meeren, P. (2022). Designing delivery systems for functional ingredients by protein/polysaccharide interactions. *Trends in Food Science & Technology*, *119*, 272-287.

Li, H., Yuan, Y., Zhu, J., Wang, T., Wang, D., & Xu, Y. (2020). Zein/soluble soybean polysaccharide composite nanoparticles for encapsulation and oral delivery of lutein. *Food Hydrocolloids*, *103*, 105715.

Li, S., Wang, C., Fu, X., Li, C., He, X., Zhang, B., & Huang, Q. (2018). Encapsulation of lutein into swelled cornstarch granules: Structure, stability and in vitro digestion. *Food chemistry*, *268*, 362-368.

Li, S., Yan, Y., Guan, X., & Huang, K. (2020). Preparation of a hordein-quercetin-chitosan antioxidant electrospun nanofibre film for food packaging and improvement of the film hydrophobic properties by heat treatment. *Food Packaging and Shelf Life*, *23*, 100466.

Li, X., & de Vries, R. (2018). Interfacial stabilization using complexes of plant proteins and polysaccharides. *Current Opinion in Food Science*, *21*, 51-56.

Li, Y., Guo, X., Lin, P., Fan, C., & Song, Y. (2010). Preparation and functional properties of blend films of gliadins and chitosan. *Carbohydrate Polymers*, *81*(2), 484-490.

Li, Y., Zhang, Y., Liu, X., Wang, M., Wang, P., Yang, J., & Zhang, S. (2018). Lutein inhibits proliferation, invasion and migration of hypoxic breast cancer cells via downregulation of HES1. *International Journal of Oncology*, *52*(6), 2119-2129.

Liang, X., Cao, K., Li, W., Li, X., McClements, D. J., & Hu, K. (2021). Tannic acid-fortified zein-pectin nanoparticles: Stability, properties, antioxidant activity, and in vitro digestion. *Food Research International*, *145*, 110425.

Linko, R., Lapvetelainen, A., Laakso, P., & Kallio, H. (1989). Protein composition of a high-protein barley flour and barley grain. *Cereal Chem*, *66*(6), 478-482.

Liu, F., Ma, C., McClements, D. J., & Gao, Y. (2017). A comparative study of covalent and non-covalent interactions between zein and polyphenols in ethanol-water solution. *Food Hydrocolloids*, *63*, 625-634.
Liu, G., Zhou, Y., & Chen, L. (2019). Intestinal uptake of barley protein-based nanoparticles for β-carotene delivery. *Acta pharmaceutica sinica B*, *9*(1), 87-96.
Ma, X.-Y., Chen, X.-X., Ma, M.-Y., Xu, Y., Wu, X.-M., Mu, G.-Q., & Zhu, X.-M. (2021). Lutein transport systems loaded with rice protein-based self-assembled nanoparticles. *Food Bioscience*, *42*, 101061.
Maria, A. G., Graziano, R., & Nicolantonio, D. O. (2015). Carotenoids: potential allies of cardiovascular health? *Food & nutrition research*, *59*(1), 26762.
Martínez-Ballesta, M., Gil-Izquierdo, Á., García-Viguera, C., & Domínguez-Perles, R. (2018). Nanoparticles and controlled delivery for bioactive compounds: Outlining challenges for new "smart-foods" for health. *Foods*, *7*(5), 72.
Martău, G. A., Mihai, M., & Vodnar, D. C. (2019). The use of chitosan, alginate, and pectin in the biomedical and food sector—biocompatibility, bioadhesiveness, and biodegradability. *Polymers*, *11*(11), 1837.
Miguel, M. G. (2010). Antioxidant and anti-inflammatory activities of essential oils: a short review. *Molecules*, *15*(12), 9252-9287.
Mihindukulasuriya, S., & Lim, L.-T. (2014). Nanotechnology development in food packaging: A review. *Trends in Food Science & Technology*, *40*(2), 149-167.
Miller, L. M., Bourassa, M. W., & Smith, R. J. (2013). FTIR spectroscopic imaging of protein aggregation in living cells. *Biochimica et biophysica acta (BBA)-biomembranes*, *1828*(10), 2339-2346.
Mohamed, S. A., El-Sakhawy, M., & El-Sakhawy, M. A.-M. (2020). Polysaccharides, protein and lipid-based natural edible films in food packaging: A review. *Carbohydrate Polymers*, *238*, 116178.
Mohammadian, M., Waly, M. I., Moghadam, M., Emam-Djomeh, Z., Salami, M., & Moosavi-Movahedi, A. A. (2020). Nanostructured food proteins as efficient systems for the encapsulation of bioactive compounds. *Food Science and Human Wellness*, *9*(3), 199-213.
Moleyar, V., & Narasimham, P. (1992). Antibacterial activity of essential oil components. *International journal of food microbiology*, *16*(4), 337-342.
Momin, J. K., Jayakumar, C., & Prajapati, J. B. (2013). Potential of nanotechnology in functional foods. *Emirates journal of food and agriculture*, *25*(1), 10-19.
Moraru, C. I., Panchapakesan, C. P., Huang, Q., Takhistov, P., Liu, S., & Kokini, J. L. (2003). Nanotechnology: a new frontier in food science understanding the special properties of materials of nanometer size will allow food scientists to design new, healthier, tastier, and safer foods. *Nanotechnology*, *57*(12), 24-29.
Mun, S., Cho, Y., Decker, E. A., & McClements, D. J. (2008). Utilization of polysaccharide coatings to improve freeze–thaw and freeze–dry stability of protein-coated lipid droplets. *Journal of food engineering*, *86*(4), 508-518.
Munarin, F., Tanzi, M. C., & Petrini, P. (2012). Advances in biomedical applications of pectin gels. *International journal of biological macromolecules*, *51*(4), 681-689.
Nasrollahzadeh, M., Sajjadi, M., Sajadi, S. M., & Issaabadi, Z. (2019). Green nanotechnology. In *Interface science and technology* (Vol. 28, pp. 145-198). Elsevier.
Nazzaro, F., Fratianni, F., Coppola, R., & De Feo, V. (2017). Essential oils and antifungal activity. *Pharmaceuticals*, *10*(4), 86.
Nidhi, B., & Baskaran, V. (2013). Acute and subacute toxicity assessment of lutein in lutein-deficient mice. *Journal of food science*, *78*(10), T1636-T1642.
Nostro, A., & Papalia, T. (2012). Antimicrobial activity of carvacrol: current progress and future prospectives. *Recent patents on anti-infective drug discovery*, *7*(1), 28-35.
Oakenfull, D., & Scott, A. (1984). Hydrophobic interaction in the gelation of high methoxyl pectins. *Journal of Food Science*, *49*(4), 1093-1098.

Omerović, N., Djisalov, M., Živojević, K., Mladenović, M., Vunduk, J., Milenković, I., . . . Vidić, J. (2021). Antimicrobial nanoparticles and biodegradable polymer composites for active food packaging applications. *Comprehensive Reviews in Food Science and Food Safety*, *20*(3), 2428-2454.

Opanasopit, P., Apirakaramwong, A., Ngawhirunpat, T., Rojanarata, T., & Ruktanonchai, U. (2008). Development and characterization of pectinate micro/nanoparticles for gene delivery. *Aaps Pharmscitech*, *9*, 67-74.

Otoni, C. G., Avena-Bustillos, R. J., Azeredo, H. M., Lorevice, M. V., Moura, M. R., Mattoso, L. H., & McHugh, T. H. (2017). Recent advances on edible films based on fruits and vegetables—a review. *Comprehensive Reviews in Food Science and Food Safety*, *16*(5), 1151-1169.

Pascoli, M., De Lima, R., & Fraceto, L. F. (2018). Zein nanoparticles and strategies to improve colloidal stability: A mini-review. *Frontiers in chemistry*, *6*, 6.

Pathak, L., Kanwal, A., & Agrawal, Y. (2015). Curcumin loaded self assembled lipid-biopolymer nanoparticles for functional food applications. *Journal of food science and technology*, *52*, 6143-6156.

Pathak, Y., & Thassu, D. (2009). Drug delivery nanoparticles formulation and characterization. *Drugs and Pharmaceutical Science Series. informa healthcare USA*, *67*, 1-30.

Perrocheau, L., Rogniaux, H., Boivin, P., & Marion, D. (2005). Probing heat-stable water-soluble proteins from barley to malt and beer. *Proteomics*, *5*(11), 2849-2858.

Peñalva, R., Esparza, I., González-Navarro, C. J., Quincoces, G., Peñuelas, I., & Irache, J. M. (2015). Zein nanoparticles for oral folic acid delivery. *Journal of Drug Delivery Science and Technology*, *30*, 450-457.

Peñalva, R., Morales, J., González-Navarro, C. J., Larrañeta, E., Quincoces, G., Peñuelas, I., & Irache, J. M. (2018). Increased oral bioavailability of resveratrol by its encapsulation in casein nanoparticles. *International journal of molecular sciences*, *19*(9), 2816.

Rani, M., Sogi, D. S., & Gill, B. S. (2021). Characterization of gliadin, secalin and hordein fractions using analytical techniques. *Scientific Reports*, *11*(1), 23135.

Rathod, N. B., Kulawik, P., Ozogul, F., Regenstein, J. M., & Ozogul, Y. (2021). Biological activity of plant-based carvacrol and thymol and their impact on human health and food quality. *Trends in Food Science & Technology*, *116*, 733-748.

Ravichandran, R. (2010). Nanotechnology applications in food and food processing: innovative green approaches, opportunities and uncertainties for global market. *International Journal of Green Nanotechnology: Physics and Chemistry*, *1*(2), P72-P96.

Reza Mozafari, M., Johnson, C., Hatziantoniou, S., & Demetzos, C. (2008). Nanoliposomes and their applications in food nanotechnology. *Journal of liposome research*, *18*(4), 309-327.

Rhim, J.-W. (2004). Increase in water vapor barrier property of biopolymer-based edible films and coatings by compositing with lipid materials. *Food Science and Biotechnology*, *13*(4), 528-535.

Ro, J., Kim, Y., Kim, H., Jang, S. B., Lee, H. J., Chakma, S., . . . Lee, J. (2013). Anti-oxidative activity of pectin and its stabilizing effect on retinyl palmitate. *The Korean Journal of Physiology & Pharmacology: Official Journal of the Korean Physiological Society and the Korean Society of Pharmacology*, *17*(3), 197.

Rostamabadi, H., Falsafi, S. R., Boostani, S., Katouzian, I., Rezaei, A., Assadpour, E., & Jafari, S. M. (2021). Design and formulation of nano/micro-encapsulated natural bioactive compounds for food applications. In *Application of nano/microencapsulated ingredients in food products* (pp. 1-41). Elsevier.

Roy, I., & Gupta, M. N. (2004). Freeze-drying of proteins: some emerging concerns. *Biotechnology and applied biochemistry*, *39*(2), 165-177.

Saffarionpour, S. (2019). Preparation of food flavor nanoemulsions by high-and low-energy emulsification approaches. *Food Engineering Reviews*, *11*(4), 259-289.

Sanguansri, P., & Augustin, M. A. (2006). Nanoscale materials development–a food industry perspective. *Trends in Food Science & Technology*, *17*(10), 547-556.

Sant'Anna, V., Gurak, P. D., Marczak, L. D. F., & Tessaro, I. C. (2013). Tracking bioactive compounds with colour changes in foods–A review. *Dyes and Pigments*, *98*(3), 601-608.
Schols, H. A., Bakx, E. J., Schipper, D., & Voragen, A. G. (1995). A xylogalacturonan subunit present in the modified hairy regions of apple pectin. *Carbohydrate Research*, *279*, 265-279.
Seibert, J. B., Bautista-Silva, J. P., Amparo, T. R., Petit, A., Pervier, P., dos Santos Almeida, J. C., . . . de Souza, G. H. B. (2019). Development of propolis nanoemulsion with antioxidant and antimicrobial activity for use as a potential natural preservative. *Food chemistry*, *287*, 61-67.
Sekhon, B. S. (2010). Food nanotechnology–an overview. *Nanotechnology, science and applications*, 1-15.
Selleckchem. Lutein. In.
Selling, G. W., Hamaker, S. A., & Sessa, D. J. (2007). Effect of solvent and temperature on secondary and tertiary structure of zein by circular dichroism. *Cereal chemistry*, *84*(3), 265-270.
Sharifi-Rad, M., Varoni, E. M., Iriti, M., Martorell, M., Setzer, W. N., del Mar Contreras, M., . . . Tajbakhsh, M. (2018). Carvacrol and human health: A comprehensive review. *Phytotherapy Research*, *32*(9), 1675-1687.
Shinde, P., Agraval, H., Srivastav, A. K., Yadav, U. C., & Kumar, U. (2020). Physico-chemical characterization of carvacrol loaded zein nanoparticles for enhanced anticancer activity and investigation of molecular interactions between them by molecular docking. *International Journal of Pharmaceutics*, *588*, 119795.
Shtriker, M. G., Hahn, M., Taieb, E., Nyska, A., Moallem, U., Tirosh, O., & Madar, Z. (2018). Fenugreek galactomannan and citrus pectin improve several parameters associated with glucose metabolism and modulate gut microbiota in mice. *Nutrition*, *46*, 134-142. e133.
Shukla, R., & Cheryan, M. (2001). Zein: the industrial protein from corn. *Industrial crops and products*, *13*(3), 171-192.
Shutava, T. G., Balkundi, S. S., Vangala, P., Steffan, J. J., Bigelow, R. L., Cardelli, J. A., . . . Lvov, Y. M. (2009). Layer-by-layer-coated gelatin nanoparticles as a vehicle for delivery of natural polyphenols. *ACS nano*, *3*(7), 1877-1885.
Silva, H. D., Cerqueira, M. Â., & Vicente, A. A. (2012). Nanoemulsions for food applications: development and characterization. *Food and bioprocess technology*, *5*, 854-867.
Singh, S. K., Dey, S., Schneider, M. P., & Nandi, S. (2022). d-Mannitol based surfactants for cosmetic and food applications and hydrogels to produce stabilized Ag nanoparticles. *New Journal of Chemistry*, *46*(13), 6193-6200.
Singthong, J., Cui, S. W., Ningsanond, S., & Goff, H. D. (2004). Structural characterization, degree of esterification and some gelling properties of Krueo Ma Noy (Cissampelos pareira) pectin. *Carbohydrate polymers*, *58*(4), 391-400.
Sivam, A., Sun-Waterhouse, D., Perera, C., & Waterhouse, G. (2012). Exploring the interactions between blackcurrant polyphenols, pectin and wheat biopolymers in model breads; a FTIR and HPLC investigation. *Food Chemistry*, *131*(3), 802-810.
Song, H., He, A., Guan, X., Chen, Z., Bao, Y., & Huang, K. (2022). Fabrication of chitosan-coated epigallocatechin-3-gallate (EGCG)-hordein nanoparticles and their transcellular permeability in Caco-2/HT29 cocultures. *International Journal of Biological Macromolecules*, *196*, 144-150.
Song, J., Sun, C., Gul, K., Mata, A., & Fang, Y. (2021). Prolamin-based complexes: Structure design and food-related applications. *Comprehensive Reviews in Food Science and Food Safety*, *20*(2), 1120-1149.
Song, Y., Zhou, J., Li, Q., Guo, Y., & Zhang, L. (2009). Preparation and characterization of novel quaternized cellulose nanoparticles as protein carriers. *Macromolecular bioscience*, *9*(9), 857-863.
Sonkaria, S., Ahn, S.-H., & Khare, V. (2012). Nanotechnology and its impact on food and nutrition: a review. *Recent patents on food, nutrition & agriculture*, *4*(1), 8-18.
Souza, V. G. L., & Fernando, A. L. (2016). Nanoparticles in food packaging: Biodegradability and potential migration to food—A review. *Food Packaging and Shelf Life*, *8*, 63-70.

Sozer, N., & Kokini, J. L. (2009). Nanotechnology and its applications in the food sector. *Trends in biotechnology*, *27*(2), 82-89.
Srinivas, P., Philbert, M., Vu, T., Huang, Q., Kokini, J., Saos, E., . . . McDade-Ngutter, C. (2010). Nanotechnology research: Applications in nutritional sciences (Journal of Nutrition (2010) 140,(119-124)). *Journal of Nutrition*, *140*(5), 1062.
Steigerwald, H., Blanco-Perez, F., Albrecht, M., Bender, C., Wangorsch, A., Endreß, H.-U., . . . Scheurer, S. (2021). Does the food ingredient pectin provide a risk for patients allergic to non-specific lipid-transfer proteins? *Foods*, *11*(1), 13.
Steiner, B. M., McClements, D. J., & Davidov-Pardo, G. (2018). Encapsulation systems for lutein: A review. *Trends in food science & technology*, *82*, 71-81.
Stoffelen, C., & Huskens, J. (2016). Soft supramolecular nanoparticles by noncovalent and host–guest interactions. *Small*, *12*(1), 96-119.
Sun, C., Dai, L., He, X., Liu, F., Yuan, F., & Gao, Y. (2016). Effect of heat treatment on physical, structural, thermal and morphological characteristics of zein in ethanol-water solution. *Food Hydrocolloids*, *58*, 11-19.
Suntres, Z. E., Coccimiglio, J., & Alipour, M. (2015). The bioactivity and toxicological actions of carvacrol. *Critical reviews in food science and nutrition*, *55*(3), 304-318.
Tarhini, M., Greige-Gerges, H., & Elaissari, A. (2017). Protein-based nanoparticles: From preparation to encapsulation of active molecules. *International journal of pharmaceutics*, *522*(1-2), 172-197.
Technavio. (2022). *Food Nanotechnology Market to record a CAGR of 25.32% by 2025*.
Teng, Z., Luo, Y., & Wang, Q. (2012). Nanoparticles synthesized from soy protein: preparation, characterization, and application for nutraceutical encapsulation. *Journal of agricultural and food chemistry*, *60*(10), 2712-2720.
Thankappan, D. A., Raman, H. K., Jose, J., & Sudhakaran, S. (2020). Plant-mediated biosynthesis of zein–pectin nanoparticle: Preparation, characterization and in vitro drug release study. *Journal of King Saud University-Science*, *32*(2), 1785-1791.
Trenkenschuh, E., & Friess, W. (2021). Freeze-drying of nanoparticles: How to overcome colloidal instability by formulation and process optimization. *European Journal of Pharmaceutics and Biopharmaceutics*, *165*, 345-360.
Uerpmann-Wittzack, R. (2017). European Directorate for the Quality of Medicines and Healthcare (EDQM).
Van Buren, J. (1991). Function of pectin in plant tissue structure and firmness. *The chemistry and technology of pectin*, 1-22.
Vishwanathan, R., Kuchan, M. J., & Johnson, E. J. (2011). Lutein is the predominant carotenoid in infant brain. *Acta Biologica Cracoviensia. Series Botanica. Supplement*, *53*(1).
Wagoner, T., Vardhanabhuti, B., & Foegeding, E. A. (2016). Designing whey protein–polysaccharide particles for colloidal stability. *Annual review of food science and technology*, *7*, 93-116.
Wang, C., Tian, Z., Chen, L., Temelli, F., Liu, H., & Wang, Y. (2010). Functionality of barley proteins extracted and fractionated by alkaline and alcohol methods. *Cereal chemistry*, *87*(6), 597-606.
Wang, P., & Wu, Y. (2021). A review on colloidal delivery vehicles using carvacrol as a model bioactive compound. *Food Hydrocolloids*, *120*, 106922.
Wang, X., Peng, F., Liu, F., Xiao, Y., Li, F., Lei, H., . . . Xu, H. (2020). Zein-pectin composite nanoparticles as an efficient hyperoside delivery system: Fabrication, characterization, and in vitro release property. *Lwt*, *133*, 109869.
Wang, Y., Yang, J., & Chen, L. (2015). Convenient fabrication of electrospun prolamin protein delivery system with three-dimensional shapeability and resistance to fouling. *ACS Applied Materials & Interfaces*, *7*(24), 13422-13430.
Wathoni, N., Shan, C. Y., Shan, W. Y., Rostinawati, T., Indradi, R. B., Pratiwi, R., & Muchtaridi, M. (2019). Characterization and antioxidant activity of pectin from Indonesian mangosteen (Garcinia mangostana L.) rind. *Heliyon*, *5*(8), e02299.

Wei, Z., & Huang, Q. (2019). Assembly of protein–polysaccharide complexes for delivery of bioactive ingredients: A perspective paper. *Journal of agricultural and food chemistry*, *67*(5), 1344-1352.
Weibull, J. (1987). Seasonal changes in the free amino acids of oat and barley phloem sap in relation to plant growth stage and growth of Rhopalosiphum padi. *Annals of Applied Biology*, *111*(3), 729-737.
Weiss, J., Decker, E. A., McClements, D. J., Kristbergsson, K., Helgason, T., & Awad, T. (2008). Solid lipid nanoparticles as delivery systems for bioactive food components. *Food biophysics*, *3*, 146-154.
Weiss, J., Gaysinsky, S., Davidson, M., & McClements, J. (2009). Nanostructured encapsulation systems: food antimicrobials. In *Global issues in food science and technology* (pp. 425-479). Elsevier.
Wikepedia. (2007). Carvacrol structure. In.
Willats, W. G., Knox, J. P., & Mikkelsen, J. D. (2006). Pectin: new insights into an old polymer are starting to gel. *Trends in Food Science & Technology*, *17*(3), 97-104.
Wilson, R. J., Li, Y., Yang, G., & Zhao, C.-X. (2022). Nanoemulsions for drug delivery. *Particuology*, *64*, 85-97.
Wu, W., Kong, X., Zhang, C., Hua, Y., & Chen, Y. (2018). Improving the stability of wheat gliadin nanoparticles–Effect of gum arabic addition. *Food Hydrocolloids*, *80*, 78-87.
Wu, Y., Luo, Y., & Wang, Q. (2012). Antioxidant and antimicrobial properties of essential oils encapsulated in zein nanoparticles prepared by liquid–liquid dispersion method. *LWT-Food Science and Technology*, *48*(2), 283-290.
Xue, J., & Luo, Y. (2023). Protein-polysaccharide nanocomplexes as nanocarriers for delivery of curcumin: a comprehensive review on preparation methods and encapsulation mechanisms. *Journal of Future Foods*, *3*(2), 99-114.
Yada, R. Y., Buck, N., Canady, R., DeMerlis, C., Duncan, T., Janer, G., . . . Noonan, G. (2014). Engineered nanoscale food ingredients: evaluation of current knowledge on material characteristics relevant to uptake from the gastrointestinal tract. *Comprehensive Reviews in Food Science and Food Safety*, *13*(4), 730-744.
Yalçın, E., & Çelik, S. (2007). Solubility properties of barley flour, protein isolates and hydrolysates. *Food chemistry*, *104*(4), 1641-1647.
Yamaguchi, M. (2012). Role of carotenoid β-cryptoxanthin in bone homeostasis. *Journal of Biomedical Science*, *19*(1), 1-13.
Yao, K., Chen, W., Song, F., McClements, D. J., & Hu, K. (2018). Tailoring zein nanoparticle functionality using biopolymer coatings: Impact on curcumin bioaccessibility and antioxidant capacity under simulated gastrointestinal conditions. *Food Hydrocolloids*, *79*, 262-272.
Yazici, A., Marinelli, L., Cacciatore, I., Emsen, B., Eusepi, P., Di Biase, G., . . . Türkez, H. (2021). Potential anticancer effect of carvacrol codrugs on human glioblastoma cells. *Current drug delivery*, *18*(3), 350-356.
Zarekarizi, A., Hoffmann, L., & Burritt, D. (2019). Approaches for the sustainable production of fucoxanthin, a xanthophyll with potential health benefits. *Journal of Applied Phycology*, *31*, 281-299.
Zhang, J., Chen, X. G., Li, Y. Y., & Liu, C. S. (2007). Self-assembled nanoparticles based on hydrophobically modified chitosan as carriers for doxorubicin. *Nanomedicine: Nanotechnology, Biology and Medicine*, *3*(4), 258-265.
Zhang, L., Zheng, J., Wang, Y., Ye, X., Chen, S., Pan, H., & Chen, J. (2022). Fabrication of rhamnogalacturonan-I enriched pectin-based emulsion gels for protection and sustained release of curcumin. *Food Hydrocolloids*, *128*, 107592.
Zhang, T., Xu, J., Chen, J., Wang, Z., Wang, X., & Zhong, J. (2021). Protein nanoparticles for Pickering emulsions: A comprehensive review on their shapes, preparation methods, and modification methods. *Trends in Food Science & Technology*, *113*, 26-41.
Zhao, C., Shen, X., & Guo, M. (2018). Stability of lutein encapsulated whey protein nano-emulsion during storage. *PLoS One*, *13*(2), e0192511.

Zhao, J., Tian, Z., & Chen, L. (2010). Effects of deamidation on structure and functional properties of barley hordein. *Journal of agricultural and food chemistry*, *58*(21), 11448-11455.
Zhao, T., Liu, F., Duan, X., Xiao, C., & Liu, X. (2018). Physicochemical properties of lutein-loaded microcapsules and their uptake via Caco-2 monolayers. *Molecules*, *23*(7), 1805.
Zhao, W., Kim, Y., & Cameron, R. G. (2022). A novel multiplex lateral flow assay for rapid assessment of pectin structural/functional properties. *Food Hydrocolloids*, *133*, 107988.
Zheng, H., Wang, J., Zhang, Y., Xv, Q., Zeng, Q., & Wang, J. (2022). Preparation and characterization of carvacrol-loaded caseinate/zein-composite nanoparticles using the anti-solvent precipitation method. *Nanomaterials*, *12*(13), 2189.
Zou, L., Zhang, Z., Zhang, R., Liu, W., Liu, C., Xiao, H., & McClements, D. J. (2016). Encapsulation of protein nanoparticles within alginate microparticles: Impact of pH and ionic strength on functional performance. *Journal of Food Engineering*, *178*, 81-89.
Åssveen, M. (2009). Amino acid composition of spring barley cultivars used in Norway. *Acta Agriculturae Scandinavica Section B–Soil and Plant Science*, *59*(5), 395-401.